Wideband Spectrum Sensing in Cognitive Radio using Uniform and Non-Uniform Filter Banks

A thesis submitted
in partial fulfillment for the degree of

Doctor of Philosophy

by

S. CHRIS PREMA

DEPARTMENT OF AVIONICS
INDIAN INSTITUTE OF SPACE SCIENCE AND TECHNOLOGY
THIRUVANANTHAPURAM - 695547

October 2016

CERTIFICATE

This is to certify that the thesis titled **Wideband Spectrum Sensing in Cognitive Radio using Uniform and Non-Uniform Filter Banks**, submitted by **S. Chris Prema**, to the Indian Institute of Space Science and Technology, Thiruvananthapuram, in partial fulfillment for the award of the degree of **Doctor of Philosophy**, is a *bona fide* record of the research work done by her under my supervision. The contents of this thesis, in full or in parts, have not been submitted to any other Institute or University for the award of any degree or diploma.

Dr. K. S. Dasgupta
Supervisor
Former Director, IIST

Counter Signature of **HOD**
(with seal)

Place: Thiruvananthapuram
Date: October 2016

DECLARATION

I declare that this thesis titled **Wideband Spectrum Sensing in Cognitive Radio using Uniform and Non-Uniform Filter Banks** submitted in fulfillment of the Degree of Doctor of Philosophy is a record of original work carried out by me under the supervision of **Dr. K. S. Dasgupta**, and has not formed the basis for the award of any degree, diploma, associateship, fellowship or other titles in this or any other Institution or University of higher learning. In keeping with the ethical practice in reporting scientific information, due acknowledgments have been made wherever the findings of others have been cited.

S. Chris Prema
SC11D013

Place: Thiruvananthapuram
October 2016

ACKNOWLEDGEMENTS

First of all let me bow my head before God Almighty for giving me the strength and confidence throughout the course of this study.

I would like to express my special appreciation and thanks to my advisor and mentor Professor Dr. K. S. Dasgupta, for his patient guidance, encouragement and advice he has provided throughout my research. He had spent hours for critically going through my thesis chapters and guided me to think and work differently, while maintaining scientific soundness and academic rigor. His advice on both research as well as on my career has been priceless. I would like to thank you for eliciting the best in my research and for allowing me to grow as a researcher.

I express my sincere thanks to Dr. Thomas Kurien, Dr. Devendra Jalihal, Dr. N. Selvaganesan, Dr. J. Sheeba Rani, and Dr. Lakshminarayanan for serving as members of my doctoral committee and whose insightfulness and timely advice had helped in refining this study. I would like to thank Dr. V. K. Dadhwal, Director, IIST, Dr. Raju K. George, Dean (R & D), IIST, Dr. A. Chandrasekar, Dean (Academics), IIST for the continuous support provided for the successful completion of this work.

I express my sincere gratitude to Dr. B. S. Manoj, Head, Department of Avionics and Dr. N. Selvaganesan, former Head, Department of Avionics for the commendable support provided in many critical situations. I acknowledge all my colleagues in Department of Avionics for the healthy technical interactions and support in various stages of this work. I am also grateful to the teaching community of IIST, especially the Department of Avionics, who have ignited the spark in me with their ideas and knowledge in the subject. The inputs and the expertise provided by the faculty and the tremendous help extended by the non-teaching staff of IIST were incredible.

My appreciation to all my friends, research scholars, and students of IIST who stood with me, motivated me to strive towards my goal, and remembering me in their prayers. A very special thanks to Sarath Babu, Research Scholar, IIST, for giving the much needed support in writing the thesis.

Words cannot express how grateful I am to my family members for the sacrifices they have made on my behalf. A very special note of love and gratitude for my husband, without whose help, patience, and support, the thesis would not have found light on time. I am indebted to my parents for making lot of sacrifices to provide me the best of opportunities that they never had. Your prayer for me was what sustained me thus far. I also thank my sisters, sister-in-law, and my brother for being there whenever I needed them.

S. Chris Prema

ABSTRACT

Rapid growth in wireless communication services has increased the demand for spectrum resources. A recent report by Federal Communications Commission (FCC) reveals the fact that major part of the spectrum is underutilized. The existing static frequency allocation schemes are not able to accommodate the requirements of increasing data rate and wireless services. Such scenarios demand innovative techniques to exploit the available spectrum. Cognitive Radio (CR) techniques have proven to be a solution to alleviate the spectrum scarcity using spectrum sensing techniques.

In this thesis, we focus on wideband spectrum sensing using filter bank techniques. Even though narrowband spectrum sensing makes a binary decision on the whole spectrum, it is unable to identify spectral holes and spectral opportunities within a wideband spectrum. On the other hand, in wideband spectrum sensing, the available bandwidth is divided into multiple subbands or subchannels for spectrum sensing. A solution to this would be filter bank spectrum sensing.

Filter banks can be derived using modulation of a single prototype filter having high stopband attenuation, narrow transition width, and small passband ripple. Architectures based on filter banks allow sensing multiple subbands simultaneously with low spectrum leakage from adjacent channels when properly designed subband filters are used. We have designed a variable step prototype filter iteratively for the filter banks satisfying Near Perfect Reconstruction (NPR) condition. Cosine Modulated Filter Bank (CMFB) was used for spectrum sensing using the designed prototype filter as they provide higher bandwidth efficiency and lower sidelobes desirable for spectrum sensing. The sensing performance depends on the granularity of filter banks. Finer granularity band improves the probability of detection at the cost of increase in computational complexity. In order to reduce computational complexity, a coarser to finer multistage CMFB was proposed to detect narrowband users in a wideband spectrum. In such cases, only the bandwidth of interest is sensed with finer resolution instead of the entire bandwidth. Since polyphase filter banks are computationally efficient compared to CMFB, the later work was done with polyphase filter banks.

Since the spectrum bands are predefined for commercial communication scenarios, CR system requires to check whether a spectrum band is free or occupied. Then the detected spectral band can be utilized opportunistically. However, in multi-channel military wireless communication, there exists a requirement to identify the center frequency and the spectral edges of the primary users for fractional utilization of the available bandwidth. In order to address this problem, a novel *centroid* based low complexity polyphase filter bank multistage approach was proposed. The sensing was performed from coarser to finer spectral resolution using filter banks. Depending on the energy distribution at each stage, narrowband users were detected in wideband channels. Using our approach, the primary users can be detected in the first stage itself in cases they appear between two subbands. As the first stage has coarser subbands (number of subbands are less), the complexity in computation as well as hardware is drastically reduced. However, if the primary user appears exclusively within a single subband, the detection process can be completed in the second stage without ambiguity. We have considered IEEE 802.22 Wireless Regional Area Network (WRAN) standard as an application for validating our algorithm using multistage polyphase filter banks to detect Wireless Microphones (WM) in Television (TV) channels. The proposed scheme was analyzed and validated through extensive simulations for the detection of WM.

A novel *center of mass* approach was proposed for the detection of multiple users in wideband spectrum. Further, mathematical relation for the estimation of center frequency and spectral boundaries/edges were also established. To reduce the complexity, the detection is carried from a coarser to finer spectral resolution depending on the energy distribution at each stage. The subbands whose energy lies within the predefined thresholds are further sensed with finer resolution in the subsequent stages. For simulations, the signal having three different communication standards such as Bluetooth, Zigbee, and Wideband Code Division Multiple Access were considered.

Applications such as digital channelizers in Software Defined Radios (SDR), digital audio industry, biomedical signal processing, subband adaptive filtering, and communication requires non-uniform frequency partitioning to better exploit the signal characteristics. In such applications, implementation of non-uniform filter banks has elicited enormous interest in multirate signal processing. Non-uniform filter banks were implemented with channel combiner using single and multi-prototype approaches. The non-uniform bands are generated by directly combining the adjacent subbands of uni-

form filter bank. The prototype filter is optimized in such a way that they are combined at 3 dB cut-off frequency and, thereby satisfies the NPR condition. Single prototype approach had the limitation of more distortion in case of large number of combiners while generating wideband from a narrowband prototype this was overcome by multi-prototype approach. The multi-prototype based method is found to have less complexity and distortions when compared to the single prototype channel combiner based approach.

In order to efficiently use the detected spectral holes, a rate request sequenced bit loading secondary user reallocation algorithm for Discrete Multi Tone (DMT) systems in CR was also proposed. Our algorithm is applicable to DMT systems for secondary user reallocation. DMT systems support different modulation techniques on different subchannels according to the Signal to Noise Ratio (SNR). The maximum bits and power that can be allocated to each subband is determined depending on the Channel State Information (CSI) and secondary user modulation scheme. The spectral holes or free subbands are allocated to secondary users depending on the user rate request as well as subchannel capacity. A comparison is done between random rate request and sequenced rate request of secondary user for subchannel allocation. Through simulations, it is concluded that with sequenced rate request, higher spectral efficiency is achieved.

TABLE OF CONTENTS

LIST OF TABLES

LIST OF FIGURES

ABBREVIATIONS

ADC	Analog to Digital Converters
AWGN	Additive White Gaussian Noise
AFB	Analysis Filter Bank
CMFB	Cosine Modulated Filter Bank
CR	Cognitive Radio
CLT	Central Limit Theorem
CSI	Channel State Information
CFD	Cyclostationary Feature Detection
CAF	Cyclic Auto-correlation Function
CMT	Cosine Modulated Multitone
DFT	Discrete Fourier Transform
DMT	Discrete Multi Tone
ED	Energy Detection
EME	Energy Minimum Eigenvalue
FCC	Federal Communications Commission
FBMC	Filter Bank Multi-Carrier
FMT	Filtered Multitone
FFT	Fast Fourier Transform
FIR	Finite Impulse Response
FRM	Frequency Response Masking
FFB	Fast Filter Bank
ISM	Industrial Scientific and Medical
ISI	Inter Symbol Interference
ICI	Inter Carrier Interference
MF	Matched Filter
MTM	Multi-Taper Method
MME	Maximum Minimum Eigenvalue
MDFT	Modified Discrete Fourier Transform

NPR	Near Perfect Reconstruction
NUFB	Non-Uniform Filter Bank
OFDM	Orthogonal Frequency Division Multiplexing
PSD	Power Spectral Density
PU	Primary User
PR	Perfect Reconstruction
PDFB	Progressive Decimation Filter Bank
OQAM	orthogonal multiplexed quadrature amplitude modulation
QMF	Quadrature Mirror Filter
RF	Radio Frequency
SMT	Staggered Modulated Multitone
SS	Spectrum Sensing
SFB	Synthesis Filter Bank
SU	Secondary User
SNR	Signal to Noise Ratio
TV	Television
UHF	Ultra High Frequency
VHF	Very High Frequency
WRAN	Wireless Regional Area Network
WM	Wireless Microphones
WLAN	Wireless Local Area Networks
WPAN	Wireless Personal Area Network

CHAPTER 1

Introduction

Recent developments in wireless communication services lead to an increase in the demand for spectrum resources. Moreover, most of the existing wireless networks follow a fixed spectrum assignment policy. A recent report by Federal Communications Commission (FCC) reveals that most of the spectrum are underutilized. Cognitive Radios (CR) have proven to be a solution to alleviate the spectrum scarcity by utilizing different spectrum sensing techniques. Another problem is the interference between users operating at the same frequency. When primary users share the spectrum with secondary users, the secondary users have to be intelligent enough to give up the spectrum when the primary user starts transmission. Therefore, the CRs have to be dynamic and adapt to the spectral environment, spectrum policies and utilize the spectrum efficiently. As a solution to these challenges advanced Cognitive Radio (CR) signal processing techniques are being researched.

CRs find application in different areas of communication systems. In communication there are certain frequency bands globally available for low cost wireless systems. The frequency band 2.4 GHz industrial, scientific and medical (ISM) is available globally and can be used by low cost wireless systems such as Wireless Local Area Network (WLAN) and Wireless Personal Area Network (WPAN). Since no effective co-ordination or radio spectrum management scheme exist, the frequency bands are utilized inefficiently. CR techniques can be a solution to the problem of inefficient utilization of spectrum. IEEE 802.22 working group is constructing Wireless Regional Area Network (WRAN) to utilize the white spaces in TV spectrum using CR techniques.

The idea of CR systems is to identify the spectral holes in a sensing bandwidth and reallocate secondary users (unlicensed) to occupy those spectral holes without causing harmful interference to the primary users (licensed). This chapter briefly describes the functionality and applications of CR. The current trends towards CR and the important issues related to the spectrum utilization are discussed. The motivation, objectives, and contribution of the thesis are outlined.

1.1 Cognitive Radio

Cognitive radio system has been proposed as a promising solution to improve the spectrum utilization. The concept of cognitive radio was proposed by Joseph Mitola [5]. CR systems have intelligent mechanism for monitoring the radio spectrum to detect spectral holes and, thereby, allocate the same to secondary users without causing any harmful interference to the primary users in wideband spectrum. Particularly, CR is considered for obtaining spectrum usage characteristics across multiple dimensions such as time, space, frequency, and code. CR comprises of determining the type of signals in addition to parameters such as modulation, waveform, bandwidth, and carrier frequency occupying the spectrum [6].

FCC defines CR as *"A radio or system that senses its operational electromagnetic environment and can dynamically and autonomously adjust its radio operating parameters to modify system operation, such as maximize throughput, mitigate interference, facilitate inter-operability, access secondary markets."*

CRs are considered to be the most promising future wireless communication technology that may potentially mitigate the radio scarcity problem using dynamic spectrum access [7]. The underutilisation of spectrum is due to the extremely low spectrum utilization in some localized temporal and geographical spectrum bands. Spectral opportunities have to be detected without any assistance from primary users. The primary users do not have any constraints to share or change the operating parameters for sharing spectrum with cognitive radio networks [8].

A CR system consists of the following entities:

1. **Primary User**: The users who have higher priority or legacy rights on the usage of a specific part of the spectrum are defined as primary users [6].

2. **Secondary User**: The unlicensed users, who transmit and receive signals over the licensed spectra or portions of it when primary users are inactive are called secondary users [6].

3. **Spectral hole**: A band of frequencies assigned to a primary user, which is unused at a particular time and at a specific geographic location is called a spectrum hole [3].

The spectral holes are classified into two types: (i) temporal and (ii) spatial spectral holes. A temporal spectral hole appears when a primary user is not transmitting for a certain period of time. When the primary users transmission are confined within an area spatial spectral holes appears and the secondary users can use the spectrum outside that area [9].

The four major functions of cognitive radio are [10]:

1. **Spectrum sensing**: The process of identification of spectrum holes by efficiently detecting the primary user and allocating the same with other users without harmful interferences is spectrum sensing. In general spectrum sensing techniques are classified into three categories [10]

   (a) Transmitter detection

   (b) Cooperative detection

   (c) Interference based detection

   Transmitter detection identifies whether the signal from a primary transmitter is locally present in a certain spectrum. There are three different approaches for transmitter detection such as matched filter detection, energy detection, and cyclostationary detection [11]. Different spectrum sensing techniques are discussed in detail in Section 2.1. In cooperative detection method, information from multiple users are incorporated for a primary user detection taking the advantages of the spatial diversity to improve the reliability of spectrum sensing.

   Interference based detection is performed based on the transmitter-centric approach. The transmitter radiated power, out-of-band emission and location of individual transmitters are regulated in this approach. FCC has introduced a model called as interference temperature model to measure the interference [12]. Depending on the increase in interference temperature model the interfering signals can be identified. The secondary users can determine the vacant spectrum from the interference temperature model.

2. **Spectrum management**: Cognitive radio captures the best available spectrum to meet user communication requirements. The best spectrum band to meet the QoS requirements over the available spectrum bands is decided by cognitive radio. The spectrum management can be further classified as spectrum analysis and

spectrum detection. The challenges in spectrum management include decision model, multiple spectrum band decision, and spectrum decision over heterogeneous spectrum bands.

3. **Spectrum mobility**: The process where a cognitive radio user can exchange its frequency of operation is the spectrum mobility. This allows the cognitive radio user to dynamically use the spectrum by allowing the radio terminals to operate in the best available frequency band. Therefore, seamless communication requirements are maintained during the transition of one spectrum to another. The challenges in spectrum mobility include spectrum handoff and spectrum mobility among multiple users

4. **Spectrum sharing**: The sharing of spectrum provides a fair spectrum scheduling method among existing next generation users. Spectrum sharing can be divided into two types: (i) open spectrum sharing and (ii) licensed spectrum sharing [10]. All the secondary users have equal rights to access the channel in open spectrum sharing. The licensed spectrum sharing follows a hierarchical spectrum access model. The hierarchical spectrum access model can be further divided into spectrum underlay and spectrum overlay. The secondary users are allowed to transmit simultaneously when the primary users are transmitting in a spectrum underlay system. However, the secondary users need to be constrained to avoid interference with primary users. In spectrum overlay system the secondary users can transmit only when primary users are not transmitting [13].

Cognitive radios have two main features which distinguish them from the conventional radio devices, they are *cognitive capability* and *reconfigurability* [10].

The cognitive ability allows a CR system to sense and capture the information from the surrounding radio environment. These features allows a cognitive user to be aware of different parameters such as transmitted waveform, Radio Frequency (RF) spectrum, and geographical information. The gathered information are analyzed to identify any unused spectrum at a specific time and location [14]. The interaction between CR and radio environment is known as cognitive cycle. The cognitive ability of CR explained through cognitive cycle is shown in Figure 1.1. A cognitive cycle consists of the following three components namely, spectrum sensing, spectrum analysis, and spectrum decision [3].

1. **Spectrum sensing**: In spectrum sensing, a cognitive radio observes the frequency band and gathers necessary information regarding its surrounding radio environment. Based on the information captured, the cognitive radio is able to detect spectrum holes.

2. **Spectrum analysis**: Once the spectrum holes are detected using spectrum sensing, each of the spectrum band is characterized based on the local observation of the cognitive radio as well as the statistical information of primary user network. Moreover, characteristics of spectrum holes are also analyzed and estimated.

3. **Spectrum decision**: Depending on the spectrum analysis, the cognitive radio determines the operating parameters such as the data rate, the transmission mode, and the bandwidth available for transmission. The most appropriate spectrum band is selected based on the spectrum band characterization and the user requirements.

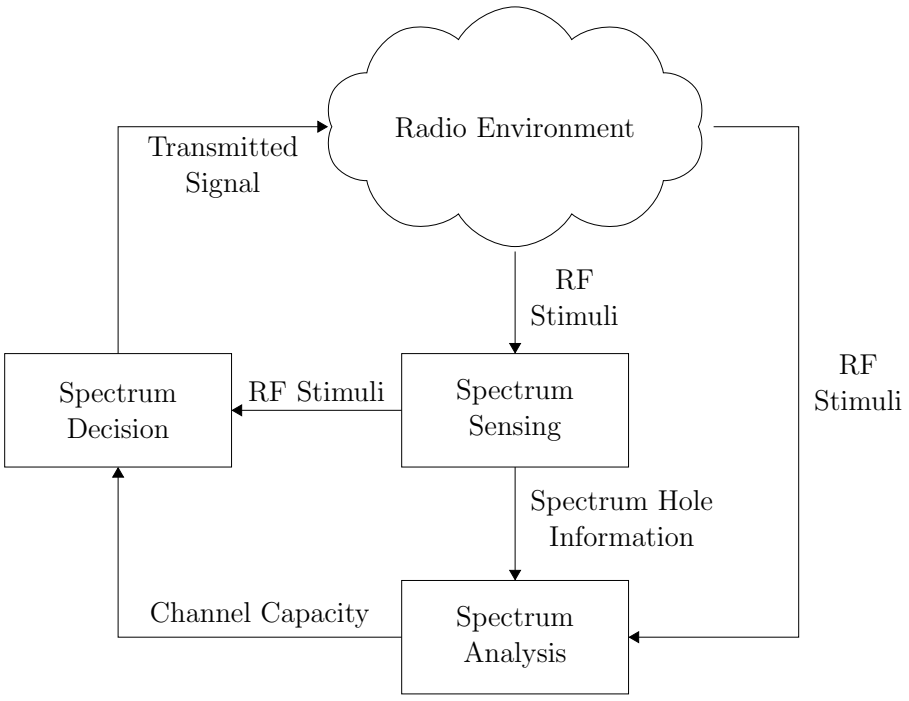

Figure 1.1: Cognitive cycle [3]

As mentioned earlier, the second key feature of a cognitive radio that distinguishes it from a traditional radio is its reconfigurability. The ability of a cognitive radio to intelligently adapt to the radio environment by adjusting its operating parameters, according to the sensed environmental variations, in order to achieve the optimal performance is

referred to as reconfigurability. Cognitive wireless networks are capable of reconfiguring their infrastructure in order to adapt to the continuously changing environment. The reconfiguration actions takes place in the PHY/MAC layers for the selection of appropriate technology and spectrum for operation. Different transmission access technologies can be supported by its hardware design such that transmission and reception are possible in a variety of frequencies [10], [15].

1.1.1 Application Scenarios of Cognitive Radio

Cognitive Radio finds application in many areas of communication. In disaster scenarios such as earth quake or hurricane the communication infrastructure might get damaged. In such situations adhoc cognitive wireless communication becomes useful. The applications of CR include defense, TV bands, and emergency networks [11]:

The portion of TV bands that are unused by licensed wireless services are referred to as TV white spaces (TVWS). Large portions of the spectrum in the VHF/UHF bands are available on a geographical basis due to the analog to digital switch over for higher spectral efficiency in digital TV. The digital switch-over is intended to be carried out in many countries around the world. For instance, FCC has proposed opportunistic access to TV bands to access TV white spaces [16]. IEEE has formed a working group (IEEE 802.22) to develop a cognitive radio standard with an air interface for opportunistic secondary access to the TV spectrum. The utilization of TVWS relies on the ability of cognitive devices to successfully detect TVWS and allocate secondary users without causing harmful interference to the licensed users of these bands [17]. When the information regarding the primary user are available such as modulation the feature detection can be performed to detect spectral holes. However, in most of the cases the primary user information is unavailable and the energy detection technique is applied for spectral analysis in TVWS.

CR techniques are useful in military application to identify wireless communication services of enemies and protect their own wireless services. In disputed regions, the adversary may send jamming signals to disturb the radio communication. In such scenarios, the CR can hands-off frequency over a wide range and use different frequency band, thereby, avoiding the frequency band with jamming signal. CR can offer flexibil-

ity which is vital in battle fields for high level of communication such as upgrade and allow the radio to use a variety of different waveforms or signals. In addition, CRs are capable of monitoring their own performances on a regular basis in order to deliver a high quality of service. The operational environment is recognized in CR and adjusted in such a way that high quality of service required for military radios are provided [18]. Military communications are also limited by radio spectrum scarcity due to the static frequency assignment, where a large amount of spectrum remains idle. CR using dynamic spectrum access can alleviate spectrum congestion through efficient allocation of bandwidth and flexible spectrum access. Therefore, CRs are capable of providing military systems with adaptive, seamless, and secure communication [14], [19]. The detection of spectral edges or spectral boundaries using CR are also useful for such military radio applications [20].

CR networks are useful to enhance public safety and homeland security [14]. Under unforseen circumstances such as accidents and natural calamities, there exists a need to maintain reliable communication. Infrastructure of the current wireless systems are inadequate for these emergency situations. Therefore, emergency networks are required to aid the search and rescue operations. CR can recognize spectrum availability and reconfigure itself for efficient communication with dynamic spectrum selectivity and reliable communication to minimize information delay [21]. In an unanticipated condition, the public networks may get overloaded due to specific group of users. To alleviate the spectrum shortage, dynamic access of free spectrum is considered to be a feasible solution using CR [22]. Further, CR can facilitate interoperability between different communication systems. In order to accommodate the requirements and conditions of other networks, the CR devices can support multiple service types, such as voice, data, and video.

1.2 Motivation and Objectives

Wireless communication has grown rapidly with several wireless applications and hence there exists a scarcity of spectrum. To accommodate new wireless technologies, dynamic spectrum access techniques are essential. CR systems can intelligently monitor the radio spectrum to detect spectral holes and allocate the free spectrum to secondary

users without causing any harmful interference to the primary users. Significant amount of work has been done in narrowband sensing with reconfigurable and low complexity spectrum sensing techniques.

The narrowband spectrum sensing makes a binary decision and is unable to identify spectral holes within the available spectrum. Therefore, spectral opportunities within a wideband spectrum has to be identified by mutiband spectrum sensing. Multiband spectrum sensing has gained significance in CR due to its promising enhancement in cognitive radio networks due to simultaneous access of secondary users. Moreover, this improves the network throughput and reduces interference with primary user as secondary users can seamlessly handsoff with other users. Further research is required towards realizing multiband spectrum access.

When narrowband users are present in a wideband spectrum, the precision of spectral detection depends on the number of subbands (granularity) used for spectrum sensing. This implies that the computational complexity gets increased if finer granularity subbands are chosen. Therefore, there exist a need to propose different spectrum sensing algorithms with lower computational complexity and latency. An in depth research is being carried out to address these two issues. Detection accuracy also plays an important role in efficient utilization of the spectrum (unused spectrum holes). There is a need for precise and faster spectrum sensing algorithms for efficient spectrum sensing and real time spectrum reallocation schemes for the unused spectrum.

Commercial CR applications require identification of the spectral holes to opportunistically exploit the available spectrum bands. Since the commercial spectrum bands are predefined, identification of the spectral holes is sufficient to allocate secondary users in the vacant frequency bands. However, in multi-channel military wireless communication, there is a need to identify the center frequency and the spectral edges of the primary users for fractional bandwidth utilization. Methods to estimate the center frequency and spectral edges are limited in literature. Accurate detection of narrowband users in wideband spectrum is also needed for fractional bandwidth utilization. Therefore, techniques to detect spectral information such as center frequency and spectral edges need to be investigated. Similarly, significant research has been done to detect the spectral holes. However the spectral utilization is improved only when the detected spectral holes are reallocated to secondary users. Spectrum reallocation techniques also

need to be analyzed for efficient utilization of detected spectral holes.

The main objective of the thesis is to address the problem of wideband spectrum sensing using filter bank techniques in CR. To overcome the computational complexity of detection with finer spectral resolutions, a multistage filter bank techniques are needed. Different filter bank techniques are to be analyzed for wideband spectrum sensing for narrowband users and multiple users with different bandwidth. Therefore proper design of prototype filters are required to enhance the overall filter bank performance. There is a need to address the center frequency detection and estimation of spectral edges/boundaries of both single and multiple users in a wideband spectrum sensing using filter banks. In addition, we need to address the reallocation of secondary users for efficient utilization of unused spectrum (spectrum hole).

In this thesis, we focus on sensing Wireless Microphone (WM) in TV channel. FCC has permitted the unlicensed wireless devices to utilize the vacant bands (white spaces) in TV spectrum [23]. IEEE 802.22 wireless standard is considered to apply cognitive radio technology to utilize the white spaces in TV spectrum. WMs have narrowbands of less than 200 kHz and appear in wideband TV (6 MHz) spectrum. Filter bank techniques are applied for the detection of WMs in such wideband spectrum. The detection of multiple users in wide band spectrum with center frequency and spectral edge detection is also addressed using filter banks

1.3 Contributions of Thesis

The contribution of the thesis is in the field of wideband spectrum sensing and non-uniform bandwidth allocation using filter bank techniques. We summarize the contribution of the thesis as follows:

1. The filter banks are used for wide band spectrum sensing in CR. The performance of spectrum estimation is characterized by frequency resolution, spectrum leakage, and subband attenuation. The three parameters can be regulated using proper design of prototype filters, since the overall performance of the filter bank depends on the design of prototype filter. Considering frequency resolution, spectrum leakage, and subband attenuation, a systematic and self controlled prototype

filter is designed iteratively for complex modulated filter banks. The primary goal of the design of prototype filters is to enhance the performance, i.e., minimizing amplitude distortion and aliasing error. In order to achieve the goal, an objective function is chosen to approximate 3 dB cut-off frequency, very close to $\frac{\pi}{2M}$, by varying the step size, which is a function of transition width.

2. Cosine modulated filter banks (CMFB) can provide higher bandwidth efficiency and lower sidelobes desirable for spectrum sensing. Moreover, cosine modulated filter banks can be designed by modulating a single prototype filter. The detection performance with varying granularity (number of subbands) bands using CMFB was analyzed. The detection performance is found to be improved with finer granularity bands at the cost of computational complexity as the number of subbands in the filter banks was increased. Therefore, multistage cosine modulated filter banks from coarser to finer resolution for reducing computational complexity were investigated. Two thresholds are calculated depending on different probability of false alarm. Only the subbands with energy between the two thresholds are sensed further with finer resolution rather than the entire bandwidth.

3. Polyphase filter banks have computationally efficient filter bank structure. In order to reduce the computational complexity, multistage polyphase filter banks were implemented for spectrum sensing in widebands. The proposed method allows to detect the presence of single user and estimate the center frequency. As narrowband users were considered, the number of detected subbands was found to be atmost two. Therefore, the energy distribution in the subbands was modeled as a trapezoid and the center frequency was calculated using the centroid method. The novelty of the proposed method is the estimation of center frequency with higher precision and reduced computational complexity. In addition, the method allows to detect Wireless Microphone (WM) in the presence of signal which follows IEEE 802.22 Wireless Regional Area Network (WRAN) standard within TV channels. In the first stage, the presence of WM along with the estimation of center frequency can be performed, in case the WM lies partly in one subband and partly in the adjacent subband. However, if the WM appears anywhere exclusively within a single subband, the detection process can be completed in the second stage without ambiguity. A mathematical expression for calculating the center frequency of WM from the subband energy (power) using centroid method

was derived and presented.

4. Multistage polyphase filter banks were implemented for the detection and estimation of spectrum edge for multiple users in a wideband spectrum. The spectral edges were estimated from the center frequency and detected subband from energy detection at the output of each subband. Since multiple users are considered, primary users may occupy more than two subbands. In such cases, a novel method based on center of mass was proposed to estimate the center frequency and spectral edges of multiple users with higher precision and reduced computational complexity. The mathematical relation for the calculation of center frequency and estimation of spectral edges was also established. The rationale behind the method is that the, mass is related to energy and and distance is related to frequency.

5. Non-uniform frequency partitioning is required to better exploit the signal characteristic in applications such as digital channelizer in Software Defined Radio (SDR), digital audio industry, biomedical signal processing, subband adaptive filtering, and communication. Non-uniform bandwidth allocation using filter bank techniques with single and multiple prototype filter approaches was designed and analyzed using channel combiner approach. The non-uniform filter banks were implemented from uniform cosine modulated filter banks with proper design of prototype filters.

6. Upon detecting the spectral holes, secondary users needs to be allocated to the identified spectral holes for efficient spectral utilization. A rate request sequenced bit loading secondary user reallocation algorithm for Discrete Multi Tone (DMT) systems in CR was proposed.

1.4 Structure of Thesis

The remaining of this dissertation is organized as follows: Chapter 2 provides an exhaustive literature survey of different spectrum sensing methods. In addition, different types of wideband spectrum sensing methods are discussed with an emphasis on filter bank based techniques relevant to the scope of this thesis.

Chapter 3 proposes an iterative prototype filter design for filter banks satisfying near perfect reconstruction conditions. The design issues of different prototype filters are also discussed. The design conditions and significance of prototype filters in complex modulated filter banks are briefly explained. Further, the simulation results are validated through comparison with existing methods.

Chapter 4 explores cosine modulated filter banks designed using the proposed prototype filter for wideband spectrum sensing. The effects of varying granularity bands were analyzed in wideband spectrum sensing. From the analysis, it is inferred that the probability of detection improved when the number of subbands is increased, which increases the computational complexity. In order to reduce computational complexity, we investigate the scope of multistage filter banks.

Chapter 5 discusses wideband spectrum sensing using multistage polyphase filter banks for single as well as multiple user detection. Issues related to the estimation of center frequency and spectral edges of primary users for fractional bandwidth utilization is examined. Two methods based on center of mass and centroid are proposed for the detection of single and multiple user. In cases where only two subbands were detected by a primary user, a centroid method was applied for estimation of center frequency. When more than two subbands were detected, the idea of center of mass method is used for estimation of center frequency. In multiuser detection the spectral edges are also estimated from the center frequency. Multistage polyphase filter banks are used to reduce the computational complexity. The performance of the proposed spectrum sensing method was analyzed with different simulation environments. Simulations include detection of wireless microphones in TV white space and detection of spectral holes in a wideband comprising of different standards such as Blutooth, Zigbee, and WCDMA.

Chapter 6 discusses non-uniform bandwidth allocation techniques using cosine modulated filter banks. A single prototype approach and multiple prototype approach is detailed for the design of non-uniform filter banks from uniform cosine modulated filter banks. A comparison is done between both methods in terms of distortions introduced in the filter bank design. The procedure for the design of non-uniform filter bank using the single and multiple prototype approaches are explained in detail.

Chapter 7 addresses the issue of allocating secondary users to the identified spectral holes using DMT systems. The bit loading algorithm was used to determine the maxi-

mum number of bits that can be allocated to each channel. An analysis was presented between random allocation along with sequenced and pooled rate requests for efficient spectrum utilization.

Chapter 8 summarizes the thesis and draws the conclusions with possibilities for future research. We conclude that filter banks can be useful for wideband spectrum sensing in cognitive radio applications. Various areas of research using filter bank in cognitive radio are also presented. The need for further research in filter bank based spectrum sensing for adaptive and co-operative spectrum sensing is discussed.

CHAPTER 2

Literature Survey on Spectrum Sensing

The emergence of new wireless devices and applications has increased the communication requirements and hence there is a scarcity of spectrum. The available radio spectrum is used inefficiently due to the fixed spectrum allocation policy as each wireless service is assigned spectrum band to operate in certain frequency bands. Since most of the spectrum are licensed, it becomes difficult to find vacant frequency bands for new wireless services or enhance existing services. To accommodate new wireless technologies, dynamic spectrum access techniques are required. The underutilized spectrum bands due to fixed frequency band allocation policy can be efficiently utilized by spectrum sensing techniques using Cognitive Radio (CR).

In this chapter, a literature survey of different spectrum sensing methods is provided in Section 2.1. The related works and classification of wideband spectrum sensing into Nyquist and sub-Nyquist spectrum sensing is discussed in Section 2.2. The different filter bank spectrum sensing methods are discussed in Section 2.3.

2.1 Spectrum Sensing Methods

Spectrum sensing is an inevitable part of cognitive radio systems that allows us to use the available spectrum efficiently. The different spectrum sensing methods provide the key to monitor and reuse the spectrum without interference. One of the major task of CR is to obtain underutilized and non-interfered spectrum for allocation of secondary users. The channel conditions keep changing due to the noise uncertainity, multipath fading, and shadowing effects in wireless channels. Therefore, there exists a need for monitoring and co-operation among secondary users for efficient spectrum utilization. The usefulness of the spectrum sensing techniques are based on the sensing performance and complexity in implementation.

Spectrum sensing techniques can be classified as non-cooperative and cooperative methods. The cognitive radio acts on its own in non-cooperative spectrum sensing,

while in cooperative spectrum sensing, multiple CRs work together, which results in an increase of accuracy in spectrum detection and spectrum awareness. Cooperative spectrum sensing is further classified into three categories depending on how cooperating CR users share the sensing data: (i) centralized [24], [25], (ii) distributed [26], and (iii) relay assisted [27], [28]. In mutipath fading and shadowing environment, cooperative spectrum sensing is considered to be an effective approach. The common spectrum sensing techniques are Energy Detection (ED), Matched Filter (MF), and Cyclostationary Feature Detection (CFD), which are discussed in subsequent sections. Apart from common spectrum sensing methods, other techniques existing in literature include Eigenvalue based methods, co-variance matrix method, and wavelet based methods [29], [30]. After spectrum sensing, the secondary users are allowed to access the spectrum holes. In order to access the spectrum holes effectively, spectrum sharing and spectrum allocation techniques are important [11]. The common spectrum sensing methods are briefly explained in the following sections:

2.1.1 Energy Detection

Energy detection method is further classified as traditional energy detection and subband based energy detection.

Traditional energy detection is the most widely used method of spectrum sensing due to its low computational complexity [31], [32]. The receiver does not require any prior knowledge of the primary user signal as energy detection is a non-coherent method of detection. The primary user is detected by measuring the energy and comparing it with a predetermined threshold. The threshold λ is computed using the assumed noise variance σ_w^2 and probability of false alarm P_{fa}, which generally depends on the channel characteristics. The problem of detecting the presence and absence of signal in spectrum sensing is typically formulated by the following binary hypothesis test,

$$\begin{aligned} H_0 &: y[n] = w[n] \\ H_1 &: y[n] = x[n] + w[n] \end{aligned} \tag{2.1}$$

where, $y[n]$ represents the received signal, $x[n]$ is the transmitted wireless signal, and $w[n]$ is the zero mean complex circularly symmetric Additive White Gaussian Noise

(AWGN). Further, $x[n] = s[n] \bigotimes h[n]$ where $s[n]$ denotes the primary user signal and $h[n]$ the channel impulse response [33]. Hypothesis H_0 represents the absence of a primary user signal and consist only the noise $w[n]$. On the other hand, hypothesis H_1 represents presence of primary user signal $x[n]$ along with noise $w[n]$. The test statistic is computed as the energy of the received signal,

$$T(y) = \frac{1}{N_s} \sum_{n=0}^{N_s-1} |y[n]|^2, \tag{2.2}$$

where N_s is the total number of samples sensed at the receiver. The test statistic follows a chi-square distribution. However, in practical cases, the test statistic can be approximated to a Gaussian distribution for large number of samples according to the Central Limit Theorem (CLT) [34]. According to CLT independent and identically distributed (i.i.d.) random variables with finite mean and variances approaches a normal distribution when N_s is large enough. Therefore, the distribution of test statistics can be accurately approximated with a normal distribution for sufficiently large number of samples [34]. The above hypothesis can be written as in [35], [36], [37],

$$T(y) \sim \mathcal{N}(\sigma_w^2, \frac{1}{N_s}\sigma_v^4); \text{for hypothesis } H_0$$
$$T(y) \sim \mathcal{N}(\sigma_w^2 + \sigma_x^2, \frac{1}{N_s}(\sigma_v^2 + \sigma_x^2)^2); \text{for hypothesis } H_1,$$

where, σ_x^2 is the signal variance and σ_w^2 is the noise variance. The presence of an active signal is determined by comparing the energy (test statistics) with a predetermined threshold. The threshold λ is calculated using the knowledge of probability of false alarm P_{fa} and the assumed noise variance σ_w^2 of the received signal. The probability of false alarm P_{fa} is given as

$$P_{fa} = Q\left(\frac{\lambda - \sigma_w^2}{\sqrt{1/N_s}\sigma_w^2}\right) \tag{2.3}$$

and the probability of detection P_d can be expressed as

$$P_d = Q\left(\frac{\lambda - (\sigma_s^2 + \sigma_w^2)}{\sqrt{1/N_s}(\sigma_s^2 + \sigma_w^2)}\right) \tag{2.4}$$

The threshold λ is determined from Equation 2.3 as

$$\lambda = (Q^{-1}(P_{fa})\sqrt{1/N_s} + 1)\sigma_w^2. \tag{2.5}$$

The minimum number of samples required for spectrum sensing is obtained using Equation 2.3 and Equation 2.4 [38],

$$N_{min} = 2[Q^{-1}(P_{fa}) - Q^{-1}(P_d)(1 + SNR)]^2 SNR^{-2}. \tag{2.6}$$

Subband based energy detection are used when the available wideband is split into non-overlapping subbands and the energy is computed as the test statistic at the output of each subband. Filter bank based methods are robust and efficient for multiband spectrum sensing where energy detection is performed at the subband level at the output of the FFT or Analysis Filter Bank (AFB). The wideband signal is split into narrow signal bands using FFT or AFB. Similar to traditional energy detection the subband signal can be expressed as follows:

$$\begin{aligned} H_0 &: y_k[m] = w_k[m] \\ H_1 &: y_k[m] = x_k[m] + w_k[m] \end{aligned} \tag{2.7}$$

where, $y_k[m]$ is the received signal at the k^{th} subband ($k = 1, 2, \ldots, M$), M is the total number of subbands with $x_k[m] = H_k s_k[m]$, H_k represents the complex gain of subband, $s_k[m]$ is the input signal, and $w_k[m]$ is the noise samples at the subband. Similar to traditional energy detection, noise follows the distribution $w_k[m] \sim \mathcal{N}(0, \sigma_{w,k}^2)$ and signal $x_k[m] \sim \mathcal{N}(0, \sigma_{x,k}^2)$ with $\sigma_{w,k}^2$ being the noise variance and $\sigma_{x,k}^2$, the signal variance [33]. If σ_w^2 is the noise variance of the wideband channel, the subband noise variance needs to be $\frac{\sigma_w^2}{M}$. The energy at the output of individual subbands is considered as the test statistic

$$Y_k = \frac{1}{L}\sum_{m=0}^{L-1} y_k[m]^2, \tag{2.8}$$

where $L = \left(\frac{N_s}{M}\right)$ is the number of samples in each subband with M number of subbands for sensing and N_s total number of samples received. The presence and absence

of a primary user signal is written in terms of the following two hypotheses [39]:

$$y_k(m) \sim \mathcal{N}\left(\sigma^2_{w,k}, \frac{1}{L}\sigma^4_{w,k}\right) \text{; for hypothesis } H_0$$

$$y_k(m) \sim \mathcal{N}\left(\sigma^2_{w,k} + \sigma^2_{x,k}, \frac{1}{L}\left(\sigma^2_{w,k} + \sigma^2_{x,k}\right)^2\right) \text{; for hypothesis } H_1$$

The number of samples for each stage need to be large enough to perform energy detection even in low SNR. The minimum number of samples required in each stage can be calculated using the relation in Equation 2.6.

2.1.2 Matched Filter

Matched Filter (MF) is a non-blind spectrum sensing technique with coherent detection. Prior knowledge of the primary user signal are required in MF. The known primary user information is correlated with the received signal to detect the presence of primary user signal and maximize the Signal-to-Noise Ratio (SNR). The matched filter requires short sensing time and achieves good detection performance with low probability of missed detection and false alarm [40]. The drawback of this method is that it requires knowledge about primary user signal such as operating frequency, bandwidth, modulation type, and packet format. Therefore, the technique is not applicable when the informations regarding the primary users are unknown [11], [41].

2.1.3 Cyclostationary Feature Detection

Cyclostationary Feature Detection (CFD) technique exploits the cyclostationary features of the signal for spectrum sensing. A signal is considered to be cyclostationary if its statistical properties vary cyclically with time. When the modulated signals are combined with sinusoidal signals and pulse trains, they exhibit periodicity [42]. The cyclostationary features are exploited from these periodicity using signal statistics such as mean and auto-correlation [43]. The Cyclic Auto-correlation Function (CAF) of the received signal $x(t)$ can be expressed as

$$R_x^{(\alpha)}(\tau) = E[x(t)x^*(t-\tau)\exp(-j2\pi\alpha\tau)], \tag{2.9}$$

where, α is the cyclic frequency, $E[.]$ is the expectation operation, and $*$ denotes complex conjugation. Using Fourier series expansion, CAF can be expressed as Cyclic Spectral Density (CSD) [11].

$$S(f, \alpha) = \Sigma_{\tau=-\infty}^{\infty} R_x^{(\alpha)}(\tau) \exp(-j2\pi f\tau). \tag{2.10}$$

When the cyclic frequency α and fundamental frequencies become equal, CSD exhibits peaks. Therefore, under hypothesis H_0, the noise alone is present and the CSD function does not exhibit peaks as the noise is non-stationary. On the other hand, in hypothesis H_1, peaks occur due to the signal and presence of noise. Therefore, CFD distinguishes the noise from the PU signal and can also be used for the detection of weak signal in case of very low SNR. CFD does not require prior knowledge of primary user waveform. The performance of CFD can be improved at a given SNR by increasing the number of samples, however at the cost of sensing time. The limitation of cyclostationary feature detection is that it requires longer processing time compared to the energy detection and matched filter detection techniques [44].

2.1.4 Eigenvalue Based Methods

Eigenvalue method overcomes the noise uncertainty problem and perform spectrum sensing in case the signals to be detected are highly correlated. The method does not require prior knowledge of the primary user signal such as channel, and noise variance. However, the computation complexity of this method is high. Eigenvalue methods are useful when the signals has to be detected in low SNR with fading and time dispersion. The Eigenvalues are determined from the covariance matrix of the received signal. The detection threshold is determined from random matrix theory where the ratio between the maximum Eigenvalue and minimum Eigenvalue is quantized. Since the Eigenvalue method is based on statistical covariance, the detection is robust to noise uncertainty and does not require a priori information of signal, channel, and noise power. Different Eigenvalue based approaches such as Maximum Minimum Eigenvalue (MME) method and Energy Minimum Eigenvalue (EME) method are presented in literature [29], [45]. To reduce the computational complexity, power iteration algorithms are proposed with efficient eigenvalue computation [46], [47], [48].

2.1.5 Wavelet Based Methods

Tian and Giannakis proposed a wavelet based spectrum sensing algorithm [49]. The power spectral density (PSD) of the wideband spectrum was modeled as a train of consecutive frequency subbands, where the PSD is smooth within each subband. However, the PSD exhibits discontinuities and irregularities on the border of two neighboring subbands. Wavelet transforms are capable of detecting these singularities in the signal which allows to identify the discontinuities occurring between users and thereby, detect the spectral edges from PSD [50],[30]. Wavelets provide procedures to analyze and characterize such singularities from the wavelet transform multiscale information. Wavelets are also useful in providing an effective radio sensing architecture to detect spectrum holes in signal spectrum. To improve the performance of wavelet in wideband spectrum sensing, compressive sensing techniques are employed along with the wavelet transforms [51].

2.1.6 Multistage Spectrum Sensing

A variety of multistage spectrum sensing algorithms exist in literature. Multistage spectrum sensing was introduced in IEEE 802.22 [52]. The first multistage algorithm was designed in [53] with energy detection followed by feature detection. A two stage spectrum sensing for dynamic spectrum access in TV applications was proposed in [54] with a coarse resolution sensing followed by a fine resolution sensing. A procedure of multistage orthogonal projection similar to multistage Wiener filter approach is used for wideband spectrum sensing in [55]. Combination of energy detection and maximum minimum eigenvalue based detection is applied for spectrum sensing in [56]. Two stage spectrum sensing was used to maximize the probability of detection given the constraint on the probability of false alarm. A two stage spectrum sensing with energy detection followed by covaiance absolute value detector is presented in [57]. A few multistage filter bank techniques are reported in literature. A multistage coefficient decimation filter bank technique with low complexity is proposed in [58]. For detection of wireless microphones in TV band a multistage DFT filter bank method is proposed in [59]. A tree-structured multistage DFT filter bank based spectrum sensor for estimation of radio channel edge frequencies in military wideband receivers was investigated in [60]. Most

of the multistage spectrum sensing techniques follow sensing from a coarser to finer spectral resolution.

2.2 Wideband Spectrum Sensing

An important challenge in CRs is the sensing of multiple narrowband channels over a wideband spectrum. Most of the existing spectrum sensing algorithms discussed above are suitable for narrowband spectrum sensing, which exploits the spectral opportunities over narrow frequency range. To achieve higher throughput, CR needs to exploit spectral opportunities over a wide range of frequencies, from hundreds of megahertz to several gigahertz [8]. In cases where spectral opportunities are to be identified in Ultra-High-Frequency (UHF) TV band (between 300 MHz to 3 GHz), wideband spectrum sensing techniques are to be employed. Narrowband spectrum sensing techniques cannot be applied in this scenario as they can make only binary decision on the whole spectrum and the spectral opportunities within the wideband cannot be identified. The benefits of multichannel/wideband spectrum sensing for CR networks are discussed in detail in [61]. In order to maximize the secondary user throughput capacity and reduce interference of primary users, multiband joint detection techniques are proposed in [62], [63]. The multiband spectrum sensing has a few challenges due to the following reasons as discussed in [64]

1. The available wideband for spectrum sensing may not be contiguous.
2. A small portion of bandwidth may be occupied by a wireless device and the entire bandwidth may be considered unavailable. (For example, in IEEE 802.22 , wireless microphone occupies only 200 kHz of a 6 MHz TV channel and the entire TV channel would be considered occupied).
3. If a portion of signal is in deep fade, the subbands may consider that portion as a spectral hole. Therefore, if a secondary user is allocated to that portion of the spectrum, interference would occur with the existing primary user.

The multiband spectrum sensing is categorized into serial based detectors, parallel based detectors, and wideband based detectors. Serial sensing is simple to implement,

however, the technique is slow and undesirable when the subbands are more. Parallel sensing provides faster detection at the expense of RF components and complex signal processing. The common multiband sensing techniques uses reconfigurable bandpass filters, tunable oscillators, filter banks, wavelets, and blind sensing. A comparison between the different multiband spectrum sensing methods is provided in [64]. A detailed review and comparison between the different spectrum sensing methods along with advantages, disadvantages, and challenges are also provided in [8]. The implementation challenges in wideband spectrum sensing is summarized below:

1. Reduction in sampling rate to reduce power consumption
2. Development of practically feasible spectrum sensing models
3. Improvement in the robustness of spectrum sensing
4. Relaxation in the synchronization requirements

Further, wideband spectrum sensing techniques are broadly classified into two types,

1. Nyquist wideband SS
2. Sub-Nyquist wideband SS

In Nyquist wideband spectrum sensing, digital signals are sampled at or above the Nyquist rate and in sub-Nyquist technique the signals are sampled below the Nyquist rate. The wideband spectrum sensing techniques are briefly discussed Section 2.2.1 and Section 2.2.2.

2.2.1 Nyquist Wideband Spectrum Sensing

Standard Analog-to-Digital Converters (ADC) and digital signal processing techniques are used in Nyquist wideband spectrum sensing. After the received signals are sampled, serial to parallel conversions are required for further processing of the signals. In filter bank based techniques, Fast Fourirer Transform (FFT) is used to convert the signal to a series of narrowband spectra. The spectral opportunities were identified by applying the binary hypothesis test to the individual subbands. In most of the filter bank techniques,

energy detection was chosen as the test statistic. The threshold for detection was jointly chosen using optimization techniques. Some techniques reported in literature include multiband joint detection algorithm for sensing multiple frequency bands, FFT based filterbank techniques, and wavelet based methods [63], [65], [49]. In wavelet based method, Power Spectral Density (PSD) is used to identify the spectral opportunities depending on the discontinuities present in the border of two adjacent subbands. Wavelet based methods are also useful in edge detection problem to find the spectral boundaries of primary user signals as they can locate the singularities of the wideband PSD.

The signal sampling in wideband should follow Shannon's theorem: the sampling rate must be at least twice the maximum frequency present in the signal (Nyquist rate), in order to avoid spectral aliasing. As standard ADC at or above Nyquist rate are required for sampling, this becomes unaffordable for next generation wireless networks. Therefore, sampling of wideband signals presents significant challenges on designing hardware that operate at sufficiently high rate and the design of high speed signal processing algorithm. To overcome this limitation, tunable Local Oscillators (LO) or Bandpass Filters (BPF) are utilized with superheterodyne technique that sweeps across the frequency of interest. The LO mixes with the wideband signal and down convert the spectrum to lower frequency. The down converted signals are bandpass filtered such that narrowband spectrum sensing techniques can be applied. Techniques using tunable LO are also limited as they are slow and inflexible [8]. The requirement of high sampling rate and high speed signal processing algorithms are the limitations of Nyquist wideband spectrum sensing. The implementation of hardware for high rate ADC with high resolution and reasonable power consumption is also difficult. These problems can be mitigated to some extent using filter bank techniques [65]. In case of filter banks, the baseband can be directly estimated from a prototype filter and other bands are obtained by modulating the prototype filter. The subbands in the filter bank are the corresponding portion of the spectrum in the wideband signal down-converted to basesband and lowpass filtered. Therefore, filter banks can capture the dynamic nature of wideband spectrum by using low sampling rates. Unfortunately, filter banks require a large number of RF components due to the parallel structure [8]. The filter bank spectrum sensing is discussed in detail in Section 2.3.

2.2.2 Sub-Nyquist Wideband Spectrum Sensing

The sub-Nyquist approach overcome the limitations of Nyquist approach resulting from high sampling rate and computation complexity [66]. In sub-Nyquist sensing, the wideband signal are acquired by using sampling rates lower than Nyquist rate. The sampled signals are reconstructed from partial measurement in sub-Nyquist sampling. The spectral opportunities of the wideband spectrum are detected using the reconstructed signal. Two types of sub-Nyquist approaches are reported in literature: (i) compressive sensing technique and (ii) multichannel sub-Nyquist wideband spectrum sensing. The sparseness of sensing environment is exploited in sub-Nyguist rate sampling. The sub-Nyquist wideband spectrum sensing is performed under the assumption that the sensing environment has low percentage of spectrum occupancy by active radios. The limitation of compressive sensing is the dependence of the technique on two principles, i.e., sparsity of the signal and incoherence which pertains to sensing modality. A compressive sensing technique is proposed for wideband spectrum by modeling the spectrum as sparse with wavelet and PSD estimation [67]. A joint sparsity model along with compressive sensing is proposed in [68]. For spectrum sensing with noise uncertainty, a cyclic feature detection based compressive sensing was proposed in [69] and a distributed compressive sensing for cooperative multihop cognitive radio networks was proposed in [70]. Different multichannel sub-Nyquist wideband spectrum sensing using blind spectrum sensing and non-uniform sampling are discussed in [71], [72].

2.3 Filter Bank Techniques for Spectrum Sensing

The concept of Filter bank was proposed for spectrum sensing initially by Farhang-Boroujeny [65]. Filter banks are implemented by shifting a lowpass prototype filter. The first subband is estimated using the prototype filter and other subbands are obtained by modulating the prototype filter. The total bandwidth is split into narrow non-overlapping subbands using multiple bandpass filters, i.e., filter banks. Multicarrier techniques were also suggested for spectrum sensing, where OFDM was the first multicarrier technique proposed for CR [73], [74]. OFDM was considered as a suitable candidate for CR as FFT can be used for spectral analysis and demodulator for OFDM signal. However, the limitation of using the OFDM for CR application is the presence

of large sidelobes in the response of the filters due to 13 dB attenuation of FFT, which may lead to interference between different users because of the spectral leakage [75]. Moreover, OFDM techniques lack high spectral dynamic range and are not suitable for detection of low power primary users. To overcome this issue, the rectangular pulse shape in OFDM was replaced with a smooth edge pulse shape filters called filtered OFDM. Filter Bank Multicarrier (FBMC) and filtered OFDM become alternate solutions to overcome the above limitations. FBMC reduces the spectrum leakage compared to cyclic prefixed OFDM systems and is capable of identifying multiple user with different center frequencies and spectral gaps between users efficiently with flexibility [76]. Different FBMC schemes reported in literature include Staggered Modulated Multitone (SMT), Filtered Multitone (FMT), and Cosine Modulated Multitone (CMT) [77]. A comparison of filter bank multicarrier methods in cognitive radio systems is presented in [78].

The spectrum efficiency can be increased by designing prototype filters with acceptable subband attenuation. Therefore, filter banks are considered to be an alternate solution for wideband spectrum sensing. Moreover, the energy can be computed at the output of subbands and compared with a predetermined threshold to determine the presence of primary users. To achieve high spectral dynamic range in filter banks, the length of the prototype filter also needs to be adjusted. Multi-Taper Method (MTM) is shown as a near optimal sensing method, even though its computational complexity is very high [3], [79]. However, similar performance can be achieved with filter banks using prolate filters with lower computational complexity [65]. Discrete Fourier Transform (DFT) and modified DFT filter bank with root-Nyquist filter have also been exploited for spectrum sensing in wideband cognitive radio [76].

Multistage filter bank techniques were proposed for the detection of center frequency of primary users with low computational complexity and higher precision using DFT based filter bank [80]. Polyphase DFT filter banks are applied for multichannel spectrum sensing for opportunistic CR due to its efficient implementation [81]. FFT and filter bank techniques have been used for sensing Wireless Local Area Networks (WLAN) such as OFDM based on IEEE 802.11 system and Wireless Personal Area Network (WPAN) with Bluetooth designated to operate on 2.4 GHz ISM band [82], [83]. Multi-resolution filter banks based on fast filter bank design with varying spectral bands for spectrum sensing in military radio receivers were proposed in [20]. Tree structured

DFT filter bank were proposed for estimating the center frequencies and spectral edges of primary user signals [60]. Filter bank was proposed for the detection of wireless microphones in IEEE 802.22 Wireless Regional Area Network (WRAN) and estimation of center frequency [59]. Progressive Decimation Filter Bank technique (PDFB) using variable sensing resolutions to detect different bandwidths are proposed in [84]. A theoretical framework for the analysis and design of filter bank based detectors for spectrum sensing applications in cognitive radios are discussed in detail in [76].

2.3.1 Sensing Architecture Based on Filter Banks

Filter banks consist of an Analysis Filter Bank (AFB) and Synthesis Filter Bank (SFB). Synthesis filter banks are sufficient to extract the signal components of each subband from the wideband RF signals. The basic filter bank spectrum sensing is illustrated in Figure 2.1 The RF module is followed by wideband ADC to sample the RF signal. Different filter bank structures like Cosine Modulated Filter Bank (CMFB), DFT, and Polyphase DFT can be considered. In case of complex modulated filter banks, the complete filter bank structure can be realized using complex modulation of a single prototype filter. A detailed discussion on the design of prototype filters is presented in Chapter 3.

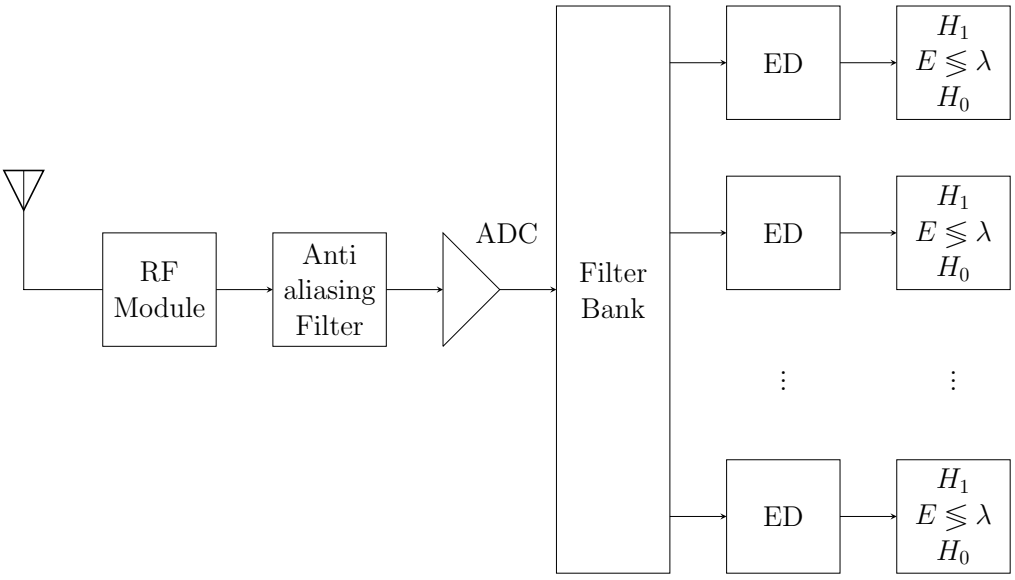

Figure 2.1: Sensing architecture based on filter banks

In general, multi-band sensing utilizes energy detection techniques. Different methods such as periodogram method, Multi-Taper Method (MTM), and filter bank meth-

ods have investigated energy detection for spectrum sensing in literature. Farhang has shown in [65] that DFT filter banks based on energy detection are more promising in terms of accuracy if noise variance are known. Energy detection is the most common method as it has low computational and implementational complexity. Energy (power) is computed at the output of individual subbands and considered as the test statistic. The presence and absence of the signal is detected by comparing the energy with a predefined threshold as explained in Section 2.1.1. The threshold is a function of probability of false alarm and noise variance of the channel.

Summary

In this chapter an exhaustive literature survey of spectrum sensing methods is provided. The classification of wideband spectrum sensing methods is discussed with special emphasis on filter bank spectrum sensing in cognitive radios relevant to the scope of the thesis. Chapter 3 discusses a prototype filter design for the filter bank implementation.

CHAPTER 3

Protoype Filter Design for Filter Banks

The design of filter banks, transmultiplexers (TMUX) and Filter Bank Multicarriers (FBMC) concentrate on the prototype filter design. Since the filter banks are generated from the modulation of a single prototype filter. The design of prototype filter plays a vital role in the overall performance of the filter bank structures. The distinctive feature of FBMC is its ability to provide improved frequency selectivity using well shaped prototype filters.

In this chapter we develop a prototype filter design using an iterative algorithm. Section 3.1 provides a survey of existing prototype filter design schemes and its significance in designing filter banks, FBMC, and TMUX structures. The conditions to be satisfied by the prototype filter for Near Perfect Reconstruction (NPR) in filter banks is explained in Section 3.2. Different filter banks implemented using complex modulation of a prototype filter is discussed in Section 3.3. Various errors that occur in filter banks and possible ways of mitigating them using prototype filters are detailed in Section 3.4. The proposed prototype filter design is explained in Section 3.5. The simulation results and comparison with existing methods are discussed in Section 3.6.

3.1 Prototype Design Schemes

The multichannel filter banks can be implemented using cosine modulation, Fast Fourier Transfor (FFT), Discrete Fourier Transform (DFT) or Modified DFT filter banks [1], [85]. The filter banks are implemented using complex modulation of a single prototype filter [86]. The analysis and synthesis subbands of the filter bank are simultaneously generated by applying an appropriate modulation scheme to the linear phase Finite Impulse Response (FIR) prototype filter. Current research aims at designing an optimal lowpass prototype filter for filter bank implementation. The significance of prototype filter design in the implementation of filter banks to improve the overall performance is well proven.

Filter Bank Multicarriers (FBMC) derived from a prototype filter has attracted recent attention due to its advantages over Orthogonal Frequency Division Multiplexing (OFDM) [73]. FBMC can provide high subband attenuation and does not require cyclic prefix as compared to OFDM. The OFDM is considered to have rectangular prototype filters from the perspective of filter banks due to the IFFT/FFT blocks. Therefore, the resulting subbands are not frequency selective and have only 13 dB attenuation. Alternative techniques such as cosine modulated multitone (CMT), filtered multitone (FMT), modified DFT (MDFT), and exponentially modulated filter banks (EMFB) are used in multicarrier modulation. Filter bank based transmultiplexers with analysis and synthesis filters derived from a prototype filter are also utilized in FBMC. The performance parameters of an FBMC system such as stopband attenuation, intersymbol interference (ISI), and interchannel interference (ICI) depend on the design of prototype filter. Therefore, the design of prototype filter is vital in the implementation of filter banks structures. The dual of the filter banks are transmultiplexers and TMUX forms the core system of FBMC.

In general, filter bank designs can be categorized into two types:

1. Perfect Reconstruction (PR)
2. Near Perfect Reconstruction (NPR) or Quadrature Mirror Filters (QMF)

Perfect reconstruction filters are alias free filters, where the output is a delayed version of input. However, the implementation of PR filters are computationally complex and for practical applications, NPR filters are adequate. The filter bank implementation focuses on NPR as they provide improved alias suppression in the subbands by relaxing PR constraint. As the same prototype filter is employed in the analysis and synthesis banks, the NPR filters have polyphase matrices which are paraunitary and, hence, have favorable numerical properties.

Extensive research has been carried out to find an optimal prototype filter for complex modulated filter banks. The optimization techniques for prototype filter design are categorized into threes types: (i) frequency sampling techniques, (ii) window based techniques and (iii) direct optimization of filter coefficients [87]. Frequency sampling techniques for prototype filter design have been proposed in [88] and [89]. The samples in the transition band are optimized using frequency sampling in [90]. Window based

prototype filter designs for transmultiplexers are proposed in [91].

Creusere and Mitra [92] have designed a prototype filter by optimizing the pass-band frequency with fixed filter length and relative error weighting. A Kaiser window approach was used by Lin and Vaidyanathan in [93] to optimize the cut-off frequency and different window based techniques with iterative algorithms are used in [94]. An investigation on perfect reconstruction filters [95] and Inter Symbol Interference (ISI) free filter banks are presented in [87], [96]. Linear optimization techniques are used in [97], and [98] to optimize the 3 dB cut-off frequency with least square method. However, in most of the existing methods, a fixed filter order and an arbitrary step size are considered for the design of prototype filters.

Other approaches include second order cone programming [99], [100] and filter designs based on gradient information [101], [102]. A prototype filter design with optimization to minimize stopband energy with NPR constraint for filter bank multicarrier modulation is proposed in [103]. The direct optimization of filter coefficients are often nonconvex and are highly nonlinear. The filter design is sensitive to the initial values and has high computational complexity. The global optimal is also not guaranteed as the solution can be trapped in local minimum [87], [104]. Prototype filters have been designed for cognitive radio systems through direct optimization of filter coefficients in [104]. A near perfect reconstruction filter bank with prototype filter having an approximate cosine-rolloff at the transition band with convex minimax optimization is solved using second order cone programming in [105].

3.2 Near Perfect Reconstruction

Perfect Reconstruction (PR) filter banks satisfy the condition that the reconstructed signal $\hat{x}(n)$ need to be a scaled and delayed version of the input $x(n)$.

$$\hat{x}(n) = cx(n - n_0) \tag{3.1}$$

The reconstructed signal can be represented using z-transform as

$$\hat{X}(z) = T(z)X(z) \tag{3.2}$$

The PR condition indicates that aliasing is canceled and distortion function $T(z)$ is forced to be a delay. The optimization of the prototype coefficients for perfect reconstruction is highly nonlinear. In case of NPR or approximate reconstruction, the analysis and synthesis filters $H_k(z)$ and $F_k(z)$ respectively, are chosen in such a way that the adjacent subband aliasing gets cancelled. The distortion function $T(z)$ is approximately a delay. The approximate systems mentioned are called pseudo Quadrature Mirror Filter (QMF) banks and are acceptable for practical applications. For near perfect reconstruction, the lowpass prototype filters have to satisfy the following conditions [92]:

1. Prototype filter has to be band-limited

$$\left|H(e^{j\omega})\right| \approx 0, |\omega| > \frac{\pi}{M} \tag{3.3}$$

2. Frequency response of prototype filter has to be pairwise power complementary

$$\left|H(e^{j\omega})\right|^2 + \left|H(e^{j(\frac{\pi}{M}-\omega)})\right|^2 \approx 1, 0 \leq \omega \leq \frac{\pi}{M} \tag{3.4}$$

3.3 Filter Bank Using Prototype Filters

In order to overcome the limitation of having M different transfer functions, which provide perfect reconstruction, the complex modulated filter banks are realized from a single lowpass prototype filter. Filter bank based on DFT, cosine modulation, DFT based polyphase filter banks, and modified DFT are examples of M analysis filters derived from a single prototype filter. The complex modulated filter banks generally use the basic pseudo quadrature mirror filter principle. The filter banks are realized by equidistant frequency shifts of a prototype filter. The transfer function of adjacent subband filters have to be power complementary as in Equation 3.4. The advantages of such filters are twofold:

1. The cost of implementing an M analysis filter bank include the cost of one prototype filter and modulation overhead. The cost of an M synthesis filter is similar to an analysis filter.

2. Optimization of prototype filter alone is required for the implementation of filter bank structure.

The prototype filters should have sufficient stopband attenuation to suppress the aliasing components. The realization of DFT, cosine modulation, and DFT based polyphase filter banks are discussed in the following subsections.

3.3.1 DFT Filter Banks

The M analysis filters $H_k(z)$, $k = 0, \ldots, M-1$, are realized using frequency shifting the transfer function $H(z)$ of the prototype filter $h(n)$. The impulse response of the prototype filter is multiplied by a factor $e^{jn\Omega_0}$. Further, the frequency response of the prototype filter $H(e^{j\Omega})$ is shifted right by Ω_0 as $H(e^{j(\Omega-\Omega_0)})$. The M analysis filter response can be expressed as in [86]

$$H_i(e^{j\Omega}) = H(e^{(j\Omega-2\pi i/M)}), i = 1, 2, \ldots, M-1. \tag{3.5}$$

In case, $W_M = e^{-j2\pi/M}$, the Z-transform of the analysis filters can be written as

$$H_i(z) = H(zW_M^i) \tag{3.6}$$

The frequency response of the prototype filter and the shifted versions of the prototype filter for the generation of subbandss filter are shown in Figure 3.1 and 3.2 respectively.

Figure 3.1: Frequency response of prototype filter

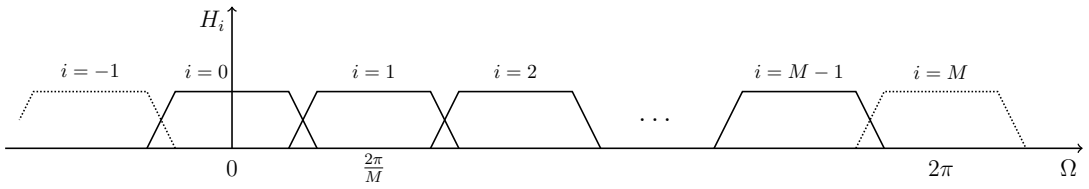

Figure 3.2: Frequency shifted versions of the prototype filter for analysis filter banks

3.3.2 Cosine Modulated Filter Bank

The Cosine Modulated Filter Banks (CMFB) are also pseudo QMF and satisfy the NPR conditions. Cosine modulated filters can easily maintain maximally decimated NPR conditions. Among the NPR FIR filter banks, CMFB is considered to be simple both in terms of design and implementation complexities. Initially, the prototype filter is designed satisfying the power complementary and band-limiting conditions specified in Equation 3.3 and 3.4. In an M channel CMFB, the impulse responses of the analysis and synthesis filters are $h_k(n)$ and $f_k(n)$ respectively. The filter banks are cosine modulated versions of the prototype filter $h(n)$ and are given by the Equation 3.7 and 3.8 for $0 \leq n \leq N-1$ and $0 \leq k \leq M-1$. The closed form expressions for analysis and synthesis filters are given in [1] as

$$h_k(n) = 2h(n)cos\left(\frac{\pi}{M}\left(k+\frac{1}{2}\right)\left(n-\frac{N-1}{2}\right)+(-1)^k\frac{\pi}{4}\right) \tag{3.7}$$

$$f_k(n) = 2h(n)cos\left(\frac{\pi}{M}\left(k+\frac{1}{2}\right)\left(n-\frac{N-1}{2}\right)-(-1)^k\frac{\pi}{4}\right) \tag{3.8}$$

The entire design of the cosine modulated filter bank is reduced to proper design of prototype filter. Therefore, the design of filter bank requires to optimize the prototype filter coefficients to reduce the complexity and computational overhead. The prototype filter has to be lowpass with linear phase and satisfy the conditions stated in Equation 3.3 and Equation 3.4 for near perfect reconstruction. The aliasing error can be cancelled when the condition in Equation 3.3 is satisfied. In case Equation 3.4 is satisfied the amplitude distortions are eliminated. By designing prototype filters with linear phase FIR the phase distortion can be eliminated completely. Therefore, the common

errors that occur in filter banks such as aliasing error, amplitude distortion and phase distortion can be eliminated.

3.3.3 Polyphase Filter Banks

The DFT filters can be modified to get a better stopband attenuation compared to 13 dB of DFT at the cost of one prototype filter. The polyphase implementation of uniform DFT reduces the computational complexity. The polyphase decomposition of the prototype filter is given in [81], and [1]. The transfer function of a FIR prototype filter $h(n)$ is given in Equation 3.9 as.

$$H(z) = \sum_{n=-\infty}^{\infty} h(n)z^{-n} \tag{3.9}$$

The transfer function in Equation 3.9 can be decomposed into polyphase components as in Equation 3.10.

$$\begin{aligned} H(z) = \sum_{n=-\infty}^{\infty} h(nM)z^{-nM} + z^{-1} \sum_{n=-\infty}^{\infty} h(nM+1)z^{-nM} + \ldots \\ + z^{-(M-1)} \sum_{n=-\infty}^{\infty} h(nM+M-1)z^{-nM} \end{aligned} \tag{3.10}$$

Equation 3.10 can be written in short as in Equation 3.11.

$$H(z) = \sum_{l=0}^{M-1} z^{-l} E_l(z^M), l = 0, 1, \ldots, M-1. \tag{3.11}$$

The above equation represents a Type-1 polyphase filter. Similarly, l^{th} polyphase component of the filter bank is defined as

$$E_l(z) = \sum_{n=-\infty}^{\infty} e_l(n)z^{-n}, \tag{3.12}$$

where, $e_l = h(nM+l)$. The Type-2 polyphase decomposition of the Equation 3.10 can be expressed as

$$H(z) = \sum_{l=0}^{M-1} z^{M-1-l} R_l(z^M) \tag{3.13}$$

Polyphase implementation simplifies the theoretical results and computationally efficient filter banks can be realized. Using Noble identities the polyphase uniform DFT filter bank structure with decimators can be drawn as shown in Figure 3.3. Since the downsampler are shifted toward the input side, the polyphase subband filters are computed at a low sampling rate, which reduces the computational complexity by a factor of M. Due to the polyphase decomposition of prototype filter, the polyphase subband filters are shorter compared to the original filters by a factor of M. Therefore, the number of coefficients of the subband filters become equal to that of a single prototype filter [1].

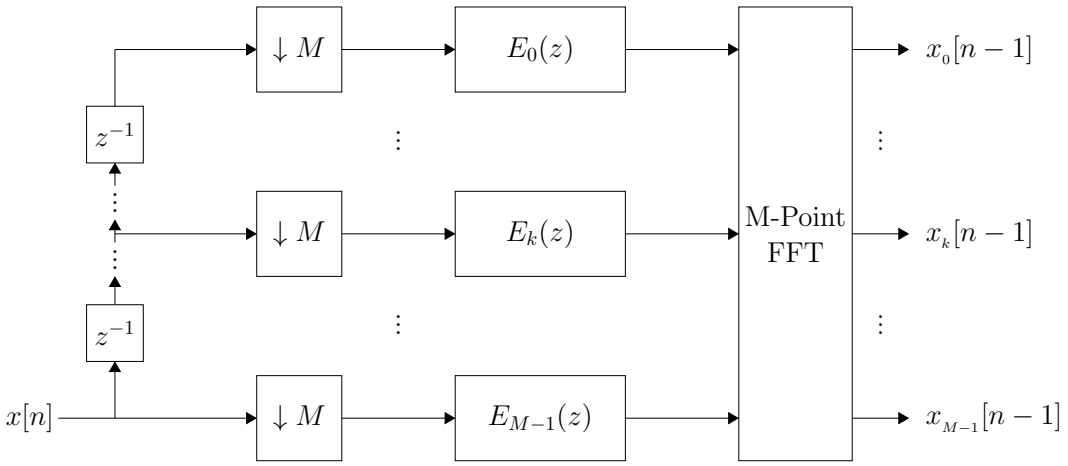

Figure 3.3: Polyphase filter bank structure [1]

3.4 Errors in Filter Banks

Errors in filter banks, occur due to the difference between the reconstructed signal $\hat{x}(n)$ and the input $x(n)$. Errors are generally classified into three types:

1. Aliasing error
2. Amplitude distortion
3. Phase distortion

In practice, the analysis filters have non-zero transmission bandwidth and stopband gain. Therefore, the signals are not bandlimited and their decimations result in aliasing. As a result, the responses of the subbands overlap and the energy in each subband

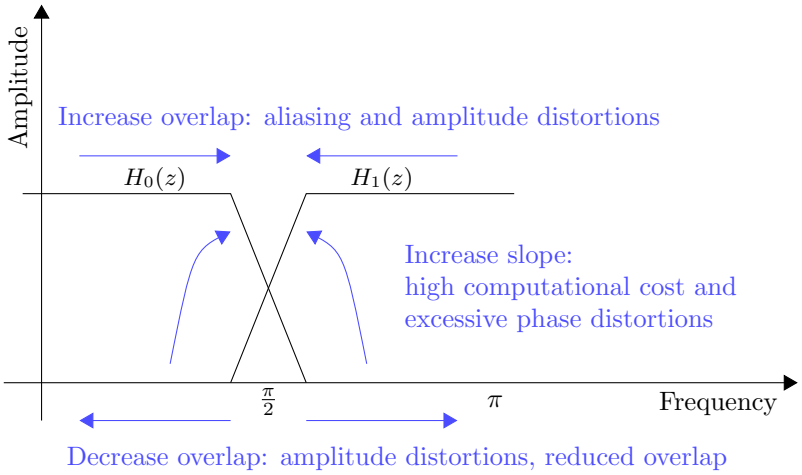

Figure 3.4: Errors in filter banks [1]

exceeds the ideal passband region. Even though the filters provide good stopband attenuation, decimation of the signals results in aliasing. However, having sufficiently large stopband attenuation, the effect of aliasing can be controlled. Implementation of narrow transition width filters is expensive as they increase the length of the prototype filter. Therefore, a feasible choice is to design subband filters with overlapping responses that are able to cancel the effect of aliasing with proper choice of synthesis filters [1].

For example if we consider a two channel filter bank, the reconstructed signal can be written as

$$\hat{X}(z) = \frac{1}{2}[H_0(z)F_0(z) + H_1(z)F_1(z)]X(z) + \frac{1}{2}[H_0(-z)F_0(z) + H_1(-z)F_1(z)]X(-z) \tag{3.14}$$

The second term in Equation 3.14 corresponds to the aliasing error. By proper choice of analysis and synthesis filters the second term can be reduced to zero for eliminating the aliasing error. Thus, the following choice of filters cancels aliasing.

$$F_0(z) = H_1(-z) \tag{3.15}$$

$$F_1(z) = -H_0(-z) \tag{3.16}$$

If the filters are designed satisfying Equation 3.15 and Equation 3.16 then $H_0(-z)F_0(z) + H_1(-z)F_1(z) = 0$. Then the reconstructed signal becomes

$$\hat{X}(z) = T(z)X(z). \tag{3.17}$$

Even though the aliasing error is cancelled the reconstructed signal suffers from linear shift-invariant distortion $T(z)$, which is also called as distortion transfer function.

$$T(z) = \frac{1}{2}[H_0(z)F_0(z) + H_1(z)F_1(z)]X(z) \tag{3.18}$$

If we consider, $T(e^{j\omega}) = |T(e^{j\omega}|e^{j\phi(\omega)}$, then

$$\hat{X}(e^{j\omega}) = |T(e^{j\omega}|e^{j\phi(\omega)}X(e^{j\omega}) \tag{3.19}$$

If $T(z)$ is allpass (i.e., $|T(e^{j\omega})| = d \neq 0$ for all ω), we say that the reconstructed signal $\hat{X}(e^{j\omega})$ suffers from amplitude distortion. Similarly, unless $T(z)$ has linear phase (i.e., $\phi(\omega) = a + b\omega$ for constant a, b), the reconstructed signal $\hat{X}(e^{j\omega})$ suffers from phase distortion [1]. The phase distortion can be completely eliminated by implementing the analysis and synthesis filter with linear phase FIR filters. The amplitude distortion gets reduced, when the band limiting condition stated in Equation 3.3 is satisfied. The prototype filters are implemented with Type-1 linear phase FIR filters. The different types of filters are discussed in detail in Section 3.4.1.

Consider the filter response $H_0(z) = \sum_{n=0}^{N} h_0(n)z^{-n}$, with $h_0(n)$ real. The linear phase constant requires $h_0(n) = \pm h_0(N-n)$. Since $H_0(z)$ has to be lowpass, the only possibility is $h_0(n) = h_0(N-n)$.

$$H_0(e^{j\omega}) = e^{-j\omega N/2}R(\omega), \tag{3.20}$$

where $R(\omega)$ is real for all ω. As long as $|H_0(e^{j\omega})|$ is an even function we can write

$$T(e^{j\omega}) = \frac{e^{jN\omega}}{2}(|H_0(e^{j\omega})|^2 - (-1)^N|H_0(e^{j(\pi-\omega)})|^2) \tag{3.21}$$

In case the length of the filter N is even at $\omega = \frac{\pi}{2}$, the above expression reduces to zero resulting in severe amplitude distortion. Accordingly, N is chosen to be odd such that

$$T(e^{j\omega}) = \frac{e^{jN\omega}}{2}(|H_0(e^{j\omega})|^2 + |H_0(e^{j(\pi-\omega)})|^2) \tag{3.22}$$

$$T(e^{j\omega}) = \frac{e^{jN\omega}}{2}(|H_0(e^{j\omega})|^2 + |H_1(e^{j\omega})|^2) \tag{3.23}$$

3.4.1 Types of FIR Linear Phase Filters

In general, the prototype filters have FIR and are designed to satisfy linear phase property. There exist different design procedures to design FIR transfer function with exact linear phase responses. A digital filter satisfies linear phase property if the phase response $\phi(\omega)$ is linear with ω. Consider, $h(n)$ as a prototype filter with response

$$H(z) = \sum_{n=0}^{N} h(n) z^{-n}. \tag{3.24}$$

The prototype filter has linear phase property only when Equation 3.25 is satisfied.

$$H(e^{j\omega}) = ce^{-jK\omega} H_R(\omega), \tag{3.25}$$

where, c is a complex constant, K is real, and $H_R(\omega)$ is a real valued function of ω. $H_R(\omega)$ is called the amplitude response or zero phase response. The response of filter can be symmetric or anti-symmetric.

$$Symmetric : h(n) = h(N-n), n = 0, 1, \ldots, N$$
$$Antisymmetric : h(n) = -h(N-n), n = 0, 1, \ldots, N$$

Depending on the length of filter N (even or odd) and whether $h(n)$ is symmetric or anti-symmetric, there are four types of real coefficient linear phase filters.

Table 3.1: Four types of real coefficient linear phase FIR filters [1]

Type	**1**	**2**	**3**	**4**
Symmetry	$h(n) = h(N-n)$	$h(n) = h(N-n)$	$h(n) = -h(N-n)$	$h(n) = -h(N-n)$
Filter Length N	N even	N odd	N even	N odd
Frequency Response	$e^{j\omega\frac{N}{2}} H_R(\omega)$	$e^{-j\omega\frac{N}{2}} H_R(\omega)$	$je^{-j\omega\frac{N}{2}} H_R(\omega)$	$je^{-j\omega\frac{N}{2}} H_R(\omega)$

The Type-3 and Type-4 filters are anti-symmetric and are not used for lowpass filter design. Type-2 is not suitable for high pass filter design. Therefore, the prototype filters are designed using Type-1 FIR filters.

3.5 Design Approach of Proposed Prototype Filter

Literature survey reveals that researchers have worked out several efficient algorithms for the design of lowpass prototype filters in filter banks. However, most of the methods start with an arbitrary fixed filter length and are optimized to get the NPR condition by varying the 3 dB cut-off frequency or passband frequency with an arbitrary step size. It is found that no systematic procedure is followed in determining the step size. Also, it is shown that the step size plays a significant role in achieving minimum amplitude distortion and aliasing error. The proposed algorithm varies the step size from a coarser to finer level with a primary objective of minimum amplitude distortion and aliasing error for CMFB.

Our scheme uses step size as a function of the transition width, which is a function of the number of subbands M. Filter bank follows the NPR condition of the prototype filter by controlling the magnitude response of the lowpass prototype filter at $\pi/2M$ close to $1/\sqrt{2}$

$$|H(e^{(j\omega)}| = \frac{1}{\sqrt{2}} \tag{3.26}$$

The following objective function approximates the 3 dB cut-off frequency very close to the ideal filter

$$\phi = ||H(e^{j\pi/2M})| - \frac{1}{\sqrt{2}}| \tag{3.27}$$

At the initial step, the cut-off frequency is calculated using the relation $\omega_c = \frac{\pi}{2M}$. The passband can be approximated as $\omega_p \approx \omega_c = \frac{\pi}{2M}$ and stopband, $\omega_s = \frac{\pi}{M}$. Thus, the approximate transition width $\omega_s - \omega_p$ is achieved from the number of subbands M as

$$\Delta\omega = \frac{\pi}{2M} \tag{3.28}$$

The filter length N can be obtained from the given attenuation A_s (in dB) and number of subbands M as

$$N = \frac{(A_s - 7.95)M}{14.36\Delta\omega/2\pi}. \tag{3.29}$$

For a fixed prototype filter length, the transition width can be computed using the Kaiser widow approach as

$$\Delta\omega = \frac{A_s - 7.95}{2.285N} \tag{3.30}$$

Further, we use step size chosen as a fraction of the transition width for the proposed iterative prototype filter design algorithm. Hence, by choosing the step size as a function of transition width and varying the step size from coarser to finer level, the minimum amplitude distortion and aliasing error can be achieved. The proposed filter is designed using two input parameters: number of subbands M and attenuation A and all other system parameters are derived from it to avoid heuristic inputs.

3.5.1 Design Procedure

The systematic procedure followed for design of prototype filter is summarized as shown in Algorithm 1. The primary goal is to design a prototype filter with enhanced performance i.e., minimum amplitude distortion and aliasing error. The proposed algorithm approximates 3 dB cut-off frequency very close to $\frac{\pi}{2M}$.

Check for Transition Point

The step size is varied from a coarser to a finer level to get the transition point, where the filter provides minimum amplitude distortion and aliasing error. Most of the existing methods in literature utilized fixed step size for the design of prototype filters. Hence, there is no mechanism to find the minimum distortion unless the step size is chosen appropriately. On the other hand in our method, the step size is varied from a coarser to a finer level in order to systematically arrive at a minimum amplitude distortion and aliasing error. Therefore, our algorithm becomes structured and does not require any heuristic input.

The relation between input signal $X(z)$ and reconstructed signal $\hat{X}(z)$ is given by

$$\hat{X}(e^{j\omega}) = T_0(e^{j\omega})X(e^{j\omega}) + \sum_{l=1}^{M-1} T_l(e^{j\omega})X(e^{j\omega - 2\pi l/M}), \tag{3.31}$$

Algorithm 1 Prototype filter design

Number of subbands M , Attenuation A in dB and Window function $W(n)$.

Step 1 Calculate:

(i) The 3 dB cut-off frequency: $\omega_c = \dfrac{\pi}{2M}$

(ii) Transition width: $\Delta\omega = \dfrac{\pi}{2M}$, Let step size, $\delta = f(\Delta\omega)$ [A fraction of the transition width $\Delta\omega$.]

(iii) Initialize: error threshold;

Step 2 (a) : Step size $\delta_j = \dfrac{\Delta\omega}{l_j}$. where, $l_j = k_1 + (j-1)k$; $j = 1, 2, \ldots, m$; k_1 is the initial value and k step increment.

Note: Iteration must start with coarser step size and move to finer step size which implies $l_{j+1} > l_j$ and $\delta_{j+1} < \delta_j$.

Step 2 (b): Iteration count for ω_c updation $i = 1 : count$;

Step 3: Calculate: $h(n)$- the lowpass prototype filter of length $N+1$, where $W(n)$ is the window function:

$$h(n) = \frac{sin\left(n - \dfrac{N}{2}\right)\omega_c}{\pi\left(n - \dfrac{N}{2}\right)} W(n).$$

Step 4: Calculate objective function, i.e., magnitude response at 3 dB $\phi = \mid\mid H\left(\dfrac{\pi}{2M}\right) \mid - \dfrac{1}{\sqrt{2}} \mid$

$Cond - a : \phi >$ error threshold

$Cond - b : \phi \leq$ error threshold

$Cond - a_1$: $\phi(i+1)^{th}$ iteration $\leq \phi(i)^{th}$ iteration

$Cond - a_2 : \phi(i+1)^{th}$ iteration $> \phi(i)^{th}$ iteration

Step 5:

if $Cond - a$ **then**

Go to **Step 5 (a)**

else

Go to **Step 6**

Step 5 (a):

if $Cond - a_1$ **then** $\omega_c = \omega_c + \delta_j; i = i + 1$ goto **Step 3**, until $i \leq count$, [if $i > count$ Go to **Step 2 (a)**]

else

if $Cond - a_2$ **then** Go to **Step 2 (a)** to update step size δ_j .

end if

end if

Step 6: $Cond - b$ is satisfied, check for transition point with amplitude distortion/aliasing error.

if error with step size $\delta_{j+1} \leq$ error with step size δ_j **then**

Go to **Step 2 (a)** to update the step size

else

Go to **Step 7**.

end if

end if

Step 7: Terminate; $h(n)$ with step size δ_j is the final prototype filter.

where, $|T_0(e^{j\omega})|$ refers to the amplitude distortion and $|T_l(e^{j\omega})|$ the aliasing error. The performance of the prototype filter is evaluated by calculating the maximum amplitude distortion R_p and the maximum aliasing error ε_a. The maximum amplitude distortion R_p is computed as

$$R_p = \max(1 - |T_0(e^{j\omega})|). \tag{3.32}$$

Similarly, maximum aliasing error ε_a is calculated as

$$\varepsilon_a = \max\left(T_l\left(e^{j\omega}\right)\right), 1 \leq l \leq M-1, \tag{3.33}$$

where, $T_l(e^{j\omega}) = \frac{1}{M}\sum_{k=0}^{M-1} F_k(e^{j\omega}) H_k\left(e^{j\omega - \frac{2\pi l}{M}}\right)$.

3.6 Simulation Results

The prototype filter designed using the proposed algorithm have been analyzed using the cosine modulated filter bank. The designed prototype is compared with some of the existing methods in literature in terms of amplitude distortion and aliasing error. The performance of the prototype filter was analyzed for different number of subbands in the filter bank. The effect of fixed filter length and the filter length calculated using Equation 3.29 are also evaluated in the prototype filter design.

The designed prototype filters were compared with existing method by choosing the filter parameters: filter length $N = 439$, number of subbands $M = 32$ and stopband attenuation of 100 dB in Table 3.2. The frequency response of the proposed prototype filter for $M = 32$, filter length $N = 439$ and stopband attenuation of 100 dB is shown in Figure 3.5. From Table 3.2 it can be inferred that the proposed method provides better performance in terms of amplitude distortion and aliasing error.

The performance of the filter bank for different subband resolutions ($M = 8, 16, 32,$ and 64) with fixed filter length $N = 439$ and stopband attenuation of 100 dB is shown in Table 3.3. The amplitude distortion increased as the number subbands increased in case of fixed filter length. A comparison in performance of prototype filter for different subband resolution with filter length using Equation 3.29 is given in Table 3.4. When filter

Table 3.2: Comparison with existing methods for $M = 32$

Algorithm	**Filter Length** N	**Amplitude Distortion** R_p	**Aliasing Error** ε_a
Creusere et al.	439	1.80×10^{-3}	1.96×10^{-6}
Lin et al.	467	2.42×10^{-3}	2.76×10^{-7}
Cruz et al.	439	3.06×10^{-3}	1.85×10^{-7}
Kumar et al.	448	1.50×10^{-3}	9.45×10^{-7}
Bergen et al.	440	3.42×10^{-3}	2.60×10^{-7}
Bergen et al.	512	1.01×10^{-3}	5.66×10^{-7}
Proposed Method	439	1.0954×10^{-4}	3.041×10^{-8}

length was evaluated for different number of subbands the variation in amplitude distortion was minimal. However, the filter length increased with increase in number of subbands. The effect of variation in filter length with increase in subband filters can be observed from Table 3.4.

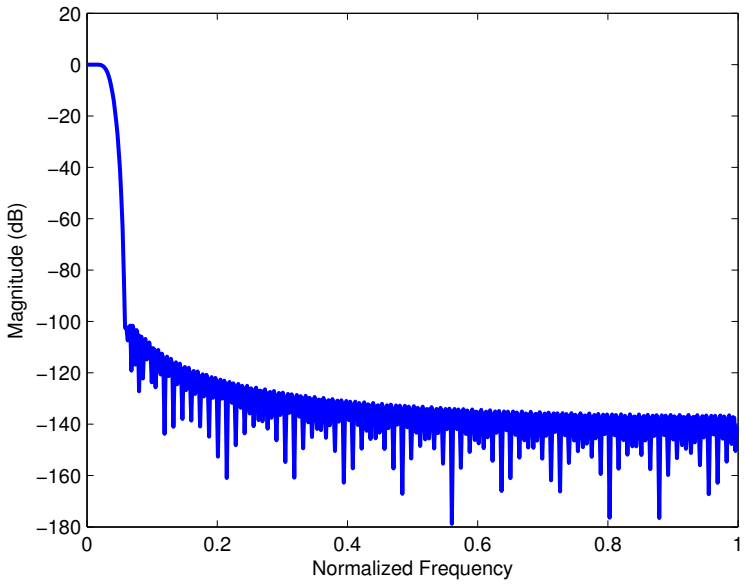

Figure 3.5: Prototype filter for $M = 32$ with filter length $N = 439$ and stopband attenuation of 100 dB

Table 3.3: Performance of the proposed prototype filter with different number of subbands M for a filter length of 439.

Subbands M	**Amplitude Distortion** R_p	**Aliasing Error** ε_a
64	2.449×10^{-4}	8.994×10^{-8}
32	1.0954×10^{-4}	3.041×10^{-8}
16	1.1051×10^{-4}	2.164×10^{-7}
8	1.0126×10^{-4}	2.128×10^{-7}

Table 3.4: Performance of prototye filter with different subbands and filter length N evaluated using Kaiser Window

Subbands M	**Filter Length** N	**Amplitude Distortion** R_p	**Aliasing Error** ε_a
64	819	1.2106×10^{-4}	5.11×10^{-8}
32	409	1.2106×10^{-4}	1.45×10^{-7}
16	205	1.2108×10^{-4}	3.92×10^{-7}
8	101	1.1747×10^{-4}	1.20×10^{-6}

3.6.1 Impact of Variable Step Size on Filter Performance

The effect of varying the step size as a function of transition width from a coarser to a finer level in the design of prototype filter is shown through simulations. A prototype filter was designed for a filter length $N = 439$, subband attenuation of 100 dB and number of subbands $M = 32$. The performance in amplitude distortion for variable step sizes $(4.55 \times 10^{-4}, 9.2 \times 10^{-4}, \text{ and } 1.84 \times 10^{-3})$ with iterations $6, 11, \text{ and } 19$ is shown in Figure 3.6. The step size is varied when the error conditions are not satisfied and thereby, the algorithm becomes computationally efficient and self controlled. From Figure 3.6, it is apparent that the minimum distortion is at the transition point.

Figure 3.7 shows the variation of step size for different subband resolution in terms of amplitude distortion. From Figure 3.7 it is apparent that there is a transition point, i.e., the amplitude distortions are minimum at a particular step size. Similarly, the different transition points for variable filter length N and the number of subbands M are shown for aliasing error in Figure 3.8. Therefore, proper selection of step size is essential to achieve minimum amplitude distortion and aliasing error for different number of subbands M.

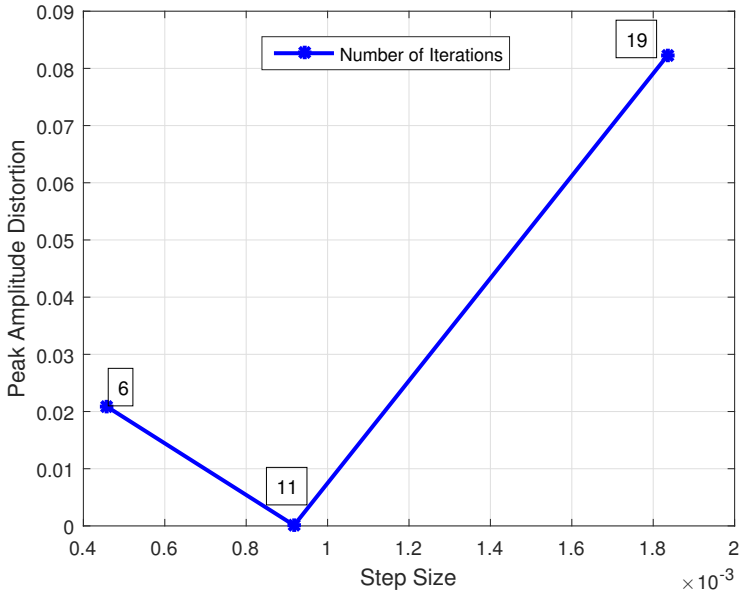

Figure 3.6: Effect of step size on amplitude distortion of the proposed method for subband $M = 32$, filter length $N = 439$, and stopband attenuation of 100 dB

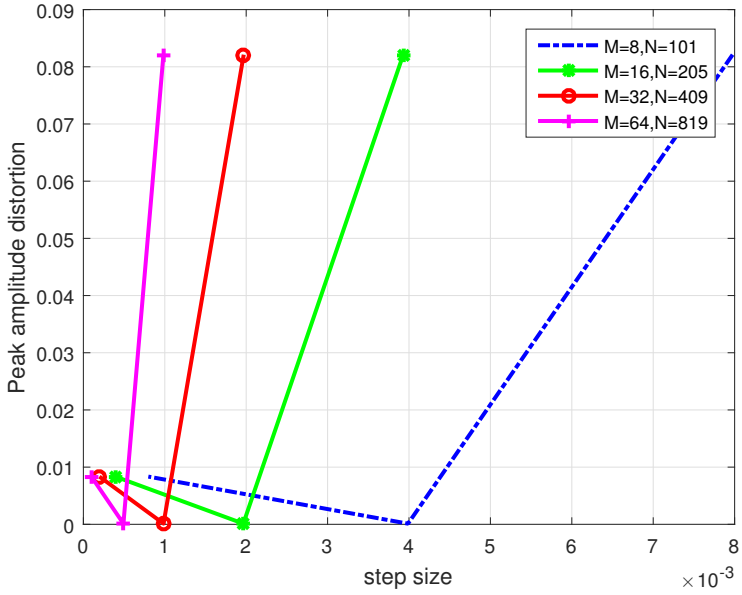

Figure 3.7: The significance of transition point variation for different filter length N and number of subbands M on amplitude distortion

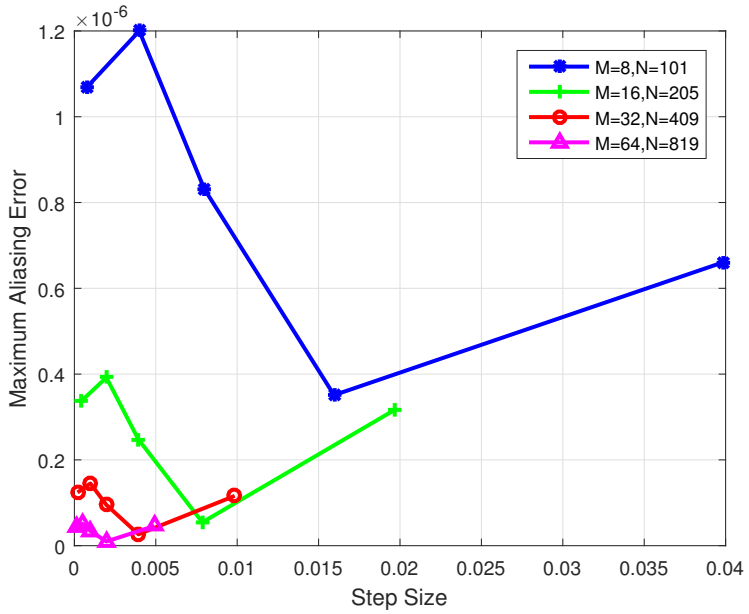

Figure 3.8: The significance of transition point variation for different filter length N and number of subbands M on aliasing error

3.7 Summary

In this chapter, literature survey of different prototype filters and the significance of prototype filter in the implementation of filter banks were discussed. A systematic and self controlled algorithm for the design of a lowpass linear phase FIR prototype

filter was proposed and the design procedure is discussed in detail. In our scheme, the prototype filter cut-off frequency is approximated to 3 dB response iteratively using a step size as a function of transition width instead of an arbitrary step size. The prototype filter is designed with two user inputs - number of subbands M and attenuation A_s. Our approach is simple and systematic compared to other widely used techniques. It can be concluded that by choosing the step size as a function of transition width and varying the step size from coarser to finer level, the minimum amplitude distortion and aliasing error can be achieved. Simulation results are presented in comparison with the results of existing methods. In Chapter 4, spectrum sensing using cosine modulated filter banks is discussed. The cosine modulated filter banks are designed using the proposed prototype filter.

Related publication

An Iterative Design with Variable Step Prototype Filter for Cosine Modulated Filter Bank, *Radioengineering*, **25**, 156-160 (2016).

CHAPTER 4

CMFB for Spectrum Sensing

Filter banks have spectral containment and are expected to provide better results in terms of spectrum sensing and spectrum utilization [73], [82]. Using complex modulation of single prototype filter, uniform multirate filter banks such as Discrete Fourier Transform (DFT), Modified DFT (MDFT), and Cosine Modulated Filter Bank (CMFB) can be implemented. These filters decompose the spectral components uniformly with efficient filter bank realization structures. The CMFB is more desirable as it provides higher bandwidth efficiency and lower sidelobes [106].

In this chapter, we discuss cosine modulated filter banks with emphasis on spectral granularity of filter banks for spectrum sensing in Cognitive Radios (CR) and multistage filter banks to reduce computational complexity. The bandwidth efficiency of the detected spectral holes can be increased by varying the granularity of prototype filter depending on the spectrum to be sensed. Spectrum sensing can be done effectively by proper choice of prototype filter with specified subband attenuation. The energy detection after subband filtering detects the spectral holes with high confidence due to spectral containment in the subband sensing using CMFB. The precision of spectral detection is increased when the number of subbands are increased, however this increases the computational complexity of the filter bank structure. We suggest a multistage filter bank structure to reduce the complexity. The subbands detected in coarser granularity bands alone would be sensed with finer granularity bands for precise spectral detection depending on the predefined threshold based on probability of false alarm. Only the spectrum of interest is sensed further with finer granularity which in turn reduces computational complexity. Using simulations, it is shown that spectrum detection with multistage granularity maintains bandwidth efficiency and reliability in spectrum detection even at low SNR.

Section 4.1 discusses the implementation of cosine modulated filter banks for wideband spectrum sensing. The significance of variable granularity bands in spectrum sensing is explained in Section 4.2. Multistage CMFB from coarser to finer spectral

resolution depending on the predefined thresholds based on probability of false alarm for reducing computational complexity is discussed in Section 4.3. Simulation results along with our observations are presented in Section 4.4.

4.1 Spectrum Sensing with Cosine Modulated Filter Banks

At the initial phase, Orthogonal Frequency Division Multiplexing (OFDM) was considered as a suitable candidate for CR systems for spectrum sensing [107]. However, the sidelobes of OFDM subcarriers introduce power leakage to adjacent channels due to the presence of FFT [75]. The FFT in OFDM is not flexible and provides a subband attenuation of only 13 dB [108]. The out-of-band rejection requirements of FCC are also not satisfied by OFDM/FFT [109]. The spectrum sensor have to provide sufficiently high spectral dynamic range in order to detect the low power primary users. The spectral resolution of sensing has to be small for better utilization of spectrum resources. Therefore, alternatively different filter bank techniques are investigated to overcome the above limitations [73]. Filter banks have been suggested as potential candidate for CR systems because of their higher spectral efficiency and lower spectral leakage compared to OFDM. Moreover, filter banks are efficient for CR signal processing as the subbbands can be designed with desired attenuation [109].

The performance of the filter banks are comparable to Thomsons Multi-Taper Method (MTM) [65]. MTM has been considered as optimal spectrum sensing technique by Simon Haykins in [3], however they are limited by the high computational complexity. Filter banks based on prolate filter also provide good spectrum sensing performance [77]. Most of the filter bank spectrum sensing methods are based on energy detection. If the energy in a subband is above a predefined threshold, the subband is considered as occupied and if the energy is below a threshold it is considered as a spectral hole. For better detection of spectral holes, the subbands in filter banks have to provide good subband attenuation and low spectral leakage to the neighbouring subbands.

Among different filter bank based methods such as orthogonal multiplexed quadrature amplitude modulation (OQAM), cosine modulated multitone (CMT), and filtered multitone (FMT), CMT is more desirable as it provides higher bandwidth efficiency

compared to FMT and lower sidelobes than OQAM [110]. The performance of spectrum estimation is characterized by different parameters such as frequency resolution, spectrum leakage, and estimation time. The above three parameters can be regulated using CMFB with a proper design of prototype filters. In wideband spectrum sensing, signals are filtered using CMFB followed by power spectrum estimation [106]. CMFB can detect primary user over contiguous channel having different bandwidth. A transceiver framework based on cosine modulated filter bank was proposed in [111] for cognitive access to TV white spaces.

In the proposed work, we discuss cosine modulated filter banks with emphasis on spectral granularity of filter banks for spectrum sensing and multistage filter banks to reduce the computational complexity. The prototype filter for CMFB was designed using Kaiser window method with attenuation A_s (in dB), filter length N, and approximating the amplitude response at $\frac{\pi}{2M}$ close to $\frac{1}{\sqrt{2}}$ using the algorithm proposed in Chapter 3. The number of subbands M determines the granularity of the filter banks. The analysis and synthesis filters are implemented by modulating the prototype filter as explained in Section 3.3.2. The closed form expressions for analysis and synthesis filters are given in [1] as

$$h_k(n) = 2h(n)\cos\left(\frac{\pi}{M}\left(k+\frac{1}{2}\right)\left(n-\frac{N-1}{2}\right)+(-1)^k\frac{\pi}{4}\right) \tag{4.1}$$

$$f_k(n) = 2h(n)\cos\left(\frac{\pi}{M}\left(k+\frac{1}{2}\right)\left(n-\frac{N-1}{2}\right)-(-1)^k\frac{\pi}{4}\right) \tag{4.2}$$

where, $0 \leq n \leq N-1$, $0 \leq k \leq M-1$ and $h(n)$ is the prototype filter. The dynamic range of the transition width of the subbands depends on the length of the prototype filter. Figure 4.1 illustrates the effect of subband attenuation for different prototype filter lengths $(N = 64, 128, 256, 512)$ with a subband attenuation of $A_s = 100$. It is apparent from Figure 4.1 that the subband attenuation increases with filter length and better spectral characteristics can be achieved.

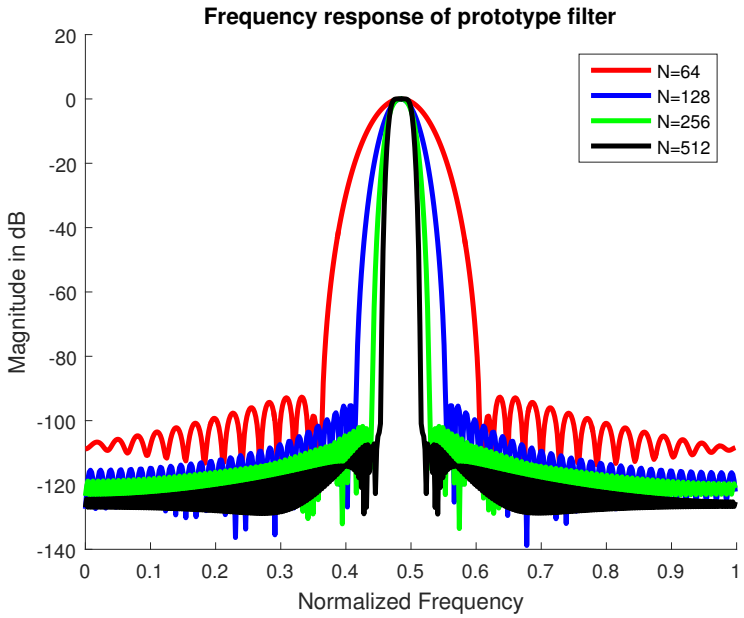

Figure 4.1: Subband attenuation with different filter lengths

4.1.1 System Model

The wideband signal for spectrum sensing are localized to various subband frequencies using filter bank structures. The available spectrum band is divided into M non-ovelapping uniform subbands, where M is the number of subbands in the filter bank. The output of each subband, $x_k(n)$, is assumed to be a random process, obtained from a random process input $s_k(n)$ passing through a linear subband filter of frequency response H_k, where $x_k(n) = H_k s_k(n)$. The received signal $y_k(n)$ can be modeled as [33],

$$y_k(n) = x_k(n) + w_k(n),\ k = 0, 1, 2, \ldots, M-1, \tag{4.3}$$

where, $x_k(n)$ is the active signal and $w_k(n)$ is the additive white Gaussian noise with zero mean and variance σ_w^2. In order to detect signal we define a binary hypothesis given as in [112].

$$H_{0,k} : y_k(n) = w_k(n) \text{ absence of signal}$$
$$H_{1,k} : y_k(n) = x_k(n) + w_k(n) \text{ presence of signal}$$

We consider the test statistic as the energy at the output of each subband and is given by Equation 4.4.

$$y_k(n) = \frac{1}{L}\sum_{n=0}^{L-1} x_k^2(n), \tag{4.4}$$

where, $L = \left(\frac{N_s}{M}\right)$, the number of samples in each subband and $k = 0, 1, 2, \ldots, M-1$. When the number of samples is increased, the chi-square distribution approximate to a normal distribution from the central limit theorem (CLT). According to CLT independent and identically distributed (i.i.d.) random variables with finite mean and variances approaches a normal distribution when N_s is large enough. Therefore, the distribution of test statistics can be accurately approximated with a normal distribution for sufficiently large number of samples [34]. The minimum number of samples required for spectrum sensing is obtained using the relation [38],

$$N_{min} = 2[Q^{-1}(P_{fa}) - Q^{-1}(P_d)(1+SNR)]^2 SNR^{-2}. \tag{4.5}$$

The presence of an active signal in a specified subband can be determined by comparing the energy in that subband with a predetermined threshold. The threshold is calculated based on probability of false alarm and noise variance depending on channel characteristics.

Calculation of Threshold

The threshold λ can be calculated using the knowledge of probability of false alarm P_{fa} and noise variance σ_w^2 of the received signal as explained in Section 2.1.1.

$$\lambda = \left(Q^{-1}(P_{fa})\sqrt{1/L} + 1\right)\sigma_v^2 \tag{4.6}$$

The energy detector gives the best performance with known noise variance and performance deteriorates when the noise variance is uncertain. To improve the detection performance, the noise variance can be estimated at the receiver before detection.

4.2 CMFB with Variable Granularity for Spectrum Sensing

The granularity of the filter banks can be chosen specifically if the bandwidth of the primary users are known apriori. At the initial stage, the prototype filter is designed with a coarse granularity. Further, using cosine modulation of the prototype filter, the filter bank structure is realized for spectrum sensing. The energy is computed at the output of individual subbands. The threshold is calculated for specified probability of false alarm P_{fa} and known noise variance σ_w^2. The procedure followed is given in Algorithm 2.

Algorithm 2 Filter bank technique for spectrum sensing

Require:

B: Bandwidth of sensing.

M : Granularity of the filter bank.

A_s: Stopband attenuation in dB of the subband filters.

1: Design prototype filter with the above specification and specify the cutoff frequency of the prototype filter to be $\pi/2M$.

2: Implement the analysis filter bank structure using Equation.4.1

3: Calculate threshold λ for specified P_{fa} with known noise variance σ_w^2.

4: Calculate the energy Y_k as test statistics at the output of each subband using Equation 4.4.

5: Apply the thresholds on the individual subband outputs and obtain the decision.

Spectrum sensing can be performed using filter bank structures for varying granularity bands. The number of subbands M determines the granularity of sensing bandwidth. For spectrum sensing with finer granularity bands, M needs to be increased, whereas for spectrum sensing with coarser granularity bands, M needs to be decreased. The advantage of varying granularity band is that the spectrum utility and re-usability can be effectively increased. Moreover, the same structure can be used for spectrum reallocation due to the flexibility offered by the filter bank structure.

The detection performance of the filter bank was evaluated for different subband resolutions varying the SNR with fixed probability of false alarm. Figures 4.2, 4.3,

and 4.4 shows the detection performance for $P_{fa} = 0.1$, $P_{fa} = 0.01$ and $P_{fa} = 0.05$, respectively, for varying granularity bands and SNR. From Figures 4.2, 4.3 and 4.4 it can be inferred that the probability of detection is increased for finer granularity bands. Simulations were performed by varying the SNR -30 dB to 10 dB and spectral granularity $M = [4, 8, 16, 32, 64]$ for fixed P_{fa}. It is also observed that the bandwidth efficiency could be effectively increased using finer granularity bands. When the number of subbands is increased the spectral resolution of the filter banks gets increased and better detection performance is achieved. The computational complexity can be further reduced with efficient structure using polyphase filter bank discussed in Chapter 5.

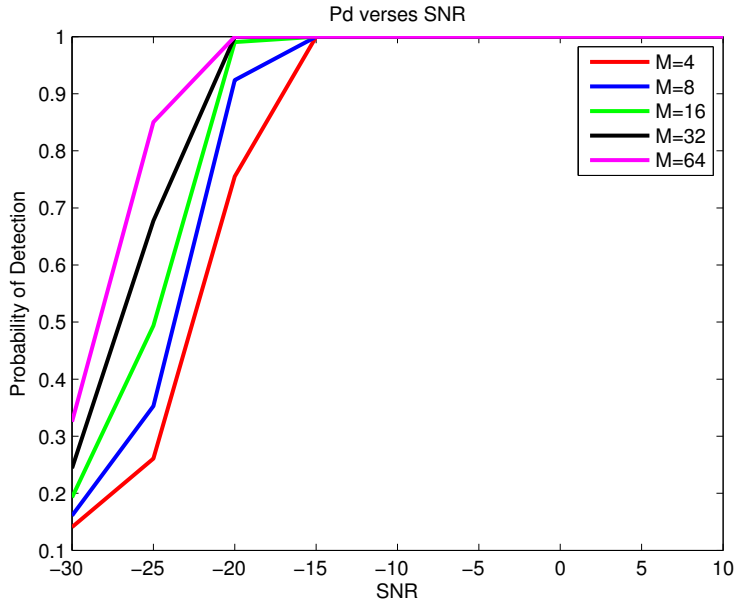

Figure 4.2: SNR vs probability of detection with different subband resolutions for $P_{fa} = 0.1$

From the Algorithm 2, it was found that finer granularity bands provide better detection performance and bandwidth efficiency. However, finer granularity bands increase the computational complexity of the filter bank structure used for spectrum sensing. In order to reduce the computational complexity, a multistage CMFB structure is proposed from coarser to finer level spectral resolution using filter bank structure.

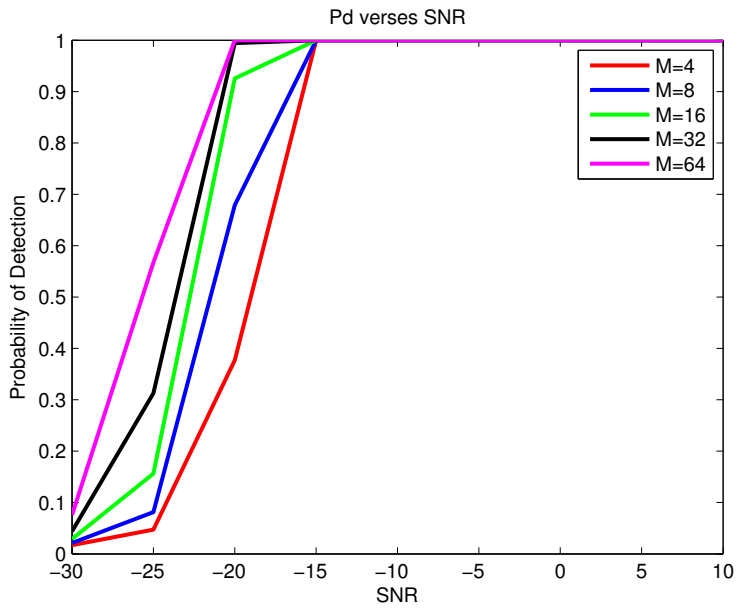

Figure 4.3: SNR vs probability of detection with different subband resolutions for $P_{fa} = 0.01$

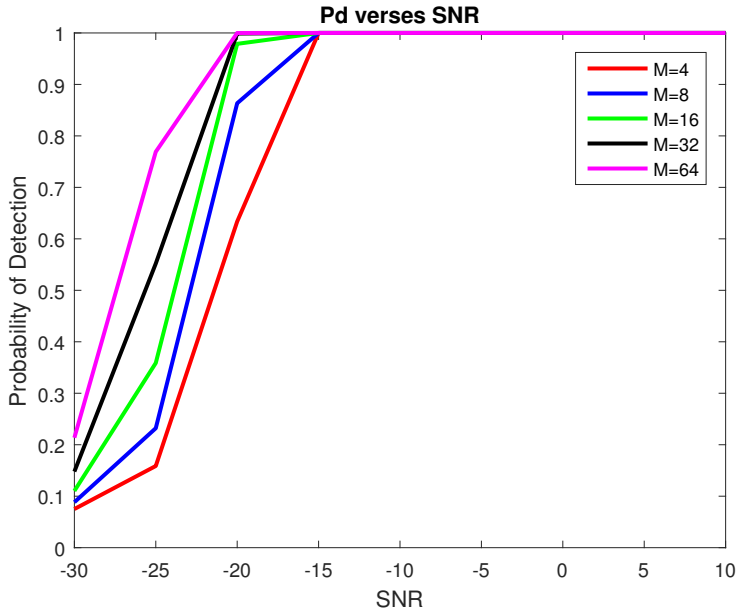

Figure 4.4: SNR vs probability of detection with different subband resolutions for $P_{fa} = 0.05$

4.3 Spectrum Detection with Multistage CMFB

Better sensing performance can be achieved in filter banks with finer resolution. However, this would increase the computational complexity of the filter bank structure. Therefore, to overcome the computational complexity multistage filter banks are in-

vestigated for sensing from coarser to finer resolution. In multistage or multi-resolution filter banks, at the initial stage the total bandwidth is sensed using coarser spectral resolution. The bandwidth of interest is identified depending on the sensing decision and only those frequency bands are further sensed with finer spectral resolution. Multiresolution filter bank techniques include Fast Filter Bank (FFB) based on Frequency Response Masking (FRM), coarser to finer spectrum sensing using wavelet transforms, and FFT based multiresolution spectrum sensing using multiple antennas [20], [113], [102].

The available bandwidth is initially divided into non-overlapping subbands with coarser spectral resolution of M_1 subbands as illustrated in Figure 4.5. When narrow band users appear in wideband spectrum and the bandwidth of sensing is sparse as shown in Figure 4.5, the subbands of interest can be detected in the first stage. The detected subbands can be sensed further with finer spectral resolution in the next stage with a spectral resolution of M_2 subbands. As the narrowband users are identified in coarser resolution, only the detected subbands are sensed further with finer resolution. Therefore, the computational complexity is reduced and better sensing performance can be achieved.

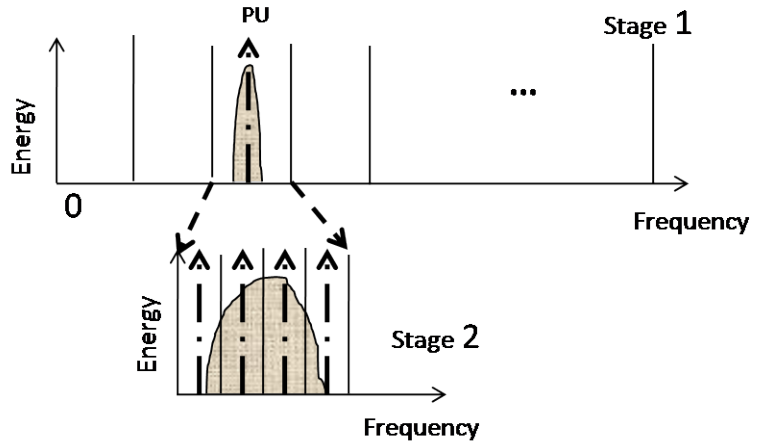

Figure 4.5: Illustration for multistage filter bank spectrum sensing

Multistage spectrum sensing can be performed by defining two thresholds based on different probability of false alarm P_{fa} depending on the channel conditions. Energy detection is performed using the predefined thresholds with different probability of false alarms, calculated as discussed in Section 4.1.1. Two thresholds, λ_1 and λ_2 are the calculated based on different probability of false alarm ($\lambda_2 > \lambda_1$). If the energy is above the threshold λ_2, it can be concluded as the presence of primary user. If the

energy is below λ_1 it is decided as the presence of a spectral hole or absence of primary user and if the energy is between λ_1 and λ_2 there is a possibility of spectral hole within the subband. The multistage spectrum sensing with energy distribution and thresholds are explained in Figure 4.6. Only the subbands having energy between λ_1 and λ_2 has to be sensed in the next level with finer granularity. Multiple spectral gaps can be identified in an efficient and flexible way using the multistage methods with reduced complexity, since the whole band need not be sensed with finer granularity.

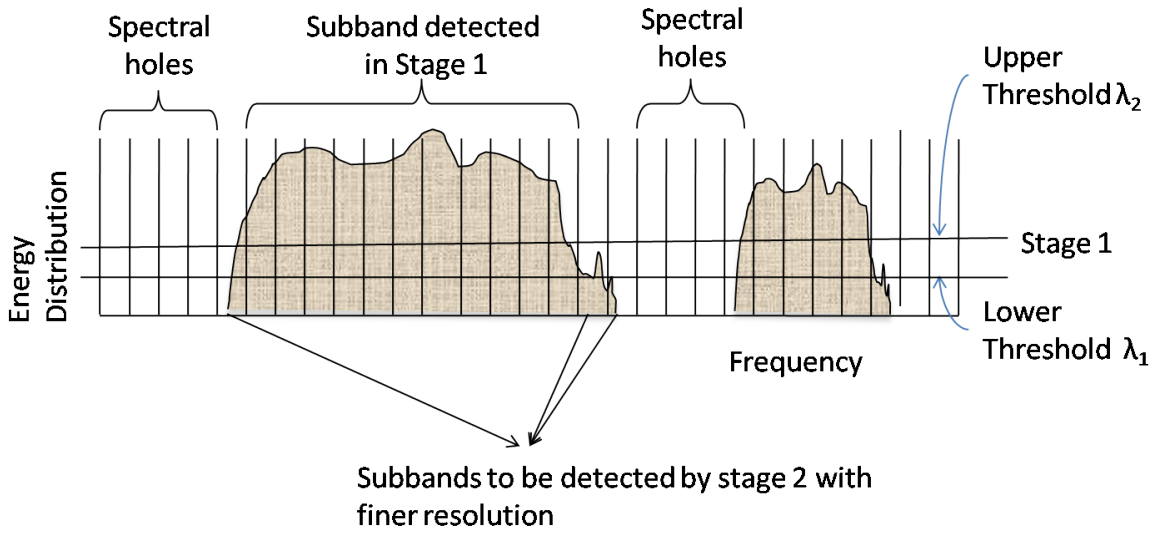

Figure 4.6: Illustration of threshold decision with multistage spectrum sensing

The proposed multistage filter bank technique for wideband spectrum sensing is elaborated in Algorithm 3.

The significance of multistage spectrum sensing is summarized as follows:

1. The probability of detection is improved with finer granularity bands [59].
2. Multistage filter banks reduce the computational complexity as the whole band need not be sensed with the finer granularity.
3. Sensing can be performed from a coarser to finer level [60].

4.4 Simulation Results

The prototype filter for the CMFB was designed for the cut-off frequency $\frac{\pi}{2M}$ for varying granularity bands with stop band attenuation $A_s = 100$ dB and filter length

Algorithm 3 Multistage filter bank technique for spectrum sensing

Require:

B: Sensing bandwidth.

M_1: Granularity of the filter bank (initial subbands should be coarse)

1: Design prototype filter with the above specification and specify the cutoff frequency of the prototype filter to be $\pi/2M_1$.

2: Implement the analysis filter bank structure using Equation.4.1.

3: Calculate λ_1 and λ_2 for different P_{fa} with known noise variance.

4: Calculate the energy Y_k as the test statistics at the output of each subband using Equation.4.4

5: Apply the thresholds on the individual subband outputs and obtain the decision

6: **if** $Y_k > \lambda_2$ **then**

7: Primary user is present

8: **else**

9: **if** $Y_k < \lambda_1$ **then**

10: Primary user is absent

11: **else**

12: **if** $\lambda_1 \leq Y_k \leq \lambda_2$ **then**

13: Perform spectrum detection with finer granularity

14: **end if**

15: **end if**

16: **end if**

17: Divide the subbands detected for finer granularity with M_2 subbands. The spectral resolution of the subbands would be $\dfrac{\pi}{M_1 M_2}$

$N = 289$. The frequency response of the CMFB for $M = 8$ and $M = 16$ is shown in Figures 4.7 and 4.8, respectively.

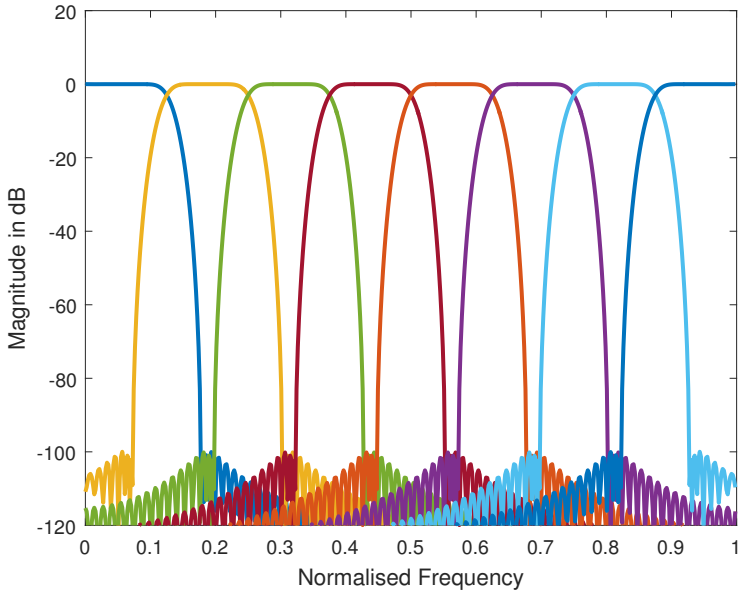

Figure 4.7: Frequency response of CMFB for $M = 8$

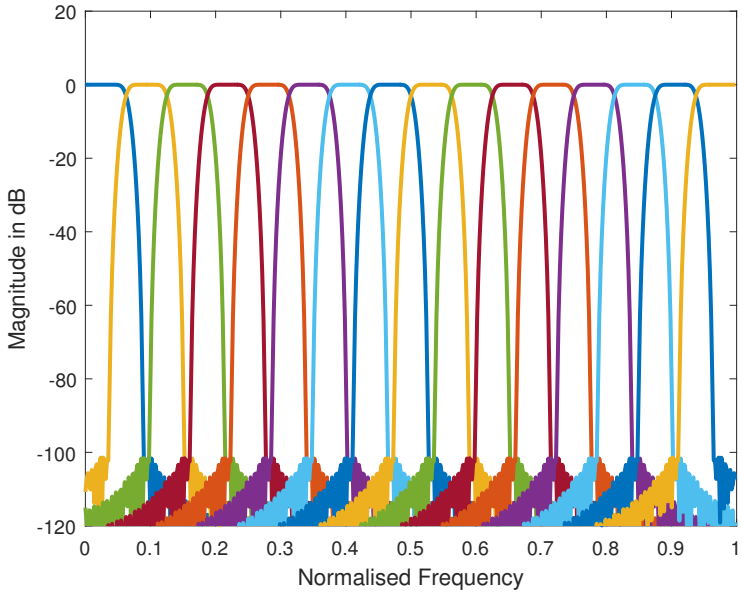

Figure 4.8: Frequency response of CMFB for $M = 16$

For our simulation, the signals having different communication standards such as Bluetooth (PU_1: $B_1 = 1$ MHz) and Zigbee (PU_2: $B_2 = 4$ MHz) are considered [2]. Simulation parameters are given in Table 4.1. Spectrum using FFT scheme with three primary users in a wide bandwidth of 12 MHz is shown in Figure 4.9. The center frequency of Bluetooth is at 2 MHz and Zigbee at 8 MHz, respectively. The signal sensed

Table 4.1: Simulation parameters [2]

Parameter	**Value**
Sensing bandwidth B MHz	12
Sampling time Ts	1/24
Capture time τ	2 sec
Number of samples	$N = \tau Ts$
Subband attenuation	100 dB
Prototype filter length	127
Primary Users : Bluetooth (PU_1), Zigbee(PU_2)	2
Bandwidth of PU in MHz	1, 4
Spectral resolution of filter bank M	8, 16, 64
Spectral decomposition of filter bank $M = M_1 M_2$,	$M_1 = 16$, $M_2 = 4$

with $M = 8$ and $M = 16$ subbands are shown in Figures 4.10 and 4.11 respectively. It can be inferred from the Figures 4.10 and 4.11 that the finer the spectral resolution, better the detection performance and spectral efficiency, since more spectral holes can be identified.

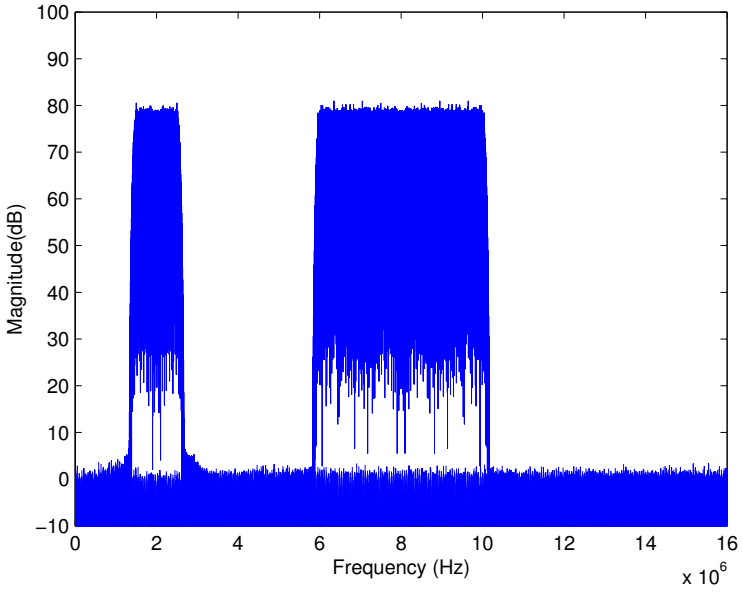

Figure 4.9: Spectrum containing Bluetooth and Zigbee using FFT scheme

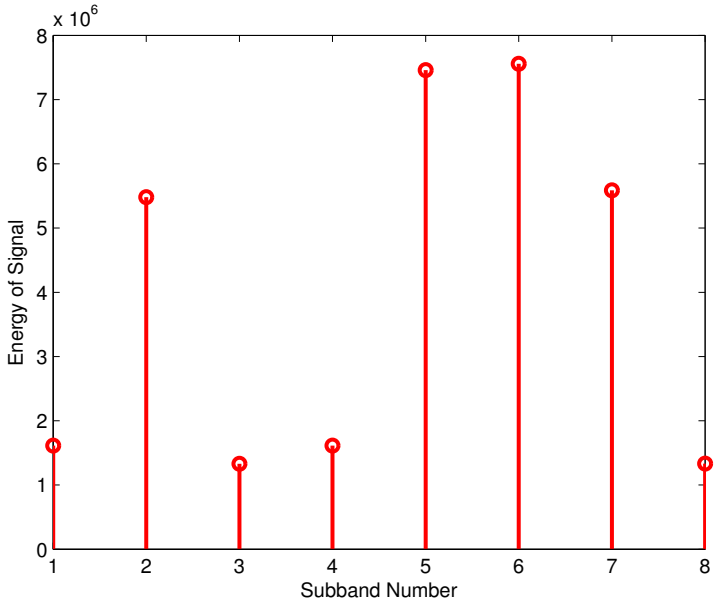

Figure 4.10: Energy distribution at the output of individual subbands with $M_1 = 8$ in the first stage of sensing for an SNR of 0 dB

From Figure 4.11, Bluetooth is identified from subbands 3 and 4 for $M_1 = 16$. Depending on the threshold decision, the subband 4 can be sensed with a finer resolution to identify holes within the subband. The subband 4 is further sensed with a spectral resolution of $M_2 = 4$ as shown in Figure 4.12. Similarly, the Zigbee is identified from subbands 9 to 14. Depending on the threshold decision, subband 14 can be sensed further with finer resolution in the second stage with $M_2 = 4$ as shown in Figure 4.12. Thus, holes within the subbands could be identified with a spectral resolution of $M = 64$ i.e., $M = M_1 M_2$.

Similarly, the simulation was done for the signal containing Bluetooth and Zigbee for an SNR of -5 dB. The energy distribution at the output of first stage for $M_1 = 16$ is shown in Figure 4.13. Depending on the threshold decision, the subband 4 and 14 can be sensed further with a finer resolution to identify holes within a subband. The energy distribution at the output of second stage for subbands 4 and 14 with $M_2 = 4$ is shown in Figure 4.14.

The significance of multistage CMFB spectrum sensing can also be illustrated assuming the Bluetooth (PU_1: $B_1 = 1$ MHz) signal appears over a wideband of 12 MHz. A signal with Bluetooth and their spectrum using FFT scheme are shown in Figure 4.15. At initial stage, the wideband is sensed with a CMFB of $M_1 = 8$ and the corresponding

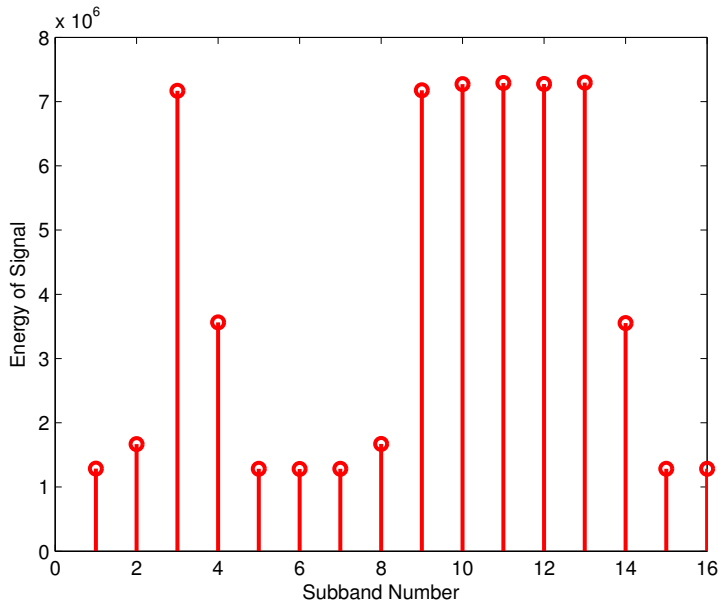

Figure 4.11: Energy distribution at the output of individual subbands with $M_1 = 16$ in the first stage of sensing for an SNR of 0 dB

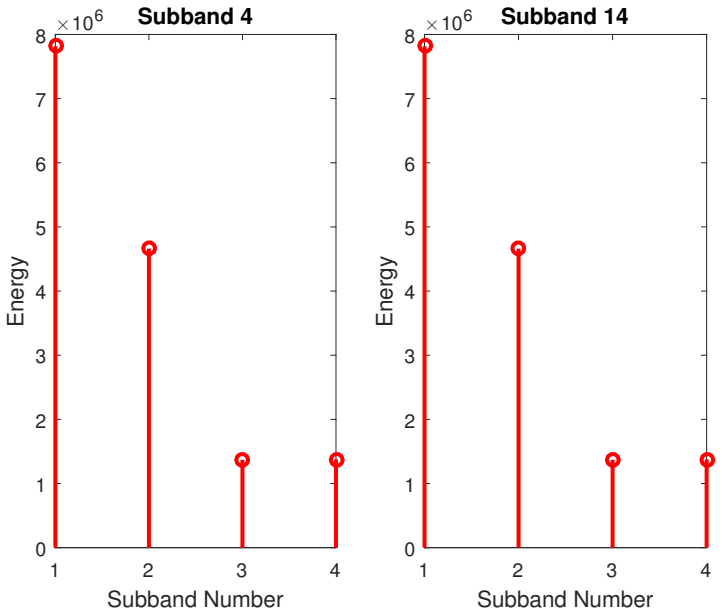

Figure 4.12: Energy distribution at the output of subbands 4 and 14 with $M_2 = 4$ in the second stage of sensing for an SNR of 0 dB

energy distribution is shown in Figure 4.16. The subbands 4 and 5 are detected in the first stage and these subbands are sensed using finer resolution with $M_2 = 4$ in the second stage and shown in Figure 4.17. Thus, the signals of interest are sensed with a spectral resolution which is equivalent to $M = M_1 M_2$, i.e., $M = 32$. The frequency band of interest could be sensed with finer spectral resolution with reduced complexity.

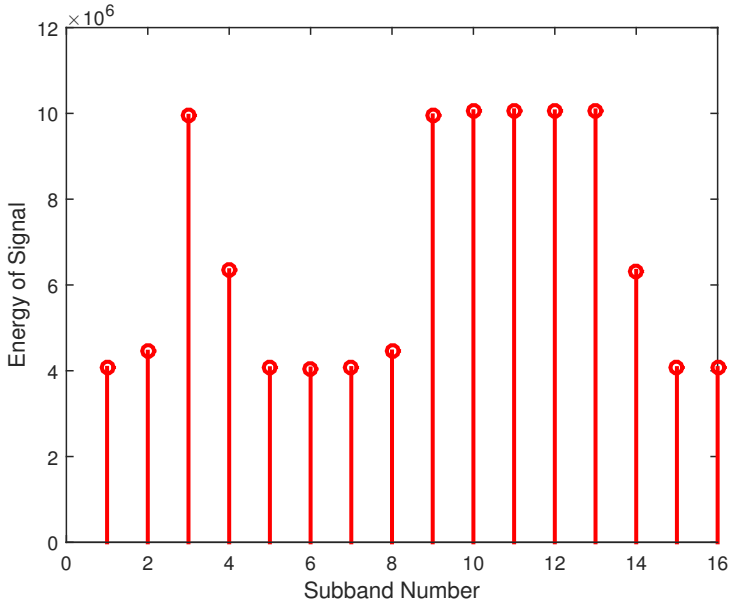

Figure 4.13: Energy distribution at the output of individual subbands with $M_1 = 16$ in the first stage of sensing for an SNR of -5 dB

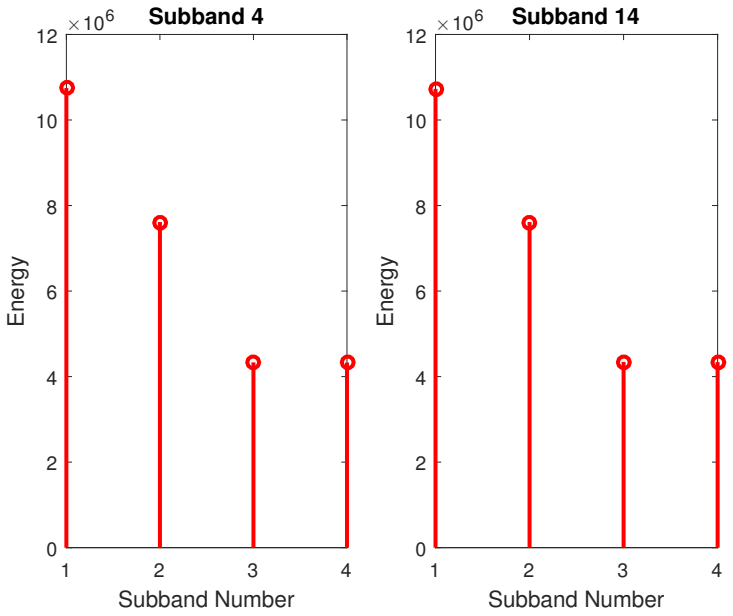

Figure 4.14: Energy distribution at the output of subbands 4 and 14 with $M_2 = 4$ in the second stage of sensing for an SNR of -5 dB

The detection of Bluetooth (PU_1: $B_1 = 1$ MHz) signal over a wide band of 12 MHz with SNR = -5 dB using multistage CMFB spectrum sensing is also considered for simulation. Initially, the signal was sensed with a CMFB of $M_1 = 8$ and the corresponding energy distribution is shown in Figure 4.18. From the energy distribution and threshold decision the subbands 4 and 5 are detected in the first stage and shown in Figure 4.18.

The detected subbands are further sensed in the second stage with $M_2 = 4$. The energy distribution of the subbands 4 and 5 in second stage is shown in Figure 4.19. Therefore, the frequency band of interest was sensed with a spectral resolution which is equivalent to $M = M_1 M_2$, i.e., $M = 32$.

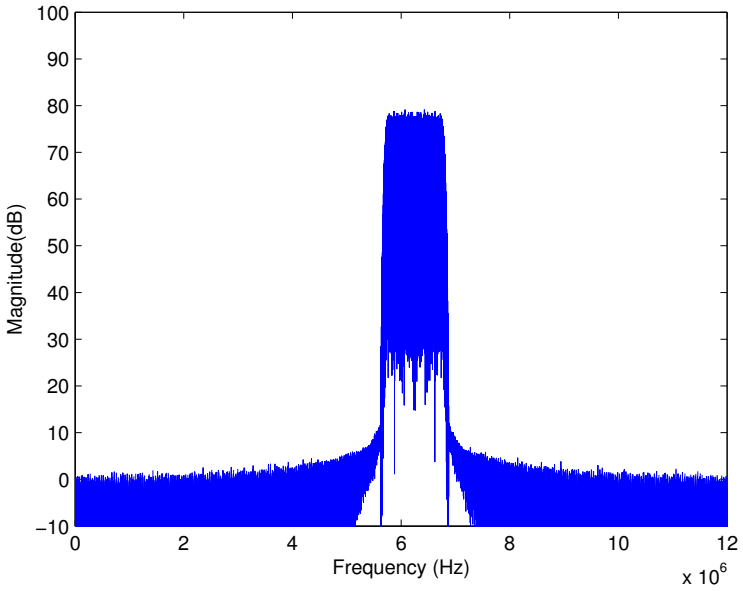

Figure 4.15: Spectrum containing Bluetooth using FFT scheme

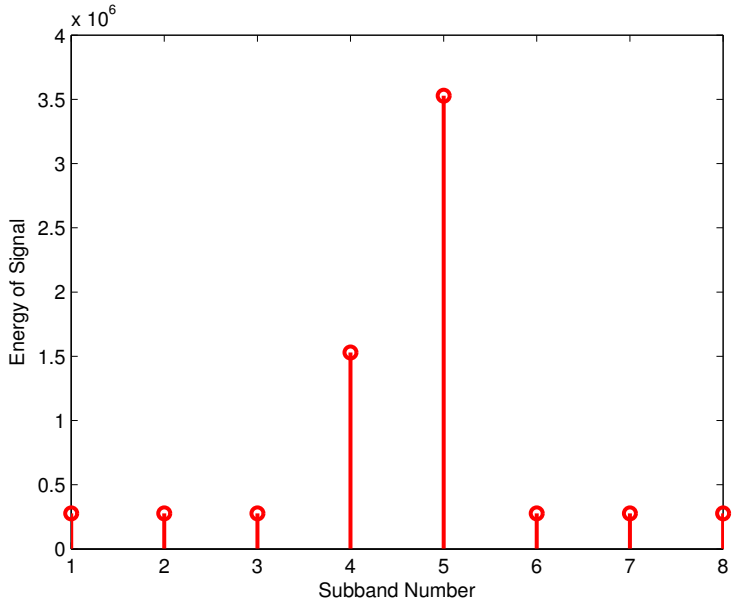

Figure 4.16: Energy distribution of the signal containing Bluetooth with $M_1 = 8$ subbands for an SNR of 0 dB

From the above examples, it can be concluded that the computational complexity can be reduced when the spectrum to be sensed is sparse. At the initial phase, the

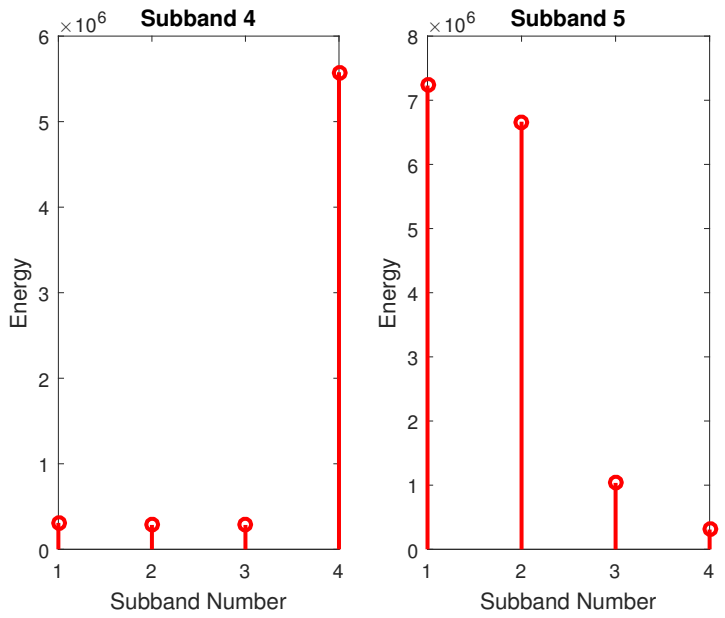

Figure 4.17: Energy distribution at the output of subbands 4 and 5 in the second stage with $M_2 = 4$ for an SNR of 0 dB

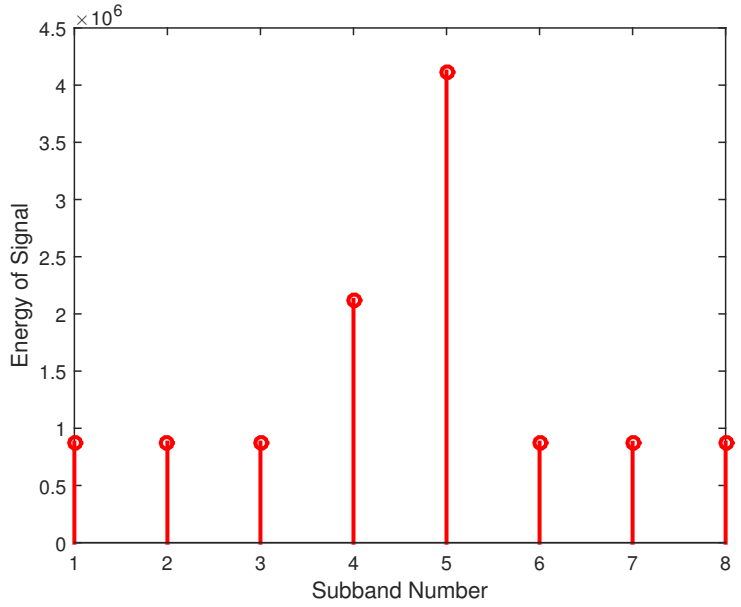

Figure 4.18: Energy distribution of the signal containing Bluetooth with $M_1 = 8$ subbands for an SNR of -5 dB

subbands are sensed with coarser level (smaller number of subbands M) to detect the presence of signal and spectral holes. Depending on the decision, the subbands are further splitted into finer bands. Since the complete spectrum need not be splitted with the finer spectral resolution, the computational complexity can be reduced further. The subbands having energy between λ_1 and λ_2 only need to be sensed with finer spectral

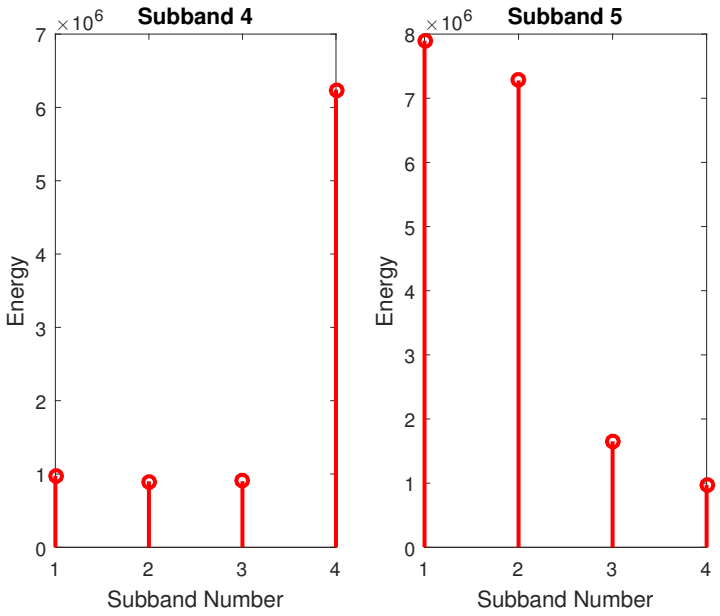

Figure 4.19: Energy distribution at the output of subbands 4 and 5 in the second stage for an SNR of -5 dB

resolution.

4.5 Summary

In this chapter CMFB was explored for wideband spectrum sensing. The filter banks provided higher bandwidth efficiency and lower sidelobes desirable for spectrum sensing. The spectral holes could be identified by the threshold determined from probability of false alarm and noise variance. The test statistic was calculated based on the energy at the output of each subband. The bandwidth efficiency could be effectively increased by finer granularity bands. It can be concluded that, finer the spectral resolution, better the detection performance and spectral efficiency. The computational complexity is reduced using multistage filter banks by processing only those subbands having energy within the predefined thresholds, instead of the entire bandwidth. Simulation results show that the detection efficiency of the free spectrum is effectively increased and the computational complexities reduced with multistage filter banks. In Chapter 5, we discuss multistage polyphase filter banks for spectrum sensing which further reduces the computational complexity.

Related publications

Spectrum Sensing in Multipath fading channels using Cosine Modulated Filter Bank for Cognitive Radio Applications at the *IEEE International conference on Electrical, Computers and Communication Technology* Tamil Nadu, 5-7th March 2015.

Spectrum Sensing with Programmable Granularity Bands Using Cosine Modulated Filter Bank for Cognitive Radio at the *IEEE International Conference on Communication and Signal Processing (ICSSP 2015)* Tamil Nadu, 2-4th April 2015.

CMFB for Spectrum Detection and Utilization in CR Application at the *International Conference on Computing and Network Communications (CoCoNet 2015)* Trivandrum, 16-19th Dec 2015.

Spectral Detection with Multistage Granularity Bands using Filter Bank Techniques for CR Applications, *International Journal of Wireless and Mobile Computing, Inderscience*, **12**, 62-67(2017).

CHAPTER 5

Polyphase Filter Bank for Spectrum Sensing

Wideband spectrum sensing using filter banks has proved to be robust and efficient. Filter bank based physical layer design for Cognitive Radio (CR) systems was introduced to perform simultaneous spectrum sensing and transmission. Filter bank techniques can reduce computational complexity and improve spectral analysis in cognitive radio applications. For fractional utilization of spectrum, the center frequency and spectral edges of the primary user need to be estimated.

In this chapter, we address the problem of estimating the center frequency and spectral edges of primary users in a wideband spectrum using polyphase filter banks. Section 5.1 discusses the general polyphase filter bank. The proposed multistage polyphase filter bank is explained in Section 5.2. Different scenarios such as narrow band users and multiple user detection in a wideband spectrum are considered. A novel centroid based method was used for the detection of narrowband users in wideband spectrum. The method was applied for the detection of Wireless Microphone (WM) in TV white spaces in the presence of a signal, following IEEE 802.22 WRAN standard. For multi-user detection, a center of mass based method was introduced. Simulation results are discussed for single user as well as multi-user detection in wideband for estimation of center frequency and spectral edges in Section 5.3.

5.1 Polyphase Filter Banks

Filter banks are often implemented based on the modulation of a single prototype filter. In general, lowpass FIR filters are used as prototype filters in realization of filter banks. The magnitude of side lobes of the filter determines spectral leakage to adjacent subbands. The overall performance of the filter bank can be improved with proper design of subband filters [81]. Polyphase filter bank structure reduces the complexity of the filter bank implementation. Polyphase filter banks are efficiently designed using FFT when the number of subbands M is a power of two. Here, M subbands are obtained

using polyphase decomposition of the prototype filter $h(n)$ having the transfer function $H(z)$. The polyphase decomposition of the prototype filter can be written as [1]

$$H_(z) = \sum_{l=0}^{M-1} z^{-l} E_l(z^M), l = 0, 1, \ldots, M-1. \tag{5.1}$$

The l^{th} polyphase component can be defined as

$$E_l(z) = \sum_{n=0}^{N-1} h(Mn + l) z^{-n}. \tag{5.2}$$

The polyphase structure of an M band filter bank is equivalent to the realization of single prototype filter and an M point FFT. The computational complexity is $N + M \log_2 M$, where N is the length of the prototype filter. Polyphase filter bank reduces the computational complexity to a large extent compared to the complexity (NM) of direct implementation. The polyphase filter bank structure can further be simplified using Noble identities of multirate signal processing [1]. The structure of polyphase filter is explained in detail in Section 3.3.

5.2 Proposed Multistage Polyphase Filter Banks

The proposed multistage polyphase filter bank method detects the presence of primary user and also estimates the center frequency with higher precision using the centroid/center of mass method. It is well known that the detection accuracy depends on the number of subbands M in the filter bank. The computational complexity of the filter bank increases with higher values of M. However, the complexity is reduced by using multistage polyphase filter bank structure. The primary users are detected by computing the signal energy (power) at output of the individual subbands. Our algorithm for the detection of unused spectrum (spectrum holes) starts with a coarser spectral resolution (smaller number of subbands) at the first stage to reduce computational complexity.

Single user and multi-user scenarios are considered in wideband for spectrum sensing using multistage polyphase filter banks. The detection of single and multiple users in widebands are elaborated in the following subsections.

5.2.1 Single User Detection in Wideband Spectrum

The proposed system can be used to detect WMs in the presence of a signal that follows IEEE 802.22 WRAN standard. In IEEE 802.22 WRAN standard, spectrum sensing has to be done to allow television (TV) services and wireless microphones to coexist. WMs are low power licensed users and are allowed by Federal Communications Commission (FCC) to operate on vacant TV channels without causing interference. The detection of WM is difficult due to the low power transmission (typically 50 mW for 100 m coverage) and small bandwidth occupancy (200 kHz). In IEEE 802.22 WRAN standard, when a WM appears anywhere in the TV channel, the whole channel of 6 MHz has to be evacuated to avoid interference [114]. However, TV channels can be utilized fractionally when the exact position of the WM is detected [115], [59]. Hence, there are several challenges in the detection of WM signals [116], [117].

Some of the conventional techniques discussed in literature include blind spectrum sensing based on Eigenvalue algorithm and power spectral density (PSD) to detect the peak of WM signal regardless of modulation type [118, 119, 120, 121]. The sensing of WM remains as an open research problem as there are no common transmission standards. Some of the filter bank techniques existing in literature include DFT filter banks, polyphase realization of DFT filter banks, and multistage coefficient decimation filter banks [81], [122], [123]. Even though multistage coefficient decimation filter bank reduces computational complexity, they are not suitable for detecting narrowband spectrum [124]. Reconfigurable filter bank methods have also been exploited for spectrum sensing in [125]. Multistage filter bank technique was proposed for the detection of a single WM and estimate the center frequency appearing in the TV channels. However, this method requires an additional modulation component to the existing DFT filter bank to move the filter response to the desired spectral region [122], [126].

The goal of the proposed multistage polyphase filter bank method is to detect the presence of WM and estimate the center frequency of the WM with better precision by using the centroid method. The important contribution of our work is the detection and estimation of center frequency with high precision and reduced computational complexity. The novelty of the proposed centroid based technique is that the presence of WM can be detected in the first stage itself, when spectrum of WM lies partly in one subband and partly in adjacent subband. As the WM is detected in the first stage it reduces the

computational complexity, latency, and thereby achieves fast sensing. However, if WM appears exclusively within a single subband, an additional stage is required to detect and estimate the center frequency of WM with finer spectral resolution. In such cases, WM can be detected in the second stage without ambiguity.

Our method is designed to detect the presence of WM anywhere within a TV channel (6 MHz) and to estimate the center frequency of WM taking into account the following scenarios:

Case 1: If the signal spectrum of WM lies partly in one subband and partly in the adjacent subband as shown in Figure 5.1, the center frequency of WM can be either in one of the subbands or between two subbands. The center frequency in such a case is estimated using the centroid method as described in Section 5.2.3.

Case 2: If the signal spectrum of WM is in the middle of two adjacent subbands as shown in Figure 5.2, the energy at the output of two subbands will be equal. That is, the center frequency of WM is at the midpoint of the two subbands. Therefore, finer level of detection is not necessary, which in turn reduces the computational complexity and latency.

Case 3: If the signal spectrum of WM appears exclusively within a subband as shown in Figure 5.3, the output of first stage is passed to the input of the next stage filter bank to estimate the center frequency with a finer spectral resolution. The process is illustrated in Figure 5.4 where only two stages are required to detect the presence of the WM and to accurately estimate its center frequency. The center frequency is estimated in the second stage using DFT polyphase filter bank and centroid method.

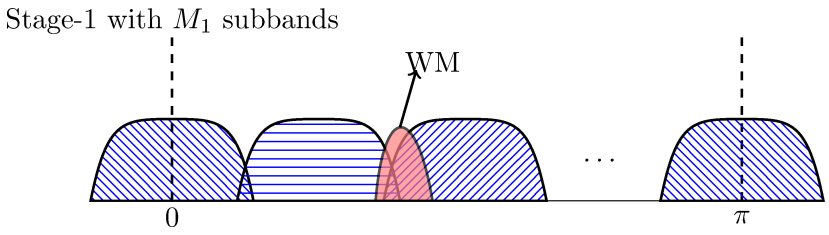

Figure 5.1: Case 1: WM appears anywhere between two consecutive subbands

The procedure followed for multistage spectrum sensing is briefed in the following two steps:

Step 1: The bandwidth of sensing is divided coarsely into M_1 subbands and sensed

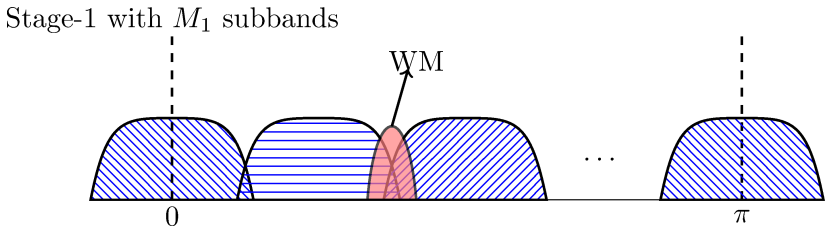

Figure 5.2: Case 2: WM appears exactly between two subband

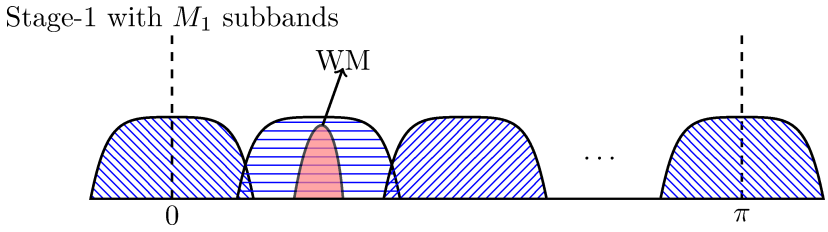

Figure 5.3: Case 3: WM appears exclusively within a subband

through the M_1 subband DFT polyphase filter bank. Energy detection is performed at the output of each subband, considering energy (power) as the test statistic to decide the presence or absence of the WM in the subbands. The detection and estimation of center frequency of WM as per Case 1 or Case 2 is done in the first stage. If the signal spectrum of WM is as per Case 3, the output of the sensed subband is further processed with finer resolution as in Step 2.

Step 2: The output of first stage is sensed in the next level with M_2 subbands. The signal energy (power) at the output of the subband is considered as the test statistic. At this level, the spectrum is sensed with a spectral resolution of π/M_1M_2.

The proposed method can be summarized as:

(i) If WM appear anywhere within consecutive subbands (Case 1 and Case 2), the center frequency of WM is estimated accurately using the centroid method in single stage.

(ii) If WM appears anywhere exclusively within any subband (Case 3), the output of the sensed subband is further processed with finer resolution as in Step 2.

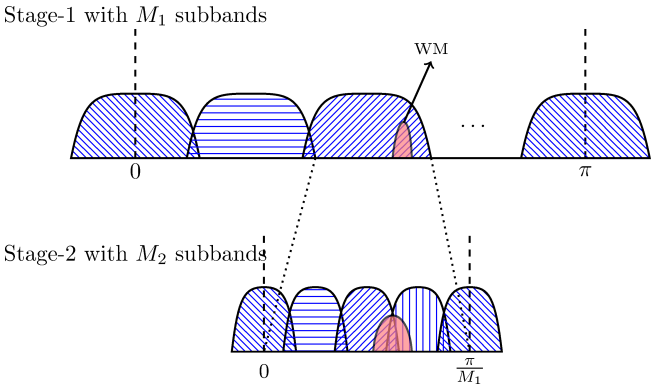

Figure 5.4: Detection of WM in a two stage filter bank

Table 5.1: Computational complexity in terms of multiplications for the proposed method for different stages and number of subands

Filter structure for a prototype filter of length $N = 51$	**Computational Complexity**	**Hardware Complexity**
32 subbands	211	Single Stage
$M_1 = 16, M_2 = 2$	168	Double Stage
$M_1 = 8, M_2 = 4$	134	Double Stage

5.2.2 Complexity Analysis

The complexity of the filter is estimated with the number of complex multiplications performed in the filter bank structure. For an M subband filter with conventional polyphase structure, complexity is equivalent to the length of the prototype filter and the M point FFT, $N + M \log_2 M$. The M subbands can be divided into two stages M_1 and M_2 such that $M = M_1 M_2$, where M_1 is the number of subbands in first stage and M_2 is the number of subbands in second stage. The complexity is $2N + M_1 \log_2 M_1 + M_2 \log_2 M_2$. The complexity of the first stage is $N + M_1 \log_2 M_1$ and the complexity of second stage is $N + M_2 \log_2 M_2$, where N is the length of prototype filter. The computational complexities of the filter bank structure for different stages and subband resolution are given in Table 5.1.

As per IEEE 802.22 standard, if the spectrum sensing is done in a 6 MHz channel to detect a WM having a bandwidth of 200 kHz, different filter bank structures can be considered. The spectral resolution to detect the WM in TV channels can be calculated

Table 5.2: Comparison of computational complexity in terms of multiplications for different filter bank methods. Example: $M = 32; M_1 = 8; M_2 = 4; N = 51$

Method	**Computational Complexity**	**Example value**
Direct Implementation	NM	1632
Conventional polyphase FB method	$N + M \log_2 M$	211
MS-DFTFB [122]	$N + M_1 \log_2 M_1 + 2N + M_2 \log_2 M_2$	185
Proposed method	$2N + M_1 \log_2 M_1 + M_2 \log_2 M_2$	134

using the relation given below,

$$M = \lceil \frac{B_{TV}}{B_{WM}} \rceil, \tag{5.3}$$

where B_{TV} is the bandwidth of the TV channel and B_{WM} is the bandwidth of the wireless microphone. The operator $\lceil \rceil$ is used to select the value of M as the least integer that is equal to or greater than power of two. When $B_{TV} = 6$ MHz and $B_{WM} = 200$ KHz then, $M = 32$ subbands are sufficient to detect WM in all scenarios. If the latency need to be reduced, a 32 subband filter can be considered in the first stage. This is sufficient to detect WM in all possible scenarios, as the spectral resolution of the subbands is 187.5 kHz. For a trade-off between complexity and latency, two stages with either $M_1 = 16$ and $M_2 = 2$ subbands or $M_1 = 8$ and $M_2 = 4$ subbands can be considered. The comparison of computational complexity of the proposed method with existing methods using filter bank structures is shown in Table 5.2.

5.2.3 Centroid Method

We use the centroid method to estimate the center frequency of the primary users. The center of each subband represents the energy in that subband resolution as shown in Figure 5.5. The energies can be modeled as a trapezoid and the center frequency can be calculated from the centroid of the trapezoid. The centroid of the trapezoid is explained in detail in Appendix A. The top edge of the distribution can be defined using a linear function $f(x) = b + \frac{x}{h}(a - b)$. The area of a trapezoid is given as $A = \frac{h}{2}(a - b)$. The

centroid in the x direction is computed as

$$A\bar{x} = \int_0^h xf(x)dx = \int_0^h x(b + \frac{x}{h}(a-b))dx = \frac{h^2}{6}(2a+b), \tag{5.4}$$

where $\bar{x} = \frac{h}{3}(\frac{2a+b}{a+b})$, and A is the area of the trapezoid. Here, $\bar{x}$ represents the centroid of the trapezoid. In case of equal energy at the output of individual subbands, i.e., when $a = b$, the midpoint can be verified as $\bar{x} = h/2$. The center frequency of WM is related to $\bar{x}$, h represents the granularity of filter bank M, a and b are related to the energies, E_1 and E_2 of the adjacent subbands. The minimum of two subband energies are represented as a, i.e., $a = \min(E_1, E_2)$, and maximum as $b = \max(E_1, E_2)$. Thus, the estimated center frequency $\hat{f}_c$ can be expressed as follows:

$$\hat{f}_c = \frac{h}{3}\left(\frac{2a+b}{E_1+E_2}\right) \tag{5.5}$$

A generalized expression is obtained by considering the energies of subband E_i and adjacent subband E_{i+1}.

$$\hat{f}_c = \frac{h}{3}\left(\frac{2\min(E_i, E_{i+1}) + \max(E_i, E_{i+1})}{E_i + E_{i+1}}\right) \tag{5.6}$$

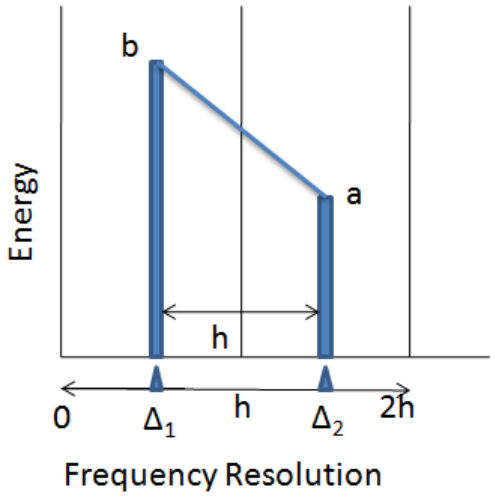

Figure 5.5: Centroid method

The centroid method provides better accuracy in center frequency estimation when the number of detected subbands is two. If the number of detected subbands is beyond two the centroid method does not provide accurate estimation of center frequency. Since the energy distribution can no longer be modeled as a trapezoid and the top edge can

not be written as a linear function. In such cases, a center of mass method is used for estimation of center frequency. The center of mass method is explained in detail in Section 5.2.5.

5.2.4 Multi-User Detection in Wideband Spectrum

One of the key features of CR, is to detect the unused spectrum bands within users in the available bandwidth. In a muti-user environment with available apriori information regarding the number of users, bandwidth of each user, and sensing bandwidth, an attempt is made to calculate the center frequency and estimate the spectral edges accurately. A center of mass method is used in multi-user environment since the number of subbands detected can be more than two as multiple users with different bandwidth can appear in the sensing bandwidth. The computational complexity can be reduced to determine the occupied spectrum using a multistage polyphase filter bank. The unused spectrum can be utilized opportunistically to improve the overall spectrum utilization. The choice of the filter bank resolution in multi-user detection in wideband scenarios is important to reduce the computational complexity and improve the detection accuracy.

The spectral resolution of the filter bank can be deterministically calculated if the apriori information regarding the bandwidth of the different primary users in the sensing bandwidth is available. Consider, N_u as the number of primary users $\{PU_1, PU_2, \ldots, PU_{N_u}\}$ having bandwidth $\{B_1, B_2, \ldots, B_{N_u}\}$ present over the available spectrum sensing bandwidth B. The sensing bandwidth is assumed to be sparse such that $\sum_{j=1}^{N_u} B_j < B$; where, $j = 1, 2, \ldots, N_u$. The number of subbands required in each stage can be calculated deterministically using the relation below:

$$M_{max} = \lceil \frac{B}{\min\{B_1, B_2, \ldots, B_{N_u}\}} \rceil \tag{5.7}$$

The operator $\lceil \rceil$ is used to select the least integer that is greater than or equal to powers of two. M_{max} determines the spectral resolution of the filter bank and is dependent on the smallest bandwidth of the primary user. In order to reduce computational complexity, M_{max} can be further decomposed using the relation $M_{max} = M_1 M_2$. The selection of M_1 and M_2 depends on the sparseness of the primary users and available bandwidth.

If the filter bank is implemented with a spectral resolution of M_{max}, the detection

of narrowband users appearing in the sensing bandwidth becomes easier. Since M_{max} is calculated considering the bandwidth of the narrowband users, the spectral resolution of the filter bank will have finer granularity. The finer granularity in filter banks inturn increases the computational complexity of the filter bank structure. If the latency need to be reduced M_{max} should be considered for filter bank implementation. For a trade-off between complexity and latency M_{max} can be decomposed and multistage filter bank structure can be considered for spectrum sensing. In our method, M_{max} is decomposed into two stages in order to reduce the computational complexity.

Two scenarios can occur when primary users of different bandwidth are sensed in a wide bandwidth as illustrated in Figure 5.6.

Case 1: When the primary users occupy more than one subband, for example PU_1 and PU_3 as shown in Figure 5.6, the center frequency can be estimated in the first stage with a computational complexity of $N + M_1 \log_2 M_1$ using the center of mass method.

Case 2: If any primary user appears exclusively within a single subband, for example PU_2 as shown in Figure 5.6, the center frequency and spectral edges can be estimated in the second stage with a computational complexity $2N + M_1 \log_2 M_1 + M_2 \log_2 M_2$.

For better accuracy in detection, the spectral edges can be sensed with finer resolution depending on the binary detection. The edges can be identified from the binary detection as they have a 10 or 01 transitions, which is illustrated in Figure 5.8. However, this increases the computational complexity of the detection process. The merit of our method is that only the spectral edges are sensed with finer granularity instead of the entire spectral band of the primary user. For most of the sensing scenarios, Case 1 and Case 2 are sufficient to detect the center frequency and estimate the spectral edges. Since multiple users are present in the sensing bandwidth the different users will have different bandwidth. The number of subbands detected by the primary users can be more than two subbands. In such cases the centroid method can not be applied to determine the center frequency. Therefore, a novel method based on center of mass is proposed to estimate the center frequency and spectral edges.

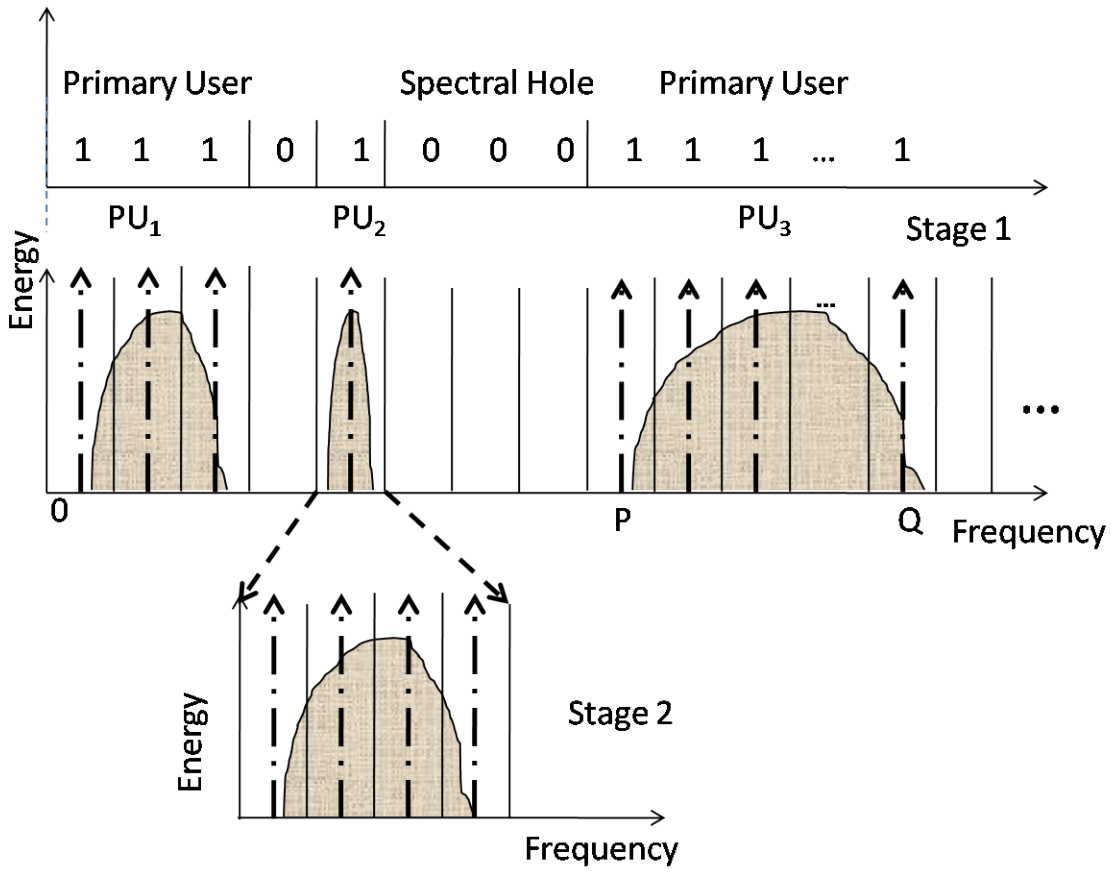

Figure 5.6: Illustration of binary detection and multistage filter banks

5.2.5 Center of Mass Method

In Section 5.2.3, a centroid based method was proposed for detection of single narrow band users in wideband spectrum along with center frequency estimation. The centroid method can be applied for center frequency estimation only when the detected subbands are at most two. When the number of detected subbands are beyond two, the center frequency can be estimated using a center of mass based method. The center frequency is calculated using the energy at the output of detected subbands and spectral resolution of the filter bank. We use center of mass method to compute center frequency, where mass is related to energy and distance is related to frequency.

The center of mass method is illustrated in Figure 5.10. Consider the energy in different subbands as $E_1, E_2, \ldots, E_k$ and $\Delta_1, \Delta_2, \ldots, \Delta_k$ as the center point of the subbands and Δ as the spectral resolution of subbands in the filter banks as shown in Figure 5.10. Then the center frequency of the k detected subbands can be calculated

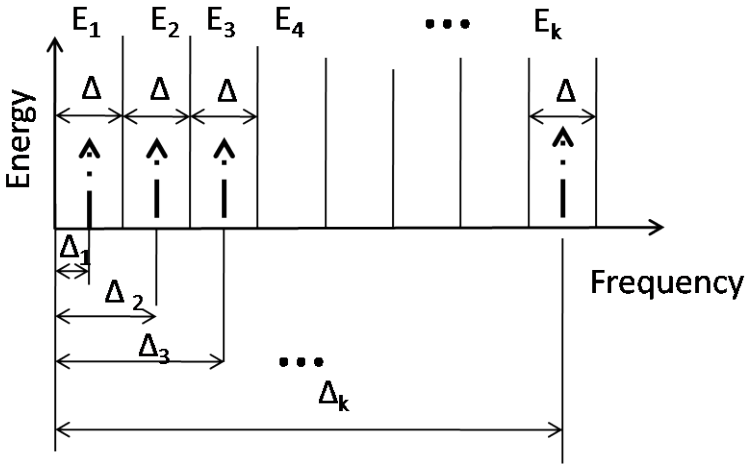

Figure 5.7: Illustration of center of mass method

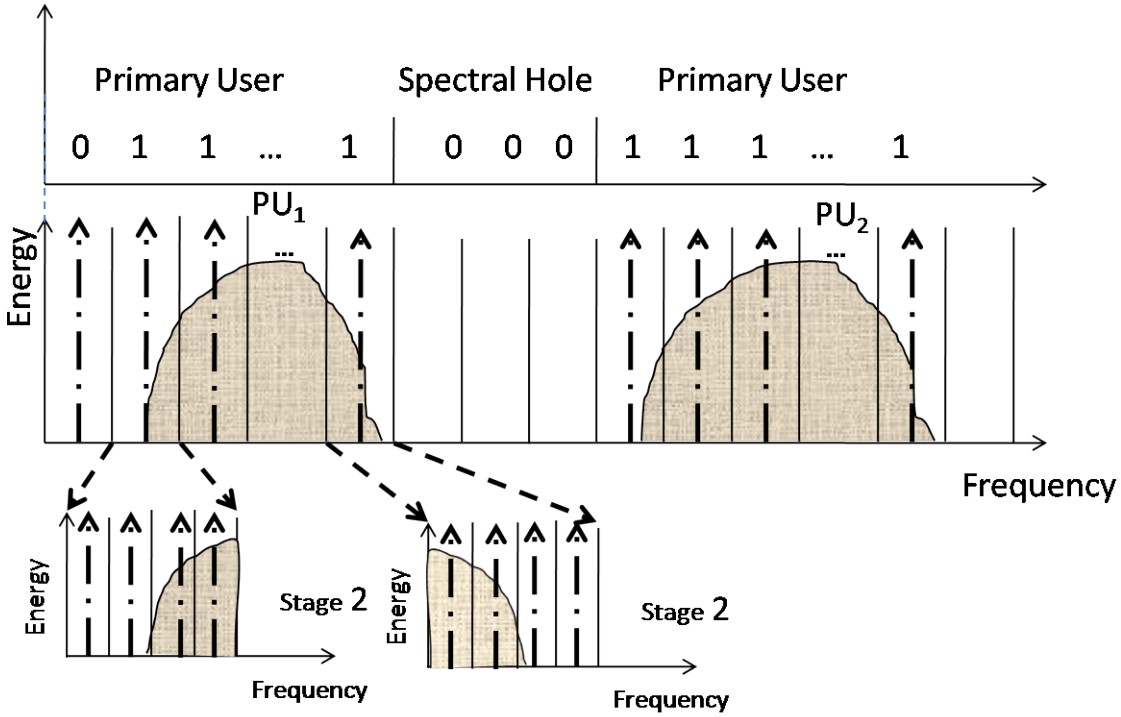

Figure 5.8: Illustration of spectral edge detection with fine resolution

using the Equation 5.8

$$\hat{f}_{cd} = \frac{\sum_{i=1}^{k} E_i \Delta i}{\sum_{i=1}^{k} E_i} \tag{5.8}$$

where, $i = 1, 2, ..., k$. For an M point DFT based polyphase filter bank, the number of subbands are $k = 1, 2, \ldots, M$. Consider (P^{th} to Q^{th}) subbands are occupied by a primary user ($E_k > \lambda$), where $k = P, \ldots Q$, which is illustrated in Figure 5.6 for

primary user PU_3. The center frequency of a primary user is estimated as,

$$\hat{f}_{cd} = \frac{\sum_{k=P}^{R} E_k \Delta_k}{\sum_{k=P}^{Q} E_k}; k = P, \ldots, R, \tag{5.9}$$

where, $\Delta_k = \Delta(k-1) + \dfrac{\Delta}{2}$. E_k represents the energy at the output of the k^{th} subband, Δ_k is the center frequency of the k^{th} subband, P is the first occupied subband number of a primary user, Q is the last occupied subband number of the same primary user, and Δ spectral resolution of each spectral band as illustrated in the Figure 5.10.

The center frequency calculation can be extended for estimating the spectral edges of the primary users. The filter bank detects the number of subbands occupied by a primary user over the available bandwidth from the energy detection method. The information regarding the number of subbands and the center frequency can be used to estimate the spectral edges of the primary user. The rising and falling edges of the detected primary user are,

$$\hat{f}_{rise} = \hat{f}_{cd} - B_x/2 \tag{5.10}$$

and,

$$\hat{f}_{fall} = \hat{f}_{cd} + B_x/2, \tag{5.11}$$

where, B_x is the bandwidth of the communication channel/primary user identified depending on the number of subbands detected using energy detection.

Center Frequency of Conventional Filter Banks

In conventional filter bank method, the center frequency is determined using the relationship given in Equation 5.12.

$$\hat{f}_{cd} = (P + Q - 1)\,\frac{\Delta}{2} \tag{5.12}$$

That is, the center frequency is the midpoint of the detected subbands. In conventional filter bank method, the center frequency is a function of spectral resolution.

5.3 Simulation

In this section, we discuss the simulation setup and results for single user and multiple users. The single user detection is explained considering the detection of WM appearing in a wideband TV channel using signal following IEEE 802.22 WRAN standard. The center frequency is calculated using the centroid method for different center frequencies. We simulated multi-users considering the different communication standards such as Bluetooth, Zigbee, and WCDMA appearing in a wideband channel . The center frequency in case of multi-user was calculated using the center of mass method and the spectral edges are estimated. In both the cases the detection accuracy of center frequency is calculated using the relative percentage error given in Equation 5.13

$$\%Error = \left(\frac{f_{cd} - \hat{f}_{cd}}{f_{cd}} \times 100 \right) \tag{5.13}$$

5.3.1 Simulation Setup for Wireless Microphone Detection

The sensing performance (detection and estimation of center frequency) of the WM is determined using simulation model provided in [127]. The WM signals are simulated using frequency modulation as in [118]. We assume the sensing bandwidth is 6 MHz.

Stage 1 has a spectral resolution of 750 kHz (π/M_1) for $M_1 = 8$ and Stage 2 has the number of subbands $M_2 = 4$, with spectral resolution 187.5 kHz (π/M_1M_2). The polyphase decomposition of spectrum in Stage 1 is [0-0.375-1.125-1.875-2.625-3.375-4.125-4.875-5.625-6] MHz. WM has three different operating modes, silent, soft, and loud. The three different operating modes in indoor environment recommended in [127], are used to generate frequency modulated WM signals. The power spectral density of the frequency modulated WM as per the specification given in Table 5.3 is shown in Figure 5.9.

The simulation parameters are given in Table 5.4. Three different scenarios are considered here.

Case 1: If WM appears with a center frequency of 1.1 MHz, the subband 2 and subband 3 are sensed as shown in Figure 5.10 and the center frequency is determined using the centroid method.

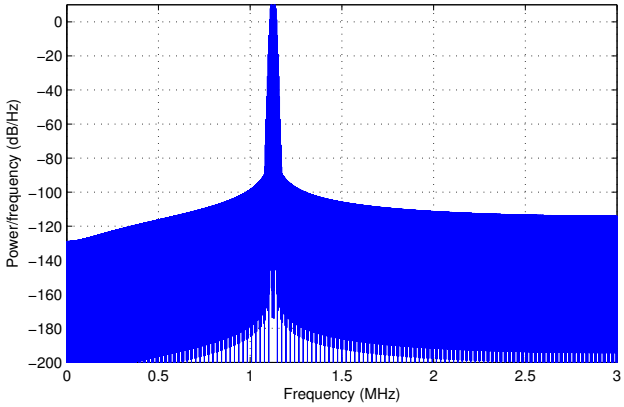

(a) Soft Mode

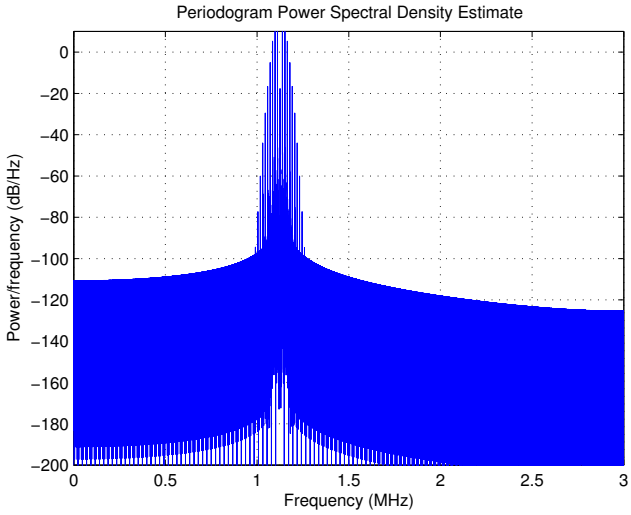

(b) Loud Mode

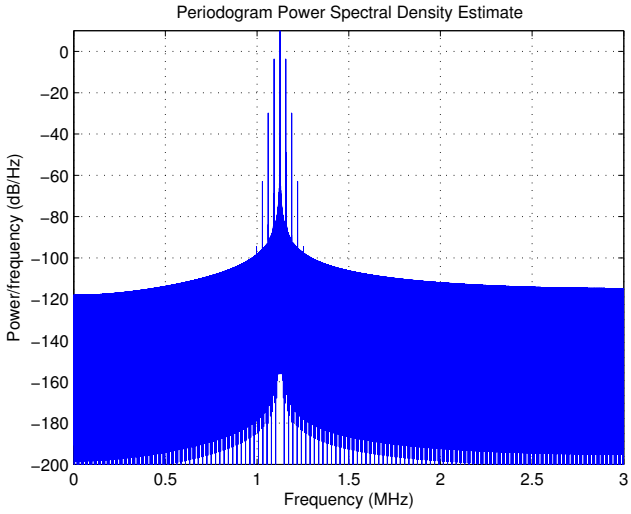

(c) Silent Mode

Figure 5.9: WM operating conditions

Table 5.3: WM operating conditions

Operating Mode	f_m **kHz**	Δf **kHz**	β
Silent	32	5	0.16
Soft	3.9	15	3.85
Loud	13.4	32.6	2.43

Case 2: If the WM appears with a center frequency of 1.125 MHz, the subband 2 and subband 3 have equal energy as shown in Figure 5.11. The center frequency of WM is at the midpoint of the two subbands.

Case 3: If the WM appears with a center frequency of 0.65 MHz, the subband 2 has higher energy compared to other subbands as shown in Figure 5.12, and the output of detected subband is further sensed with finer resolution in Stage 2 to locate the center frequency using centroid method. The condition is shown in Figure 5.13 for a spectral resolution of $M_2 = 4$.

It can be inferred, that except for Case 3, the detection and center frequency estimation of WM is completed in Stage 1 with less computational complexity and latency.

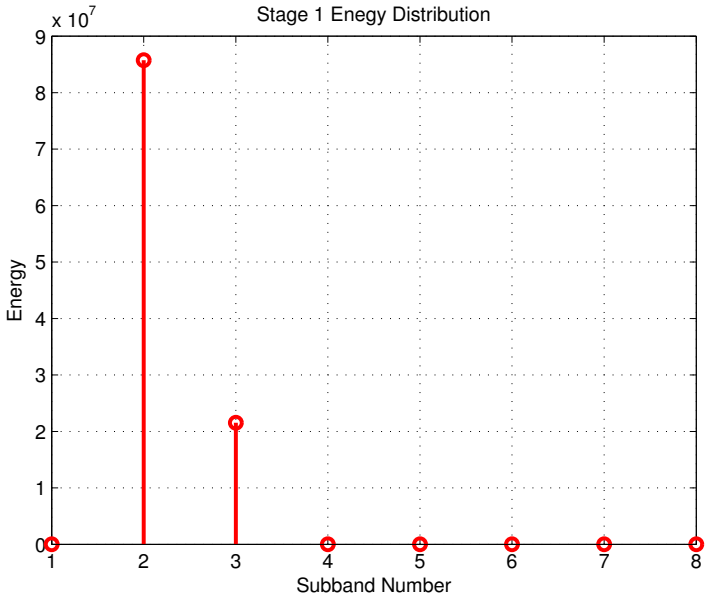

Figure 5.10: Energy distribution for Case 1

The accuracy of center frequency estimation concerning WM using the proposed method was compared with conventional polyphase DFT filter bank methods for different number of subbands $M = 8$, $M = 16$, and $M = 32$. The accuracy of the multistage

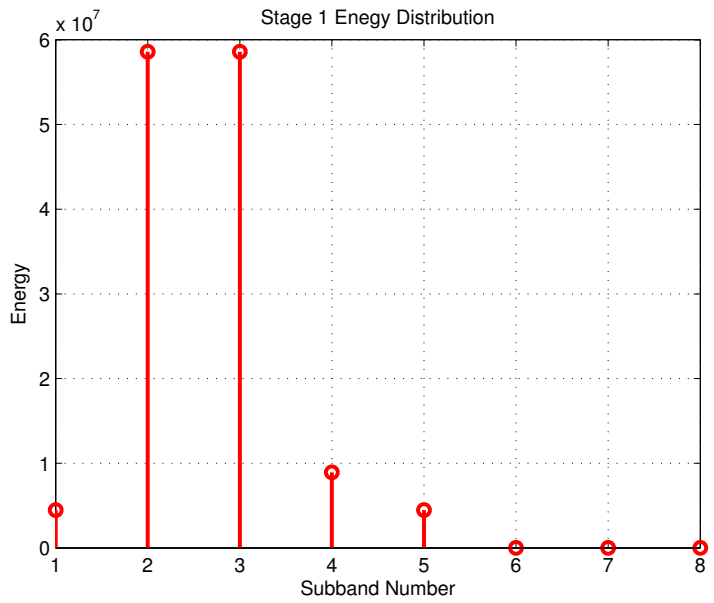

Figure 5.11: Energy distribution for Case 2

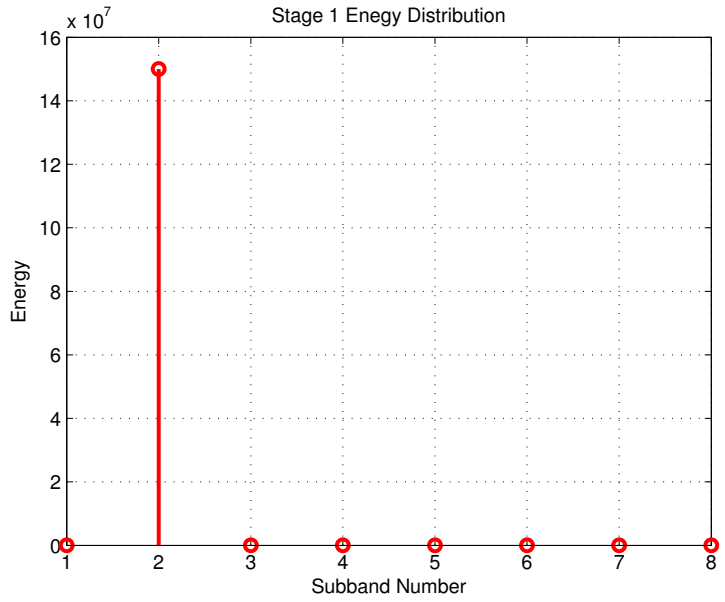

Figure 5.12: Energy distribution for Case 3

method in [122] is same as the conventional polyphase DFT filter bank method [59]. In our method, the number of subbands in the first stage was chosen to be $M_1 = 8$ and the second stage $M_2 = 4$. Simulations are performed for different center frequencies with different operating modes of WM over a sensing bandwidth of 6 MHz with SNR varying from 0 to -20 dB. A comparison of our method with the conventional methods for center frequency estimation in terms of percentage error is shown in Figure 5.14. It can be inferred from Figure 5.14 that our method has the percentage error less than

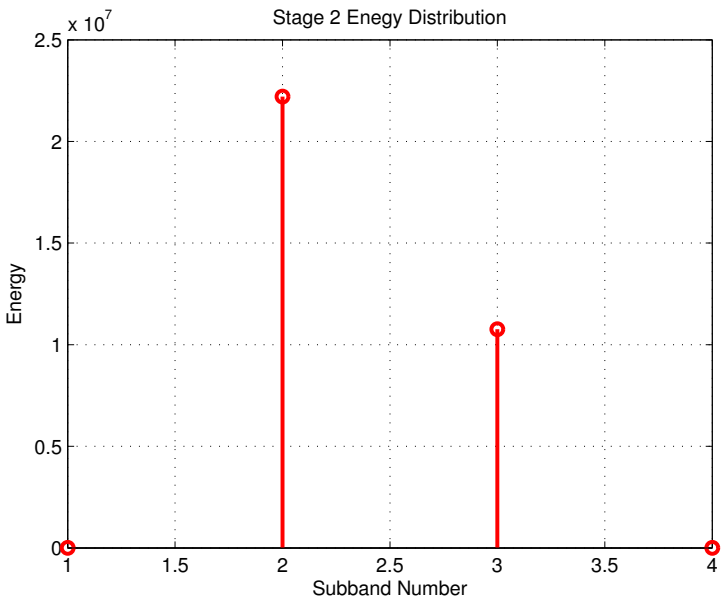

Figure 5.13: Energy distribution at the output of subband 2 in Case 3 for a spectral resolution of $M_2 = 4$ in second stage

Table 5.4: Simulation parameters

Parameter	**Value**
Capture time τ	2 sec
Bandwidth B MHz	6 MHz
Sampling time Ts	1/12 MHz
Number of samples	$N = \tau Ts$
Samples in first stage (M_1=No.of subbands in stage 1)	N/M_1
Samples in first stage (M_2=No.of subbands in stage 2)	N/M_1M_2
Latency	$N/M_1(Ts) + N/M_1M_2(Ts)$
Subband attenuation	100 dB
Prototype filter length	127

4% which is better compared to conventional filter bank methods. It is also observed that, for coarser resolution $M = 8$, the percentage error is much higher compared to finer resolutions $M = 16$ and $M = 32$. The computational complexity of proposed

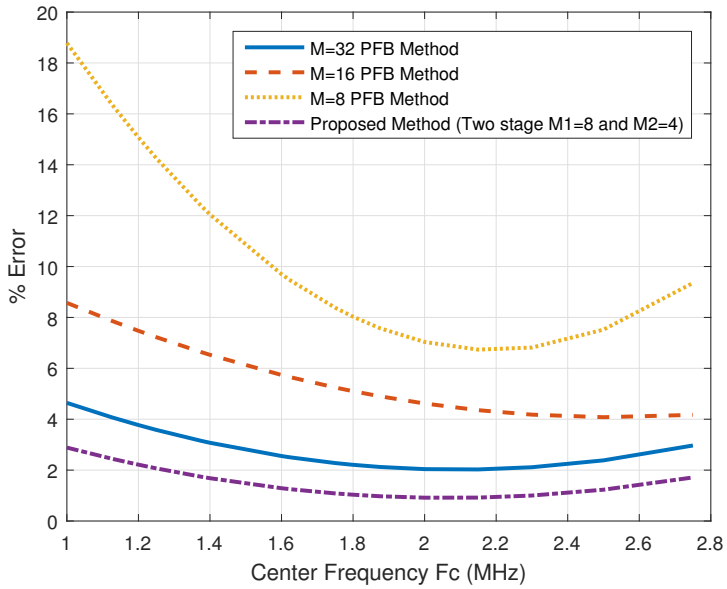

Figure 5.14: Comparison of proposed method with conventional methods for different center frequencies of WM

method along with the other methods is tabulated in Table 5.2. The proposed method provides better accuracy in the estimation of center frequency regarding WM with less computational complexity.

5.3.2 Simulation Setup for Muti-user Detection

For simulation with multi-users, we considered signals with three different communication standards Bluetooth (PU_1: $B_1 = 1$ MHz), Zigbee (PU_2: $B_2 = 4$ MHz), and Wideband Code Division Multiple Access (PU_3: $B_3 = 5$ MHz) [2]. Simulation parameters are given in Table 5.5. The simulations are performed for different values of SNR varying from 0 dB to -15 dB. A typical signal spectrum with the three primary users is shown in Figure 5.15. The center frequency of different primary users f_{c1}, f_{c2}, and f_{c3} are varied during the simulation. $\lceil M_{max} \rceil = 32$ calculated using Equation 5.7 is further decomposed into two factors with $M_1 = 16$ and $M_2 = 2$. The energy distribution for the three primary users with $M_1 = 16$ is shown in Figure 5.16. In order to show the merit of the proposed method, a comparison of relative error between filter bank method and center of mass method in the estimation of different center frequency for a primary user PU_2 with an SNR of -5 dB is shown in Table 5.6. It is inferred from the Table 5.6 that the center of mass method achieves better detection accuracy compared

to filter bank method even in a coarser level of spectrum sensing.

Table 5.5: Simulation Parameters [2]

Parameter	**Value**
Sensing Bandwidth B MHz	20
Sampling time Ts	1/40
Capture time τ	2 sec
Number of samples	$N = \tau Ts$
Subband attenuation	100 dB
Prototype filter length	127
No. of Primary Users : Bluetooth (PU_1), Zigbee(PU_2), WCDMA (PU_3)	3
Bandwidth of PU in MHz	1, 4, 5
Spectral resolution of filter bank M	32
Spectral decomposition of filter bank $M = M_1 M_2$,	$M_1 = 16$, $M_2 = 2$

Table 5.6: Comparison of relative error between center of mass method and filter bank method $\left(\frac{f_{cd} - \hat{f}_{cd}}{f_{cd}} \times 100 \right)$ for PU_2

Center Frequency	**Proposed Method**		**Filter Bank Method**	
f_{cd}	$\hat{f}_{cd}$	Error%	$\hat{f}_{cd}$	Error%
6.5	6.6197	1.8415	6.875	5.7690
7	6.9609	0.5585	6.875	1.7850
7.5	7.5025	0.0333	7.5	0.0000
8	8.0315	0.3937	8.125	1.5625
9	9.131	1.4555	9.375	4.1666
13	13.035	0.2692	13.125	0.9615

Simulations are done simultaneously for detecting the primary users and calculating the center frequency. The calculation of the center frequency of the three primary users for varying center frequencies are shown in Table 5.7. It can be inferred that filter bank methods provide better performance only when the center frequencies of the primary users appear at integer multiples of the spectral resolution.

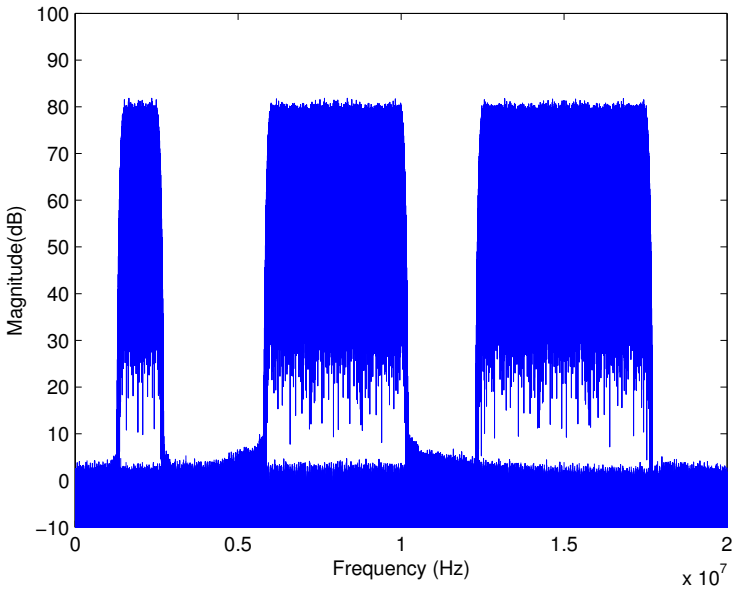

Figure 5.15: Spectrum containing BT, Zigbee and WCDMA for $f_{c1} = 2MHz$, $f_{c2} = 8MHz$, and $f_{c3} = 15MHz$

The rationale for better accuracy in the proposed center of mass method is due to the fact that the estimation of the center frequency depends on the energy in each subband as well as the spectral resolution of the filter banks. In filter bank method, the center frequency is a function of spectral resolution alone. The comparison of the proposed method with the conventional methods for center frequency estimation in terms of percentage error is shown in Figure 5.17. It can be inferred from Figure 5.17 that the proposed method has the percentage error better compared to the conventional filter bank methods. The detection precision of filter bank method can be made similar to the proposed method with finer spectral resolution at the expense of higher computational complexity. Simulation results show that the center of mass method detects center frequencies with better accuracy than conventional filter bank techniques.

5.4 Summary

In this chapter, wideband spectrum sensing using polyphase filter banks was discussed. Multistage polyphase filter banks were used to reduce computational complexity due to its efficient structure. The sensing was performed from finer to coarser spectral resolution using multistage filter banks. We proposed a centroid method for computing the

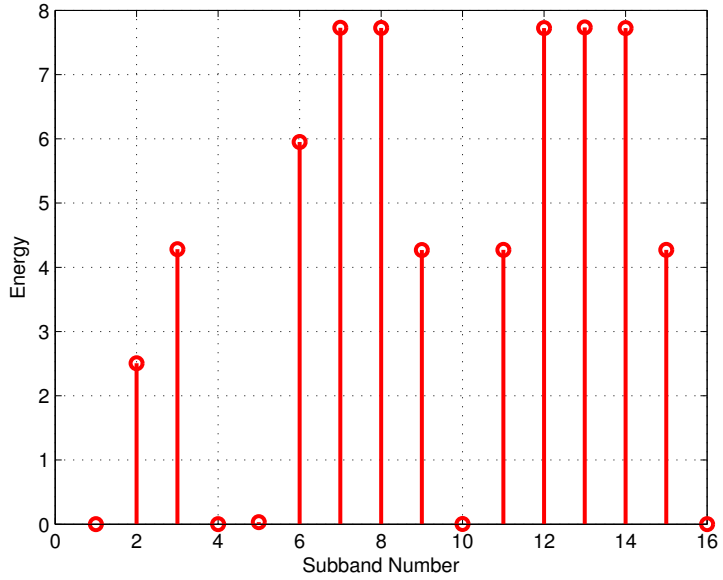

Figure 5.16: The energy distribution at the output of individual subbands for $M_1 = 16$

center frequency of WM in TV channels depending on the energy at the output of the subbands in the filter bank. The centroid method provides better accuracy in center frequency estimation when the number of detected subbands is two. The centroid method detects the presence of WM depending on the energy distribution at the output of each subband. Compared to the existing schemes, the proposed method has less computational complexity. If the number of detected subbands is greater than two, the center of mass method was used for estimation of center frequency.

The rationale behind the center of mass method was, mass is related to energy and and distance is related to frequency. A center of mass based method was useful for computing the center frequency of multiple users in a wideband spectrum and estimating the spectral edges. Computational complexity is reduced in most of the cases, using the center of mass or centroid method the detection process can be completed in the first stage with coarser resolution. It is shown through exhaustive simulation that the proposed scheme based on multistage polyphase filter bank and center of mass method can estimate the center frequency of primary user with higher precision and detect spectral edges with reduced computational complexity. The proposed method outperforms the conventional filter bank as it can exploit the uniqueness of center of mass in center frequency estimation with high precision in addition to low computational complexity due to multistage polyphase filter bank. The rationale behind adapting this method along

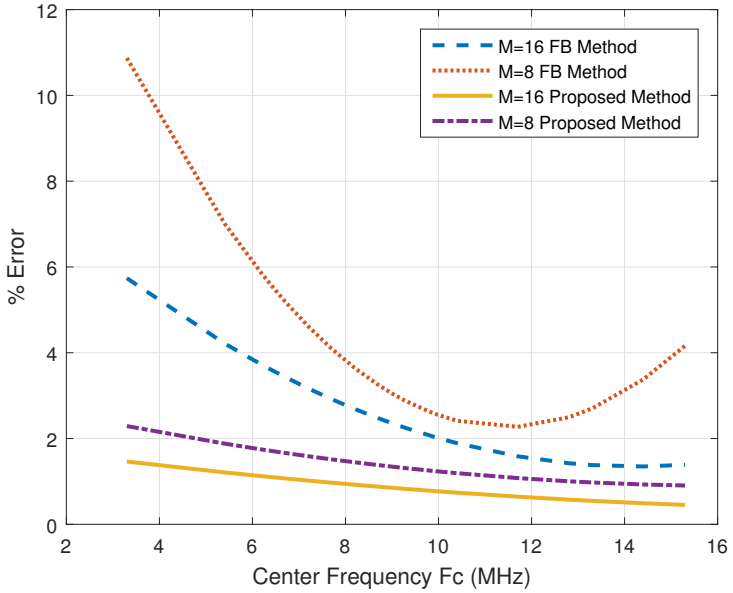

Figure 5.17: Comparison of proposed method with conventional methods for different center frequencies of Zigbee in SNR = -5 dB

with the mathematical derivation for calculation of center frequency and spectral edges are discussed in detail. In the next chapter, we discuss non-uniform digital channelizers using filter banks.

Related publication

A Low Complexity Multistage Polyphase Filter Bank For Wireless Microphone Detection in CR, *Circuits, Systems, and Signal Processing, Springer*, **36**, 1671-1685 (2016).

Table 5.7: Comparison of relative error between center of mass method and filter bank method for three primary user appearing simultaneously

User No.	**Center Frequency** f_c	**Proposed Method** $\hat{f}_{cd}$	**Filter Bank Method** $\hat{f}_{cd}$	**Proposed Method Error%**	**Filter Bank Method Error%**
Primary User - 1	2.0	1.886	1.875	5.665	6.25
	8.0	7.999	8.125	0.008	1.562
	8.5	8.464	8.125	0.415	4.411
	15.5	15.499	15.625	0.005	0.805
	10	9.998	10.000	0.018	0.000
Primary User - 2	8.0	8.029	8.175	0.308	1.562
	4.0	4.022	3.750	0.555	6.250
	4.5	4.475	4.375	0.540	2.777
	10.0	9.988	10.000	0.113	0.000
	15.0	15.000	15.000	0.000	0.000
Primary User - 3	15.0	15.000	15.000	0.000	0.000
	14.0	13.994	13.750	0.036	1.785
	15.0	15.000	15.000	0.000	0.000
	4.0	3.994	3.750	0.130	6.250
	5.0	5.000	5.000	0.000	0.000

CHAPTER 6

Non-Uniform Filter Bank Channelizer

Applications such as digital channelizer in Software Defined Radio (SDR), digital audio industry, biomedical signal processing, subband adaptive filtering, and communication require non-uniform frequency partitioning inorder to better exploit the signal characteristics [128]. In such applications, implementation of non-uniform filter banks has elicited enormous interest in multirate signal processing. Particularly, the digital channelizers are useful to select narrowband channels from wideband signal. Different wireless standards have different bandwidths, therefore non-uniform filter banks are useful in such applications. Due to the advantages of digital channelizers in SDR, more attention is given to improve the performance of non-uniform filter banks [129].

In this chapter, we discuss the design of non-uniform filter banks (NUFB) with channel combiners using single and multiple prototype filter approaches. In single prototype approach, the NUFB is realized using uniform cosine modulation filter bank (CMFB) structure. The uniform CMFB was implemented from a single FIR, Type-1 prototype filter. CMFB is designed to satisfy Near Perfect Reconstruction (NPR) conditions such that the 3 dB point of the prototype filter is optimized at $\frac{\pi}{2M}$, where M is the number of subchannels in the corresponding uniform filter bank. Channel combiners are employed to combine the subbands of uniform filter bank. The limitation of single prototype approach is that, when the number of combiners increases the distortions introduced in the filter bank increases.

The multi-prototype based method reduces the number of channel combiners and residual errors compared to single prototype based channel combination techniques. In multi-prototype method, the prototype filters with different passbands are optimized independently. In Section 6.1 the existing methods and conditions to be satisfied in the design of non-uniform filter banks are discussed. Single prototype approach is explained in Section 6.2 and multi-prototype approaches in Section 6.3. Simulation results and comparison of single and multiple prototype approaches are detailed in Section 6.4.

6.1 Introduction

Filter banks for various applications demand good frequency response with reduced implementation complexity. The frequency selectivity of the filter bank depends on the small passband ripple, high stopband attenuation, and narrow transition width. An important application of NUFB is digital channelizers in software defined radios (SDR) to select individual channels from a wideband signal. SDR require stringent specification on the design of filter banks with narrow transition width and low implementation complexities. Different non-uniform filter bank channelizers have been proposed earlier using multiplier-less cosine modulated filter banks to reduce the complexity by representing the coefficients as canonic signed digits and optimizing the filter coefficients with modified meta heuristic algorithms [130], [129].

In general the approach used for the design of a NUFB is a direct method, which involves nonlinear optimization with different parameters [131]. NUFB can be implemented indirectly by merging uniform filter banks to achieve near perfect reconstruction [132]. Tree structure based NUFB using linear optimization is also widely discussed in literature. However, this approach accumulates the system delay with a number of stages and can implement subbands in powers of two [133], [134]. Transmultiplexers (TMUX) are also used for the non-uniform partitioning of the spectrum. A multimode transmultiplexer employing Farrow structures for non-uniform decomposition of signals is proposed in [135]. The constraints for designing an NUFB are discussed in [136].

Cosine modulated filter bank is an attractive choice for the design of NUFB due to its simple design and frequency characteristics. Different methods are used for the generation of NUFB using cosine modulated filter banks. A linear phase NUFB with interpolated prototype filter is proposed in [137]. NUFB was implemented by merging uniform filter banks in cases where, the upper band edge frequency of each non-uniform filter is an integer multiple of the bandwidth of the corresponding uniform band in [138]. The design of NUFB from uniform filter banks using cosine modulation has also been addressed in [139] and [140].

Most of the literature mention NUFB design using a single prototype approach due to the simplicity in its design. A design of cosine modulated non-uniform linear phase

FIR filter bank through the stretching and shifting of a single prototype filter is proposed in [141]. Non-uniform filter banks implemented with more than one prototype (multiprototype) with different passbands are discussed in [142]. The filter banks were designed with numerical optimization of a narrowband prototype filter. All the other prototype filters were derived from the narrowband prototype filter. The multi-prototype approach in [142] was particularly suitable for the design of filter banks with large number of filter coefficients.

In this thesis, we focus on the generation of NUFB based on single and multi-prototype approaches using channel combiners. Channel combiner approach was initially used to generate non-uniform filter banks from a uniform filter bank. The uniform filter bank was implemented by modulating a single prototype filter. However, when widebands are required from a narrowband prototype filter the number of additions and subsequent distortions caused due to merging is significantly high. The distortions/residual errors in single prototype filter approach can be overcome by the multi-prototype approach. In multi-prototype approach, the number of combinations are reduced by designing prototype filters with different passbands. Hence, the amplitude distortion of the designed NUFB is also reduced.

6.1.1 Review of Non-Uniform Filter Banks

In the design of NUFB, certain conditions have to be satisfied to achieve near perfect reconstruction. The necessary and sufficient conditions required in the implementation of NUFB are detailed in [136]. Consider an NUFB shown in Figure 6.1, where decimation factors n_k are integers. The filter bank is said to be maximally decimated if the channel decimation factors n_k satisfies the following condition,

$$\sum_{k=0}^{L-1} \frac{1}{n_k} = 1, \tag{6.1}$$

where, L is the number of non-uniform subbands.

Decimation factors are not the same for all the subbands in NUFB and has to be constrained to Equation 6.1, such that the average sampling rate is preserved at the output of the analysis filter bank.

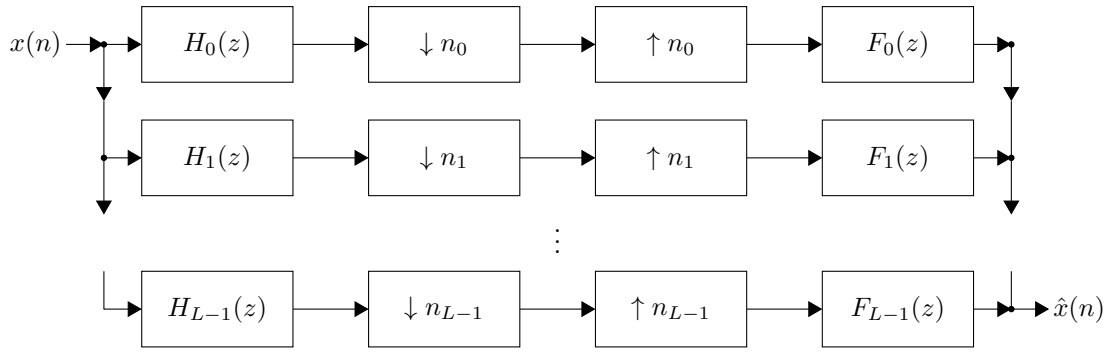

Figure 6.1: L band non-uniform filter bank [4]

In case of M maximally decimated uniform filter banks with analysis filter bank $H_k(z)$ and synthesis filters $F_k(z)$, the reconstructed signal can be written as

$$\hat{X}(z) = T(z)X(z) + \sum_{l=1}^{M-1} T_l(z)X(zW_M^l), \tag{6.2}$$

where $W_M = e^{-j(2\pi/M)}$. The distortion function $T(z)$ is given as per Equation 6.3 and also represents the amplitude distortion.

$$T(z) = \frac{1}{M}\sum_{k=0}^{M-1} F_k(z)H_k(z) \tag{6.3}$$

The aliasing error is given by Equation 6.4.

$$T_l(z) = \frac{1}{M}\sum_{k=0}^{M-1} F_k(z)H_k(zW_l^M) \tag{6.4}$$

The three main errors that occur in uniform filter banks are aliasing error, amplitude distortion, and phase distortion. Methods to cancel such errors in uniform filter banks are well proven.

In case of NUFB the reconstructed signal $\hat{X}(z)$ is given by [1] and [4], as

$$\hat{X}(z) = \sum_{k=0}^{L-1} \bar{F}_k(z)\frac{1}{n_k}\sum_{l=0}^{n_k-1} X\left(zW_{n_k}^l\right)\bar{H}_k\left(zW_{n_k}^l\right), \tag{6.5}$$

where $W_{n_k} = e^{-j2\pi/n_k}$. Unlike uniform filter banks, the two summation in Equation 6.5 is not interchangeable. Similar to uniform filter banks aliasing error, amplitude distortion, and phase distortion occur in non-uniform filter banks.

In NUFB, aliasing can be eliminated if the compatibility set condition is satisfied with the decimation factors. It is proposed that if the cut-off frequencies of each analysis filter are integer multiples of their bandwidth, aliasing errors can be avoided [139]. Based on the integer factors, Vaidyanathan et al. proposed a compatibility test on the set of possible decimation factors that can be used in NUFB design [4].

Compatibility Test on Decimators

The necessary conditions have been found for the choice of decimation factors such that the NPR condition is satisfied in the design of NUFB [4], [136]. The need for compatibility test arises as each alias frequency at the output should occur at least twice for aliasing to get cancelled. The decimation factors n_k should form a compatible set to pair the alias components in the alias cancellation matrix to cancel aliasing. Compatibility test is proposed in [4] as an algorithm to be performed on the decimator values. The definition of a compatible set is stated as follows:

Let $S = \{n_0, n_1, \ldots, n_{L-1}\}$ be a set of ordered integers $n_0 \leq n_l \leq \ldots \leq n_{L-1}$. The set S is said to be compatible if it satisfies the following conditions:

1. The decimation factors n_k has to be the constrained by $\sum_{k=0}^{L-1} \frac{1}{n_k} = 1$
2. For n_i, $l_i (l_i \leq n_{i-1})$, there exists n_j, $l_j (l_j \leq n_{j-1})$, with $n_j \neq n_i$, such that $W_{n_i}^{l_i} = W_{n_j}^{l_j}$

6.2 Single Prototype Approach

In our approach, we have designed an NUFB using uniform cosine modulated filter bank. The maximum passband ripple magnitudes and the maximum stopband ripple magnitudes of all the analysis filters and the synthesis filters depend on the prototype filter and sampling factors. If the FIR lowpass protoytpe filter are used, the cosine modulated uniform filter banks satisfy linear phase condition. The closed form expressions for analysis and synthesis filters are given in [1] as

$$h_k(n) = 2h(n)cos\left(\frac{\pi}{M}\left(k+\frac{1}{2}\right)\left(n-\frac{N-1}{2}\right)+(-1)^k\frac{\pi}{4}\right), \qquad (6.6)$$

$$f_k(n) = 2h(n)cos\left(\frac{\pi}{M}\left(k+\frac{1}{2}\right)\left(n-\frac{N-1}{2}\right)-(-1)^k\frac{\pi}{4}\right), \tag{6.7}$$

where $0 \leq n \leq N-1$ and $0 \leq k \leq M-1$. The associated NUFB is obtained by combining the adjacent channels of uniform filter banks using channel combiners or adders. Channel combiners add the frequency responses at specific locations of the uniform filter bank to produce a non-uniform bank as illustrated in Figure 6.2. If M is the number of subbands in the uniform filter bank, NUFB can be implemented with L subbands where $(1 \leq L < M)$.

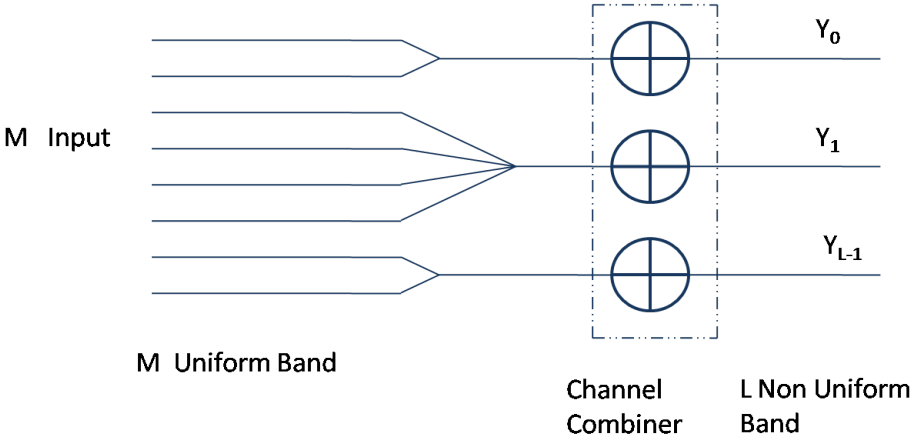

Figure 6.2: Illustration of NUFB from uniform filter bank using channel combiner

The non-uniform banks are generated by combining integer number of subbands constrained to the compatibility condition mentioned in Section 6.1.1. The frequency response of analysis and synthesis filters of non-uniform filter bank is given by,

$$\bar{H}_k(z) = \sum_{m=P_{k-1}}^{P_{k-1}+p_k-1} H_m(z) \tag{6.8}$$

$$\bar{F}_k(z) = \sum_{m=P_{k-1}}^{P_{k-1}+p_k-1} F_m(z), \tag{6.9}$$

where, $P_{l-1} = \sum_{l=0}^{k} p_{l-1}$, $l = 0, 1, \ldots, L-1$ and $P_{-1} = 0$. The number of subbands to be combined to generate the non-uniform subband is represented as p_k. Therefore, for M uniform filter bank there are L non-uniform subbands with different number of subbands p_k, $(k = 0, 1, \ldots, L-1)$ generated from the different decimation factors n_k. The number of subbands satisfies the condition $p_0 + p_1 + \ldots + p_{L-1} = M$ and the

number of subbands to be combined is obtained from the relation $p_k = \dfrac{M}{n_k}$.

For example, consider that a 3 channel NUFB has to be generated from a uniform filter bank of $M = 8$ with decimation factors $(4, 4, 2)$. Then, the corresponding combination needed in the NUFB are $(2, 2, 4)$. The 3 channel NUFB is generated from an 8 channel uniform filter bank using a single prototype filter. The prototype filter designed for a filter length $N = 187$ and subband attenuation $A_s = 100$ dB is shown in Figure 6.3. The 8 channel uniform filter bank implemented from a single prototype filter of length $N = 187$ and subband attenuation $A_s = 100$ dB is shown in Figure 6.4. The 3 channel NUFB generated from a 8 channel uniform filter bank using a single prototype filter is shown in Figure 6.5.

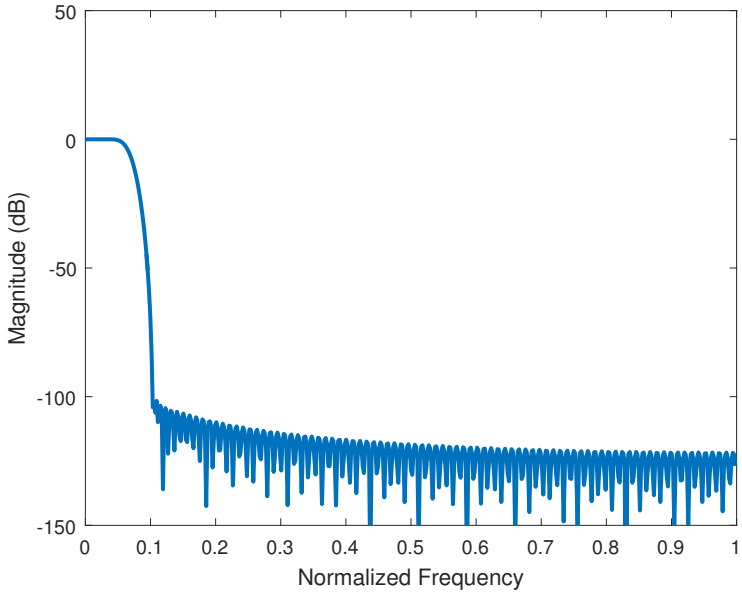

Figure 6.3: Prototype filter with filter length $N = 187$ and subband attenuation $A_s = 100$ dB for $M = 8$ subbands

The prototype filter is optimized to have the 3 dB amplitude response at $\dfrac{\pi}{2M}$. If the adjacent subbands are not combined exactly at 3 dB, distortions occur around the 3 dB as dips or bumps as shown in Figure 6.6. If the subband responses are combined properly at the 3 dB, flat in-band response can be achieved. The improper combination at the 3 dB frequency response lead to amplitude distortions in the filter bank design. Thus, it is necessary that when the adjacent subbands are combined to generate the non-uniform bandwidth, the subband filters are combined exactly at the 3 dB amplitude response to eliminate the distortions.

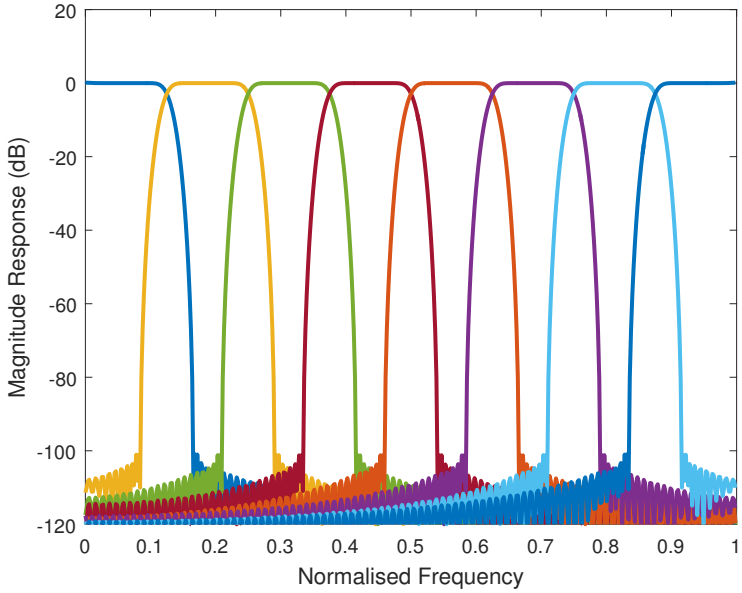

Figure 6.4: 8 channel uniform filter bank implemented from a single prototype filter length $N = 187$ and subband attenuation $A_s = 100$ dB for $M = 8$ subbands

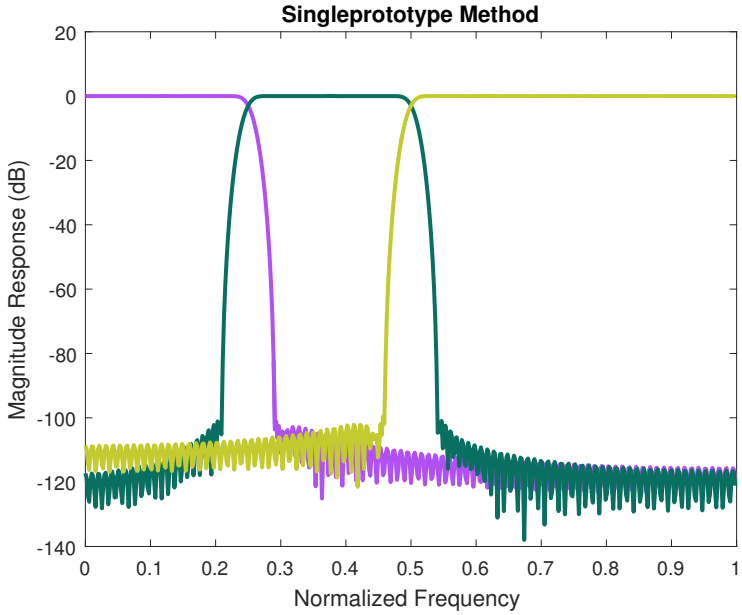

Figure 6.5: 3 Channel NUFB from an 8 channel uniform filter bank using a single prototype filter

As the decimation factors are chosen according to the compatibility condition the aliasing errors get reduced. In the absence of aliasing error the reconstructed signal can be written as

$$\hat{X}(z) = \bar{T}(z)X(z) \tag{6.10}$$

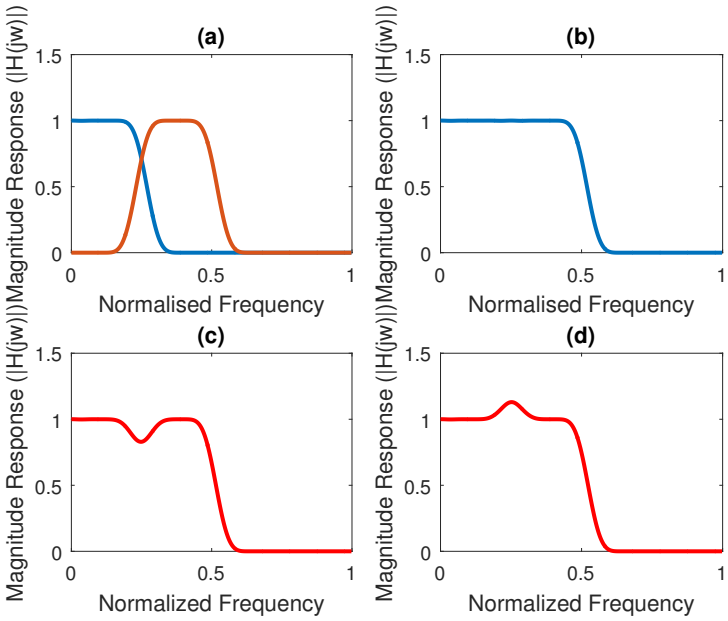

Figure 6.6: Illustration of amplitude distortions introduced due to combiner mismatch

The distortion function has to be an allpass function such that the amplitude and phase distortions can be reduced. When analysis filters $\bar{h}_k(n)$ and synthesis filters $\bar{f}_k(n)$ satisfy the relation in Equation 6.11 the NUFB satisfies linear phase condition and is free from phase distortions.

$$\bar{f}_k(n) = \bar{h}_k(N-n) \tag{6.11}$$

The amplitude distortions have to be reduced in NUFB by satisfying the power complementary condition.

The errors introduced in the NUFB in comparison with the uniform filter bank is explained through an example. Consider, we have a uniform filter bank with $M = 4$ subbands. Let an NUFB be implemented with $L = 3$ subbands with a decimation factor $(4, 4, 2)$ and combination set of $(1, 1, 2)$, such that $p_0 = 1$, $p_1 = 1$, and $p_2 = 2$. Then, the distortion function of the NUFB is given by

$$\bar{T}(z) = \sum_{j=0}^{2} \bar{H}_k(z)\bar{F}_k(z) \tag{6.12}$$

$$\bar{T}(z) = H_0(z)F_0(z) + (H_1(z) + H_2(z))(F_1(z) + F_2(z)) + H_3(z)F_3(z) \tag{6.13}$$

Table 6.1: Performance comparison with existing methods for 3 channel NUFB

	Decimation Foactor	**Method**	N	A_s **(dB)**	E_{pp}
Li et al.	(4,4,2)	Cosine Modulation	64	-60	7.803×10^{-3}
Xie et al	(4,4,2)	Recombination	63	-110	7.803×10^{-3}
Soni et al	(4,4,2)	Tree Structure	63	-80	3.85×10^{-3}
Kumar et al	(4,4,2)	Tree Structure	48	-80	3.11×10^{-3}
Proposed	(4,4,2)	Cosine Modulation	45	-80	2.60×10^{-3}

$$\bar{T}(z) = \underbrace{H_0(z)F_0(z) + H_1(z)F_1(z) + H_2(z)F_2(z) + H_3(z)F_3(z)}_{} + F_1(z)H_2(z) + F_2(z)H_1(z) \tag{6.14}$$

$$\bar{T}(z) = T(z) + \underbrace{H_1(z)F_2(z) + F_1(z)H_2(z)}_{} \tag{6.15}$$

$$\bar{T}(z) = T(z) + e(z) \tag{6.16}$$

From Equation 6.15 and 6.16, it is clear that a few additional terms are introduced in the distortion function of NUFB when compared to uniform filter banks. The limitation of single prototype approach is that when the number of combinations increases the residual error also increases. Residual error due to combiners can be reduced using the multi-prototype approach explained in Section 6.3. The single prototype approach was compared with some of the existing methods in literature and tabulated in Table 6.1. From the table, it can be inferred that the proposed single prototype approach has better performance compared to the existing methods. The 3 channel NUFB was designed from a uniform filter bank of $M = 8$, with decimation factors $(4, 4, 2)$. The prototype filter was designed with a subband attenuation of $A_s = 100\,\text{dB}$ and filter length $N = 187$.

6.3 Multi-prototype Approach

In multi-prototype approach the non-uniform filter banks are designed using a combination of more than one prototype having different passbands. The analysis and synthesis filter coefficients of the NUFB with different granularity bands can be generated by cosine modulation of the prototype filters of same filter length N. The multiple prototype filters can be optimized independently with reduced errors, unlike the method proposed in [142], thereby simplifying the design complexity. In the earlier method, the prototype filters were designed dependent on each other. Our method optimizes the 3 dB cut-off frequency of the individual prototype filter at $\omega_c = \frac{\pi}{2M}$ to eliminate the combiner mismatch and thereby, reduce amplitude distortions.

For simplicity, consider two uniform filter banks with different subbands M_1 and M_2 using prototypes hp_1 and hp_2, respectively. The impulse response of the analysis and synthesis filters are given by the closed form expressions as [142]:

Bank 1:

$$h_{1,k}(n) = 2hp_1(n)\, cos\left[(2k+1)\frac{\pi}{2M_1}\left(n - \frac{N}{2}\right) + \theta_{1,k}\right] \tag{6.17}$$

$$f_{1,k}(n) = 2hp_1(n)\, cos\left[(2k+1)\frac{\pi}{2M_1}\left(n - \frac{N}{2}\right) - \theta_{1,k}\right] \tag{6.18}$$

where, $k = 0, 1, \ldots, M_1 - 1$.

Bank 2:

$$h_{2,k}(n) = 2hp_2(n)\, cos\left[(2k+1)\frac{\pi}{2M_2}\left(n - \frac{N}{2}\right) + \theta_{2,k}\right] \tag{6.19}$$

$$f_{2,k}(n) = 2hp_2(n)\, cos\left[(2k+1)\frac{\pi}{2M_2}\left(n - \frac{N}{2}\right) - \theta_{2,k}\right] \tag{6.20}$$

where, $k = 0, 1, \ldots, M_2 - 1$.

The prototype filters have linear phase and satisfy the relation $f(n) = h(N-1-n)$. Here, $\theta_{1,k}$ and $\theta_{2,k}$ are the phase terms associated with different filter banks. The phase difference has to be $\frac{\pi}{2}$ in order to reduce the aliasing error [142]. For the design of NUFB using multiple prototype filters the phase terms are related by the matching con-

dition in Equation 6.21.

$$e^{j2\theta_{1,k}} + e^{j2\theta_{2,k}} = 0 \tag{6.21}$$

where, $\theta_{q,k} = (\pm)^k \frac{\pi}{4}$, with $q = 1, 2, \ldots, Q$ represents different prototype filters $hp_1, hp_2, \ldots, hp_Q$. The generalized expression for multiple prototype filter banks can be written as $h_{q,k}$ and $f_{q,k}$ for the analysis and synthesis filter banks, respectively. In our method, the prototype was designed using the method proposed in Chapter 3. The prototype filters which are designed to implement NUFB need to satisfy the following necessary conditions.

1. All the prototype filters have to be of the same length N.
2. The prototype filters should satisfy near perfect reconstruction, bandlimiting and power complementary conditions as in [93].

$$\left|H(e^{j\omega})\right| \approx 0, |\omega| > \frac{\pi}{M} \tag{6.22}$$

$$\left|H(e^{j\omega})\right|^2 + \left|H(e^{j(\frac{\pi}{M}-\omega)})\right|^2 \approx 1, 0 \leq \omega \leq \frac{\pi}{M} \tag{6.23}$$

3. The phase terms relative to adjacent filters must differ by $\frac{\pi}{2}$.
4. The prototype filters should satisfy the linear phase conditions $f(n) = h(N-1-n)$.

The conditions reduce the aliasing error, amplitude distortion, and phase distortion while combining different prototype filters to implement filter banks with non-uniform bandwidth. The advantage of our method is that the multiple prototypes can be optimized independently. Filter banks with different bandwidths are implemented by alternatively selecting the analysis and synthesis filter coefficients which satisfies the phase conditions. A flowchart for the design of multi-prototype filter is shown in Figure 6.7.

The procedure followed for the implementation of a multi-prototype non-uniform filter bank is summarized below:

1. Design Q linear phase FIR lowpass prototype filters of length N optimized to have their cut-off frequencies at $\omega_c = \frac{\pi}{2M_q}$, where $q = 1, 2, \ldots, Q$. All the prototype filters should be designed with the same length and satisfy the bandlimiting and power complementary condition for satisfying near perfect reconstruction.

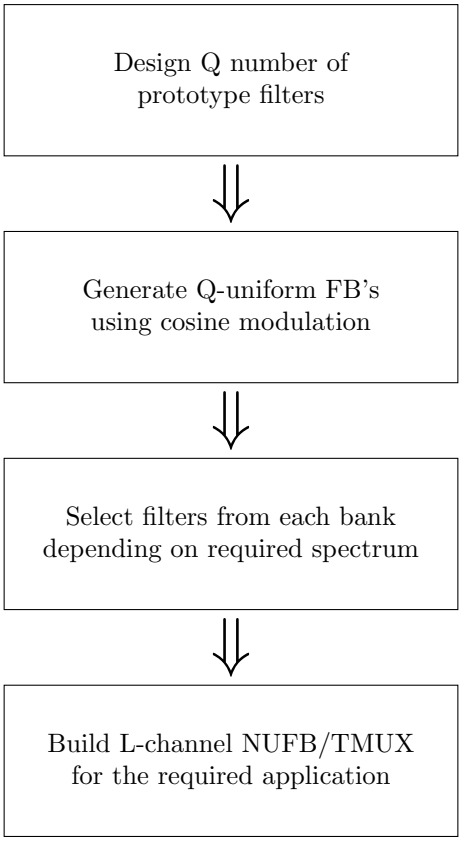

Figure 6.7: Flowchart for NUFB design using multiple prototype filters.

2. The corresponding Q uniform filter banks should be generated using cosine modulation of these prototype filters. The closed form equations as given in Equation 6.6 and 6.7 are to be used to generate the subband filter responses.

3. Implement an L channel non-uniform filter bank by selecting the subband responses from each uniform filter bank with proper compatibility set and apply the channel combination in accordance with the required bandwidth.

For example, consider an NUFB has to be designed with decimation factors $(16, 16, 8, 4, 2)$. When a multi-prototype approach is considered, four or three prototype filters can be designed depending on the flexibility. We consider three different prototype filters having resolution $M_1 = 4$, $M_2 = 8$, and $M_3 = 16$ with the same length and subband attenuation. The designed prototype filter is shown in Figure 6.8. The implemented NUFB will have 5 subbands and are shown in Figure 6.9. All the prototype filters are designed with the same length $N = 187$ and subband attenuation $A_s = 100\,\text{dB}$.

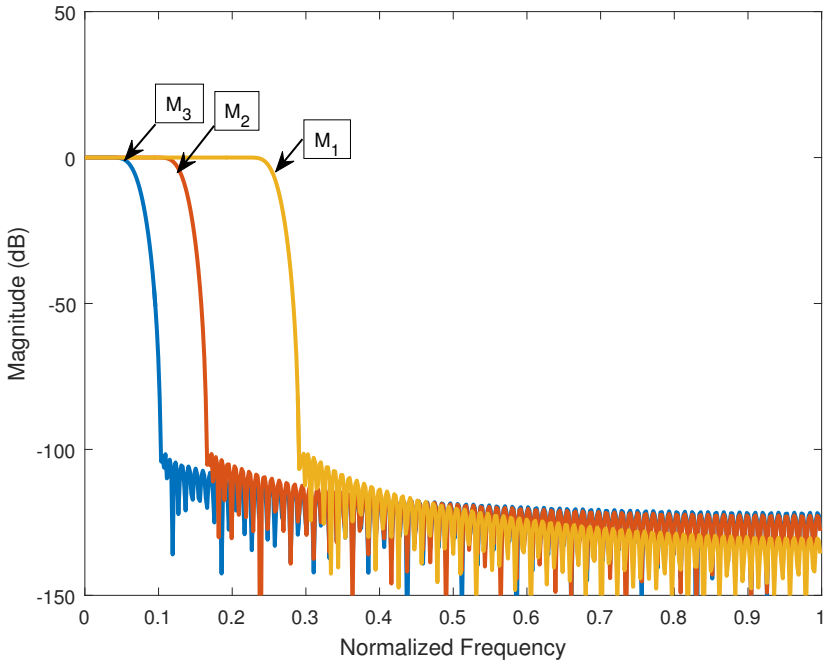

Figure 6.8: Different lowpass prototype filters with variable granularity $M_1 = 4$, $M_2 = 8$, and $M_3 = 16$

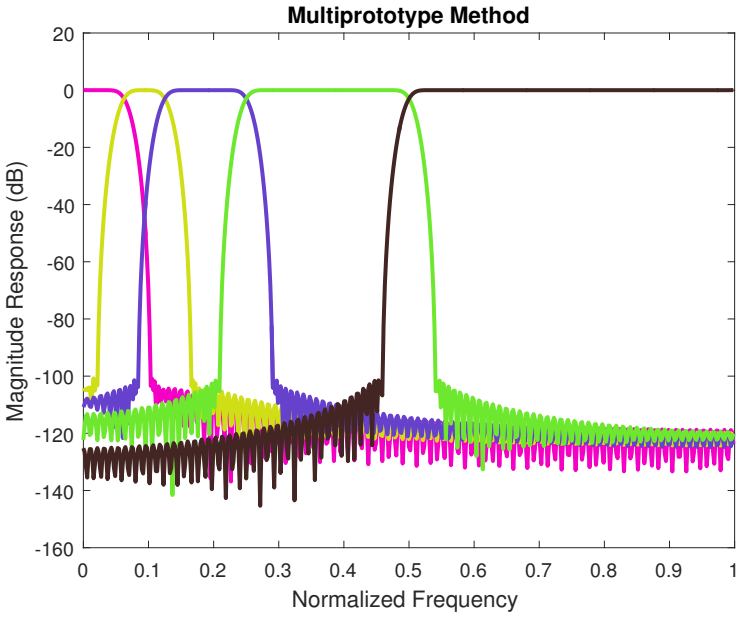

Figure 6.9: NUFB with multiple prototype filters having resolution $M_1 = 4$, $M_2 = 8$, and $M_3 = 16$ and decimation factors $(16, 16, 8, 4, 2)$

6.4 Simulation Results of Single and Multi-prototype Approaches

Comparisons between single and multiple prototype filter bank approaches are shown through simulations. A 5 channel NUFB is constructed from a 16 channel uniform CMFB designed from a single prototype filter. Consider the NUFB has decimation factors $(16, 16, 8, 4, 2)$, then the corresponding combinations required are $(1, 1, 2, 4, 8)$ using single prototype approach. The prototype filter is designed with a subband attenuation of $A_s = 100\,\text{dB}$, and filter length $N = 187$. The designed NUFB using single prototype filter is shown in Figure 6.10. The same was implemented with multiple prototype approach. Three different prototype filters were generated for $M_1 = 4$, $M_2 = 8$, and $M_3 = 16$ as explained in Section 6.3 with the same length and subband attenuation as in single prototype approach. The single prototype approach required $11N$ additions compared to $1N$ addition in multiple prototype approach. The distortions introduced in the single and multiple prototype approach are shown in Figure 6.10 and 6.11. From the comparisons of single and muti-prototype approach it can be concluded amplitude distortions are reduced in the muti-prototype approach.

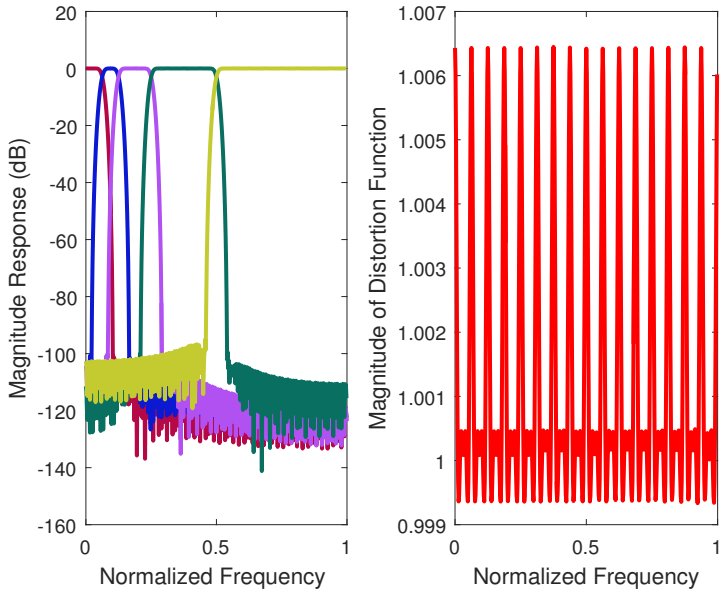

Figure 6.10: NUFB using single prototype approach and their corresponding distortion function

The performance comparison of single and multiple prototype filter bank approaches in terms of amplitude distortion E_{pp}, number of filter taps N, and stopband attenuation

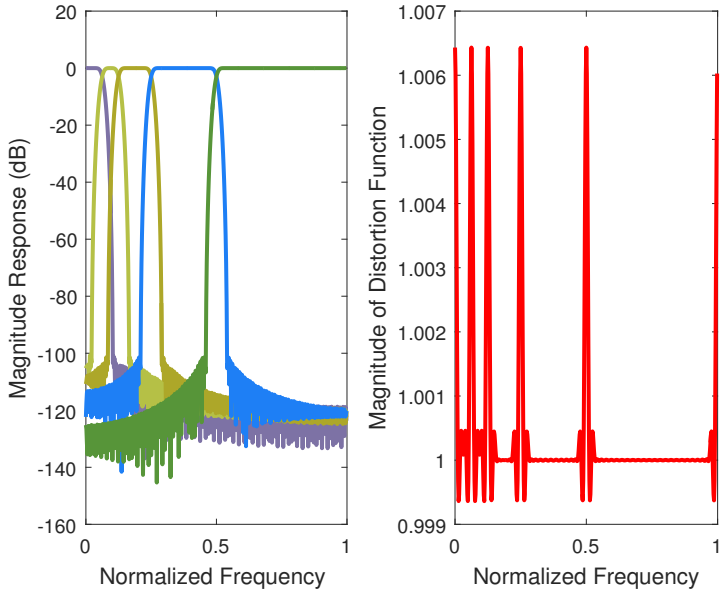

Figure 6.11: NUFB using multi-prototype approach and their corresponding distortion function

A_s is tabulated in Table 6.2. It is observed from the table that the multi-prototype approach provides better performance when the subband combinations are increased.

It was inferred that the distortion occurring in the multi-prototype method is less compared to single prototype approach when the combinations are increased. The main advantage of multi-prototype approach is that the number of additions required in the channel combiner is much reduced when compared to that of single prototype approach. Therefore, the complexity in the system and the distortions introduced by the adders are reduced.

The aliasing error of the given design is not altered as compared with the uniform bank case. Both the single and muti-prototype approaches have same values since the stop band attenuation is not altered during channel combinations. The complexity in filter additions and hence the increased distortions when using a single prototype approach is reduced using multi-prototype approach since we have the flexibility in choosing the required prototype.

Table 6.2: Comparison of single prototype approach vs mutiprototype approach

Band	A_s **(dB)**	**Filter Length** N	**Single Prototype**	**Multiple Prototype**
Three Band 4,4,2,	-80	47	2.7×10^{-3}	2.7×10^{-3}
		65	2.5×10^{-3}	2.5×10^{-3}
		71	2.6×10^{-3}	2.6×10^{-3}
Four Band 8,8,4,2	-80	65	5.4×10^{-3}	2.7×10^{-3}
		71	3.8×10^{-3}	2.6×10^{-3}
		79	5.1×10^{-3}	2.6×10^{-3}
Five Band 16,16,8,4,2	-80	95	7.09×10^{-2}	5.4×10^{-3}
		125	8.4×10^{-3}	3.2×10^{-3}

6.5 Summary

In this chapter, non-uniform bandwidth allocation techniques using cosine modulated filter banks are discussed. We implemented non-uniform filter banks from uniform cosine modulated filter banks using single and multiple prototype approaches. A performance comparison of NUFB design using single and multiple prototype filters with channel combiners is presented. The prototypes are designed using an iterative algorithm which satisfies the NPR conditions. In single prototype based method, non-uniformity is achieved by combining adjacent subbands constrained by compatibility set. As the prototype filters are generated to have the cut-off frequency at $\omega_c = \frac{\pi}{2M}$, flat passbands are generated at the merging points.

In multiple prototype method, non-uniform filter responses are obtained from design of different prototype filters with varying passbands. Different prototype filters were optimized independently in multiple prototype filter approach. The conditions to be satisfied by prototype filters in multiple prototype filter approaches were also discussed. The multi-prototype based method reduces the number of channel combiners and residual errors when compared to single prototype based method. Finally, a comparative analysis of both methods in terms of complexity as well as accuracy is presented. The complexity in filter additions and hence the increased distortions in the

single prototype filter bank is minimized in a multi-prototype based non-uniform filter bank. In both single and multi-prototype approaches, the NUFB maintains the linear phase and is found to be simple in terms of implementation

Related publications

A channel combiner approach for the design of near perfect reconstruction non uniform filter banks at the *IEEE International Conference on Communication and Signal Processing (ICSSP 2014)* Tamil Nadu, 3-5th April 2014.

Analysis of multiprototype over single prototype filters for non uniform filter banks at the *IEEE (INDICON 2014)* Pune, 11-13th Dec 2014.

CHAPTER 7

Rate Request Sequenced Bit Loading Algorithm for Secondary User Allocation

Significant research has been done to detect the spectral holes, however the spectral utilization is improved only when the detected spectral holes are reallocated to secondary users [123], [143], [144], [145]. Efficient spectrum utilization is done using bit loading algorithm based on Channel State Information (CSI) [143]. The spectrum requirements of secondary users are not known aprori and their request comes at different time slots. Therefore, it is not possible to use any static resource allocation algorithms for the secondary users in Cognitive Radio (CR). At present, an extensive research is being carried out for adaptive resource allocation techniques for secondary users allocation in CR.

The reallocation can be carried out based on instantaneous request, i.e., on a first-come-first-serve basis. However, this approach does not allow efficient resource allocation, because the secondary users may have different spectral requirements. In order to address this issue, an approach based on sequence of request available from the users and channel condition in terms of CSI need to be used. The maximum bits and power that can be allocated to each subband is determined based on the CSI and secondary user modulation schemes.

In this chapter, the performance analysis of a rate request sequenced bit loading reallocation algorithm for allocation of secondary users is examined. This work investigates subband-wise spectrum sensing followed by spectrum utilization using bit loading algorithms. The spectral holes or free subbands are allocated to secondary users depending on the user rate request and subchannel capacity. Section 7.1 provides a brief overview of the existing resource allocation techniques. The rate request sequenced algorithm is explained in Section 7.2, followed by simulation results in Section 7.3. Simulations was done to compare the spectral utility between random rate request and sequenced rate request of secondary users for subchannel allocation.

7.1 Resource Allocation Techniques

In Cognitive Radio (CR), unused spectrum need to be reallocated to secondary user for efficient spectrum utilization. The secondary users have variable spectrum requirements, therefore rate adaptive techniques have to be used for spectrum reallocation. Spectrum utilization can be maximized by using adaptive bit loading algorithms. In addition, rate adaptive loading algorithms are considered to provide better control of interference between CR and primary user receivers [143]. In adaptive bit loading algorithm the number of bits that can be transmitted in each subchannel is determined by the CSI.

Different optimization techniques have been proposed in literature for resource allocation. They are broadly classified as rate adaptive algorithms and margin adaptive algorithms. The Margin Adaptive (MA) algorithms achieve minimum transmit power given the constraints on data rate and Bit Error Rate (BER). The Rate Adaptive (RA) algorithms maximize the data rate with constraints on transmit power [146]. A maximum rate loading algorithm for DMT systems was proposed in [147], which assigns energy to different subchannels in order to maximize the data rate. Even though waterfill algorithms are optimal, it is difficult to realize this in practice. Therefore, suboptimal algorithms are used to maximize margin for a target data rate in DMT systems such as chow's algorithm [148], Fischers algorithm [149], Hughes-Hartogs algorithm [150]. Bit loading algorithms using Lagrange approach was proposed by Krongold et al. in [151]. To reduce the complexity in allocation, suboptimal techniques are used with adaptive algorithms in [152].

In order to maximize the data rate for a given transmit power, adaptive bit loading algorithm is considered to be a better choice to determine the number of bits to be allocated to each subchannel. DMT systems use maximum rate loading algorithm to assign more bits to a subchannel with higher SNR. The critical requirement of bit loading algorithms is to determine the usable subchannels [147]. A subband based water filling algorithm for spectrum utilization in CRs operating in ISM band was analyzed in [82]. As in case of spectrum sensing, the subband information is known, therefore the bit loading algorithm are examined for secondary users allocation. The performance of a rate request sequenced bit loading reallocation algorithm for allocation of secondary users in CR are analyzed. The random request for resource allocation from secondary

users is sequenced based on the data rate. The pool of sequenced rate request is analyzed to allocate spectrum resource to secondary users in order to increase the spectrum efficiency.

7.2 Rate Request Sequenced Algorithm for Subchannel Allocation

Spectral utility is said to be achieved only when the detected spectral holes are efficiently allocated to the secondary users. In our thesis, we focus on the reallocation of unused spectrum (detected spectrum holes) to the secondary users. We consider a rate request sequenced bit loading reallocation algorithm for the allocation of spectrum to secondary users. Free subchannels are allocated to the secondary users depending on the channel capacity and the user rate request. The bits to be allocated to each subchannel are determined based on the channel state information and modulation scheme used by secondary users. The channel state information takes care of the different fading channel conditions and additive white Gaussian noise present in the channels.

Bit loading algorithm is suitable for rate adaptive DMT systems as optimal distribution of discrete bits is possible over different subcarriers [153]. The number of bits per symbol in each subcarrier can be adjusted according to the channel conditions. The maximum number of bits that can be allocated to each subchannel is calculated using secondary user modulation schemes. The crucial part of bit loading algorithm is to determine the usable subchannels. Allocation of resources to subchannel other than a useable subchannels increases the probability of error.

After spectrum sensing the spectral holes are detected and the number of free subchannels is calculated. Let N_{free} be the identified free subchannels. The scheme first determines the maximum number of bits that can be allocated to each free subchannel. The energy distribution of each subchannel is calculated using subchannel SNR and the water filling constant K [147]. The optimal water filling constant is calculated using the relation in Equation 7.1

$$K = \frac{1}{N_{free}} \left(\varepsilon + \Gamma \sum_{n=1}^{N_{free}} \frac{1}{g_n} \right) \tag{7.1}$$

where ε represents the total energy distributed in the available bandwidth and Γ refers to SNR gap in each subchannel. The subchannel SNR in each subband is $g_n = \frac{|H_n|^2}{\sigma_n^2}$. The SNR gap Γ represents the additional SNR required to transmit the bit rate equal to channel capacity. The value of SNR gap varies with the modulation scheme used by the secondary user and depends on the symbol error rate requirement. For Pulse Amplitude Modulation (PAM), the symbols are real and SNR gap is calculated as in [154].

$$\Gamma_{PAM} = \frac{1}{3}\left[Q^{-1}\left(\frac{SER_{PAM}}{2\left(1-2^{-b}\right)}\right)\right]^2 \tag{7.2}$$

For Quadrature Amplitude Modulation (QAM) the symbols are complex and SNR gap is calculated as

$$\Gamma_{QAM} = \frac{1}{3}\left[Q^{-1}\left(\frac{SER_{QAM}}{4\left(1-2^{-b}\right)}\right)\right]^2, \tag{7.3}$$

where SER is the symbol error rate and b is the number of bits per symbol of the modulation scheme used by the secondary user. As the SNR gap increases, symbol error decreases. The energy in each usable channel can be calculated as per Equation 7.4

$$\varepsilon_n = K - \frac{\Gamma}{g_n} \tag{7.4}$$

Since, ε is the total energy that can be distributed in the available bandwidth, then subbands energies are $\varepsilon_n = \frac{\varepsilon}{N_{free}}$. The number of bits that can be allocated to each subchannel is obtained using the maximum rate loading algorithm [147].

$$b_n = \frac{1}{2}\left(1 + \frac{\varepsilon_n g_n}{\Gamma}\right) \tag{7.5}$$

In order to increase the data rate of each subchannel, maximum rate loading algorithm is chosen to determine the maximum number of bits that can be allocated to each subchannel. Subchannel gains are calculated and arranged in descending order to determine the usable subchannels for secondary user transmission. When noise variance is high, subchannel SNR reduces and the energy in that subchannel becomes negative. The subchannel is declared as a bad channel, when $\varepsilon_n < 0$, as it is not suitable for secondary user transmission. In such cases, the total number of usable subchannels reduces to $N^*_{free} = N_{free} - N_b$, where N_b is the number of subchannels with negative energy. Accordingly, the bit allocation is done only for the usable subchannels.

Upon determining the maximum number of bits that can be allocated to each subchannel, the available subchannels are allocated to the secondary users depending on the rate request. There exist different ways to allocate subchannels to secondary users for efficient spectrum utilization. The spectrum utility is increased as we allocate from the pool of sequenced random request received from secondary user for resource allocation instead of random allocation i.e., first-come-first-serve basis. The rate sequenced resource allocation algorithm is described in Algorithm 4.

Algorithm 4 Rate request sequenced resource allocation

1: Randomly generate L rate requests, $R = [R_1, R_2, \ldots, R_L]$, $L > N_{free}$, of secondary users using Poisson distribution with mean μ and arrange them in descending order.
2: Determine the maximum number of bits that can be allocated to each subchannel using bit loading algorithm as $B = [b_1, b_2, \ldots, b_{N_{free}}]$, where N_{free} is the number of free subbands and $b_n = \frac{1}{2} log_2(1 + \frac{\varepsilon_n g_n}{\Gamma})$.
3: **if** $R_l \leq b_n$, $l \in L$, $n \in N_{free}$ **then**
4: Allocate n^{th} subchannel to user request l
5: **else**
6: Discard that request
7: **end if**

The improvement in spectrum efficiency and reduction in computational complexity are achieved by pooling and sequencing the random rate requests R from secondary users and arranging B in descending order. Computational complexity is reduced as the sorting process is done only once at the beginning of the algorithm. Sequencing R, allocates the first user with maximum rate request to occupy the subchannel with higher capacity. In cases where the secondary user rate request does not satisfy the condition in Step 3, the request gets denied. The process is continued until all the subchannels are occupied. The allocation of secondary users can be done till the the new set of CSI is available.

The performance of rate request sequenced resource allocation method was compared with random rate request without pooling and sequencing. In random rate request allocation, the users were allocated to subchannels in a first-come-first-serve basis. The disadvantage of random allocation is that the user request with less data rate may occupy

a subchannel of higher capacity. The last user with high data rate may be denied if subchannel is not free. In such cases spectrum is not utilized efficiently and for each data request searching process takes place from the first subchannel excluding the occupied subchannels.

7.3 Simulation Results

Simulations were carried out by random generation of secondary user request based on Poisson distribution with different mean values. A comparison is done between random rate request and sequenced rate request of secondary users for subchannel allocation. Let N_{free} be the number of vacant subchannels (spectral holes). The resource allocation to secondary users is done depending on the secondary user rate request. The random rate requests are generated using Poisson distribution with different mean values and different modulation schemes (QAM, PAM). Figure 7.1 shows the bit allocation using QAM with an Symbol Error Rate (SER) of 10^{-7} and SNR gap of $\Gamma_{QAM} = 9.91$ with mean $\mu = 6$. Figure 7.2 shows the bit allocation using PAM with SER of 10^{-4} and SNR gap of $\Gamma_{QAM} = 5.05$ using bit loading algorithm. The total number of bits varies for different modulation with different SER. The simulation are done on the assumption that the free subchannels are detected and the channel state information is known. The channel state information gives the subchannel SNR to determine the maximum number of bits that can be allocated to each subchannel.

In Figure 7.3, Method 1 shows the subchannel allocation using random rate request and Method 2 shows the pooled and sequenced rate request. By arranging the rate requests and bits per subchannel in descending order, spectrum can be utilized efficiently. The proposed method was tested for 100 Monte Carlo simulations and it is observed that Method 2 has the superior performance compared to Method 1. It is observed from Figure 7.4 that the request denial rate is less when the rate requests are pooled and sequenced. Therefore, higher capacity is achieved in rate sequenced allocation when compared to random allocation. For 35 rate requests, only 9 requests are denied using Method 2 whereas 16 requests are denied using Method 1. The performance of random rate request is compared with pooled and sequenced rate request for different rate request and shown in Figure 7.4. The request denial rate gradually increases with increase

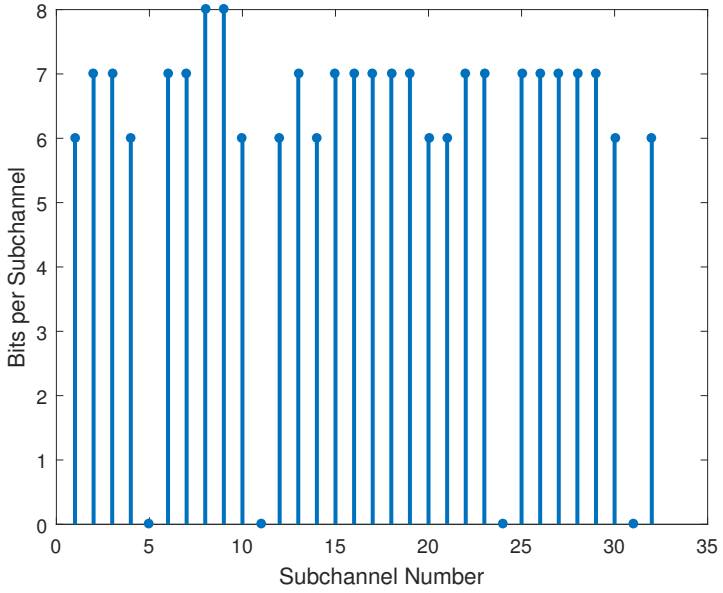

Figure 7.1: Bits distribution in each subchannel with QAM for SER of 10^{-7} and a SNR gap of 9.91

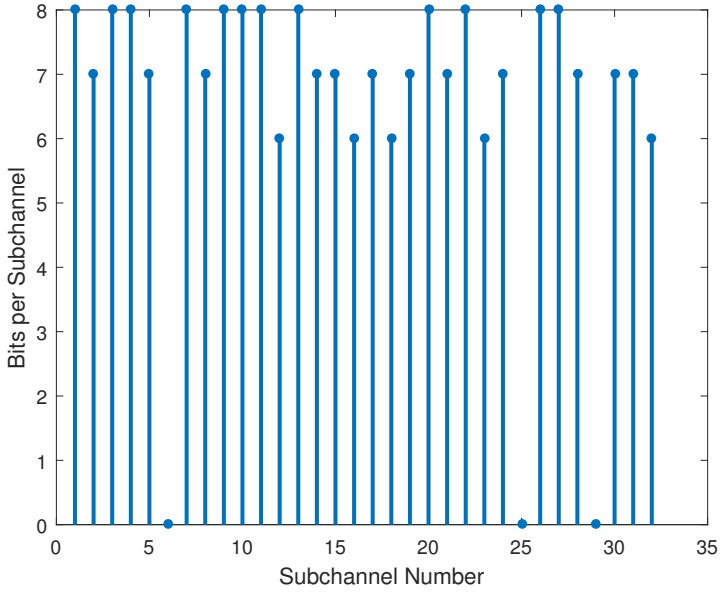

Figure 7.2: Bits distribution in each subchannel with PAM for SER of 10^{-4} and a SNR gap of 5.05

in number of rate requests.

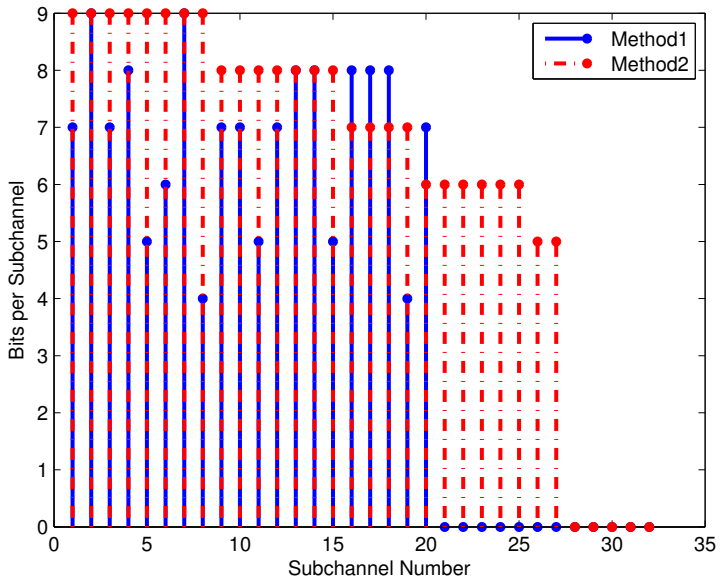

Figure 7.3: Subchannel allocation to secondary users with the two methods

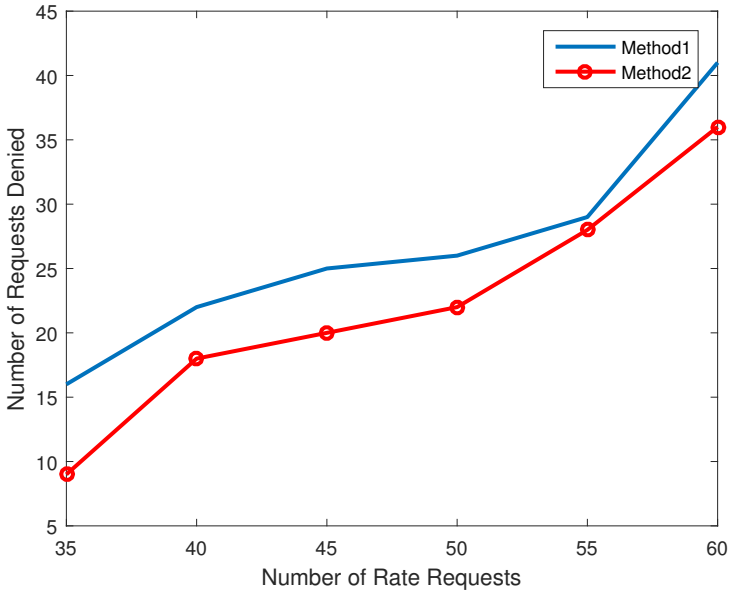

Figure 7.4: Comparison between Method 1 and Method 2 using Bit Loading algorithm

7.4 Summary

The problem of allocating spectral holes detected by cognitive radio to secondary users was addressed in this chapter. The bit loading algorithm is applicable in DMT systems for secondary user allocation. The maximum number of bits that can be allocated to each subchannel is determined using the channel state information and bit loading

algorithm. The spectral holes are free subbands are allocated to secondary users depending on the rate request and subchannel capacity. It is concluded that, compared to random allocation, a sequenced and pooled rate request of secondary users provides efficient spectral utilization. In addition, it is observed that the request denial rate is less when rate requests are pooled and sequenced and higher capacity is achieved when compared to random allocation.

Related publication

Rate Request Sequenced Bit Loading Secondary User Reallocation Algorithm for DMT Systems in Cognitive Radio, *International Journal of Vehicular Technology*, **Article ID 685491** (2015)

CHAPTER 8

Conclusions and Future Scope

In essence, our research mainly focuses on exploring wideband spectrum sensing techniques using filter banks for the efficient use of radio frequency spectrum. Various conclusions drawn are explained in Section 8.1 and future scope of the thesis is briefed in Section 8.2.

8.1 Conclusions

In this thesis, we developed various wideband spectrum sensing algorithms in cognitive radio using filter banks and addressed the issues related to non-uniform bandwidth allocation. A systematic and self controlled prototype filter was designed for filter banks satisfying near perfect reconstruction. The prototype filter was designed using two input parameters: (i) number of subbands M and (ii) subband attenuation A. All other system parameters were derived from these two parameters to avoid heuristic inputs.

Wideband spectrum sensing was performed with cosine modulated filter banks and polyphase filter banks. The filter banks provides higher bandwidth efficiency and lower sidelobes desirable for spectrum sensing. The spectral holes could be identified by the threshold determined from probability of false alarm and noise variance. The test statistic was calculated based on energy detection. The bandwidth efficiency could be effectively increased by finer granularity bands. It can be concluded that finer the spectral resolution better the detection performance and the spectral efficiency. The detection precision of primary users in a wideband spectrum sensing is directly related to the number of subbands and number of stages in the filter bank. The computational complexity of the filter bank structure was increased when the number of subbands and number of stages increased. It was shown in the thesis, computational complexity was reduced when sensing from a coarser to a finer spectral resolutions using multistage filter banks.

The proposed centroid method was used for detection of single narrowband user in wideband with multistage filter banks. The entire bandwidth was divided into consecutive non-overlapping frequency bands using DFT based polyphase filter banks. The mathematical expressions for calculating the center frequency was derived and presented in the thesis. The proposed method can be used to detect Wireless Microphone (WM) in the presence of signal which follows IEEE 802.22 Wireless Regional Area Network (WRAN) standard within TV channels. The WM is detected in the first stage with a reduced computational complexity and latency when WM appears between adjacent bands. When the WM appears exclusively within a single subband, the center frequency can be estimated in the second stage without ambiguity. The proposed method outperforms the conventional filter bank as it can exploit the uniqueness of centroid method in center frequency estimation with high precision, in addition to low computational complexity due to multistage polyphase filter bank.

In cases where the information regarding the bandwidth of different primary users are available, the spectral resolution of the filter bank is deterministically calculated. It is shown that, when multiple users appear on a wideband, the number of detected subbands can be more than two. In such scenarios, a center of mass method was used for primary user detection. Similar to single user detection, if the primary users occupy more than one subband, the detection is performed in the first stage. If a primary user appears exclusively within a single subband, the detection of center frequency and estimation of spectral edges are done in the second stage. The mathematical expressions for calculating center frequency and spectral edges are also derived using center of mass method and presented in the thesis. The proposed method can be used to detect center frequencies and spectral edges of multiple users in a wideband spectrum.

We also address the problem of non-uniform bandwidth allocation using uniform filter banks. As the initial step, a channel combiner approach was used to generate non-uniform filter banks from a uniform filter bank. Uniform filter bank was implemented by cosine modulating a single prototype filter. We could combat the issue of residual errors and amplitude distortion in single prototype filter approach by adopting a multi-prototype approach.

A rate request sequenced algorithm was proposed for efficient utilization of the spectrum to efficiently allocate spectral holes to the secondary users. It was observed

that, when secondary user requests are pooled and sequenced, we achieved higher spectral utilization compared to random allocations on first-come-first- serve basis.

Although an extensive research has been done in spectrum sensing there exist several challenges in wideband spectrum sensing which has to be appeased for making cognitive radio networks a reality. Important areas of cognitive radio such as access policy, coexistence among multiple primary users/secondary networks, cooperative communication, network security, cognitive network architecture, and hardware implementation requires further research.

8.2 Future Scope

From our research we conclude that filter banks are plausible for wideband spectrum sensing. As a result, our research lead to many other areas of research which are targeted towards filter bank based communication systems. We presented wideband spectrum sensing using filter banks for implementation in cognitive radios, where resource allocation could be done as well using filter banks. We briefly highlight some possible future scope of research in this field.

The proposed spectrum sensing was validated using additive white Gaussian noise. In future they can be extended for different fading environment. Predominantly, energy detection method is used for spectrum sensing in filter bank techniques. The detection performance can be increased, if the noise variance is known. The threshold in energy detection is a function of noise variance. Therefore, noise variance estimation techniques can be investigated in wideband spectrum sensing. The proposed method used fixed threshold for all the subbands in the filter banks. If noise variance can be estimated in individual subbands, adaptive threshold schemes can be implemented. The adaptive thresholds can be determined for different stages with different spectral resolution in order to increase the probability of detection. The sensing performance can be improved by incorporating adaptive schemes in wideband spectrum sensing. In order to improve the reliability of spectrum sensing in multipath and shadowing environments co-operative wideband sensing techniques can be investigated.

In this research, the estimation of center frequency and spectral edges were formulated for fractional bandwidth utilization. On the other hand center frequency and

spectral edge detection can be extended for coexistence among heterogeneous networks and multiple primary users in the same frequency bands. More practical scenarios can be validated with the proposed method. The resource allocation techniques available for reallocation of secondary users in the identified spectral holes are limited in literature. The filter bank techniques can be further extended for resource allocation as well.

REFERENCES

[1] P. P. Vaidyanathan, *Multirate systems and filter banks*. Pearson Education India, 1993.

[2] A. Ambede, K. Smitha, and A. P. Vinod, "Flexible low complexity uniform and nonuniform digital filter banks with high frequency resolution for multistandard radios," *IEEE Transactions on Very Large Scale Integration (VLSI) Systems*, vol. 23, no. 4, pp. 631–641, 2015.

[3] S. Haykin, "Cognitive radio: brain-empowered wireless communications," *IEEE journal on selected areas in communications*, vol. 23, no. 2, pp. 201–220, 2005.

[4] P.-Q. Hoang and P. Vaidyanathan, "Non-uniform multirate filter banks: Theory and design," in *Circuits and Systems, 1989., IEEE International Symposium on*. IEEE, 1989, pp. 371–374.

[5] J. Mitola and G. Q. Maguire, "Cognitive radio: making software radios more personal," *IEEE personal communications*, vol. 6, no. 4, pp. 13–18, 1999.

[6] T. Yucek and H. Arslan, "A survey of spectrum sensing algorithms for cognitive radio applications," *IEEE communications surveys & tutorials*, vol. 11, no. 1, pp. 116–130, 2009.

[7] E. Biglieri, A. J. Goldsmith, L. J. Greenstein, N. B. Mandayam, and H. V. Poor, *Principles of cognitive radio*. Cambridge University Press, 2012.

[8] H. Sun, A. Nallanathan, C.-X. Wang, and Y. Chen, "Wideband spectrum sensing for cognitive radio networks: a survey," *IEEE Wireless Communications*, vol. 20, no. 2, pp. 74–81, 2013.

[9] A. Ghasemi and E. S. Sousa, "Spectrum sensing in cognitive radio networks: requirements, challenges and design trade-offs," *IEEE Communications Magazine*, vol. 46, no. 4, pp. 32–39, 2008.

[10] I. F. Akyildiz, W.-Y. Lee, M. C. Vuran, and S. Mohanty, "Next generation/dynamic spectrum access/cognitive radio wireless networks: a survey," *Computer networks*, vol. 50, no. 13, pp. 2127–2159, 2006.

[11] L. Lu, X. Zhou, U. Onunkwo, and G. Y. Li, "Ten years of research in spectrum sensing and sharing in cognitive radio," *EURASIP Journal on Wireless Communications and Networking*, vol. 2012, no. 1, p. 1, 2012.

[12] E. FCC, "Docket no 03-222 notice of proposed rule making and order," 2003.

[13] Q. Zhao and B. M. Sadler, "A survey of dynamic spectrum access," *IEEE signal processing magazine*, vol. 24, no. 3, pp. 79–89, 2007.

[14] B. Wang and K. R. Liu, "Advances in cognitive radio networks: A survey," *IEEE Journal of selected topics in signal processing*, vol. 5, no. 1, pp. 5–23, 2011.

[15] F. K. Jondral, "Software-defined radio: basics and evolution to cognitive radio," *EURASIP journal on wireless communications and networking*, vol. 2005, no. 3, pp. 275–283, 2005.

[16] F. C. Commission *et al.*, "Unlicensed operation in the tv broadcast bands," *ET Docket*, no. 04-186, 2004.

[17] R. A. Saeed and S. J. Shellhammer, *TV White Space Spectrum Technologies: Regulations, Standards, and Applications*. CRC Press, 2011.

[18] A. N. Mody, S. R. Blatt, D. G. Mills, T. P. McElwain, N. B. Thammakhoune, J. D. Niedzwiecki, M. J. Sherman, C. S. Myers, and P. D. Fiore, "Recent advances in cognitive communications," *IEEE Communications Magazine*, vol. 45, no. 10, pp. 54–61, 2007.

[19] M. Sherman, A. N. Mody, R. Martinez, C. Rodriguez, and R. Reddy, "Ieee standards supporting cognitive radio and networks, dynamic spectrum access, and coexistence," *IEEE Communications Magazine*, vol. 46, no. 7, pp. 72–79, 2008.

[20] K. G. Smitha and A. P. Vinod, "A multi-resolution fast filter bank for spectrum sensing in military radio receivers," *IEEE Transactions on Very Large Scale Integration (VLSI) Systems*, vol. 20, no. 7, pp. 1323–1327, 2012.

[21] P. Pawelczak, R. V. Prasad, L. Xia, and I. G. Niemegeers, "Cognitive radio emergency networks-requirements and design," in *First IEEE International Symposium on New Frontiers in Dynamic Spectrum Access Networks, 2005. DySPAN 2005.* Ieee, 2005, pp. 601–606.

[22] Q. Zhang, F. W. Hoeksema, A. B. Kokkeler, and G. J. Smit, "Towards cognitive radio for emergency networks," 2006.

[23] E. Act and E. D. No, "Second report and order and memorandum opinion and order."

[24] A. Ghasemi and E. S. Sousa, "Collaborative spectrum sensing for opportunistic access in fading environments," in *First IEEE International Symposium on New Frontiers in Dynamic Spectrum Access Networks, 2005. DySPAN 2005.* IEEE, 2005, pp. 131–136.

[25] J. Unnikrishnan and V. V. Veeravalli, "Cooperative sensing for primary detection in cognitive radio," *IEEE Journal of selected topics in signal processing*, vol. 2, no. 1, pp. 18–27, 2008.

[26] Z. Li, F. R. Yu, and M. Huang, "A cooperative spectrum sensing consensus scheme in cognitive radios," in *INFOCOM 2009, IEEE.* IEEE, 2009, pp. 2546–2550.

[27] G. Ganesan and Y. Li, "Cooperative spectrum sensing in cognitive radio, part ii: Multiuser networks," *IEEE Transactions on wireless communications*, vol. 6, no. 6, pp. 2214–2222, 2007.

[28] W. Zhang and K. B. Letaief, "Cooperative spectrum sensing with transmit and relay diversity in cognitive radio networks-[transaction letters]," *IEEE Transactions on Wireless Communications*, vol. 7, no. 12, pp. 4761–4766, 2008.

[29] Y. Zeng and Y.-C. Liang, "Eigenvalue-based spectrum sensing algorithms for cognitive radio," *IEEE transactions on communications*, vol. 57, no. 6, pp. 1784–1793, 2009.

[30] S. Rao and G. Singh, "Wavelet based spectrum sensing techniques in cognitive radio," *Procedia Engineering*, vol. 38, pp. 880–888, 2012.

[31] H. Urkowitz, "Energy detection of unknown deterministic signals," *Proceedings of the IEEE*, vol. 55, no. 4, pp. 523–531, 1967.

[32] S. P. Herath, N. Rajatheva, and C. Tellambura, "Energy detection of unknown signals in fading and diversity reception," *IEEE Transactions on Communications*, vol. 59, no. 9, pp. 2443–2453, 2011.

[33] S. Dikmese, P. C. Sofotasios, T. Ihalainen, M. Renfors, and M. Valkama, "Efficient energy detection methods for spectrum sensing under non-flat spectral characteristics," *IEEE Journal on Selected Areas in Communications*, vol. 33, no. 5, pp. 755–770, 2015.

[34] S. Atapattu, C. Tellambura, and H. Jiang, *Energy detection for spectrum sensing in cognitive radio*. Springer, 2014.

[35] M. K. Steven, "Fundamentals of statistical signal processing," *PTR Prentice-Hall, Englewood Cliffs, NJ*, 1993.

[36] G. Taricco, "On the accuracy of the gaussian approximation with linear cooperative spectrum sensing over rician fading channels," *IEEE Signal Processing Letters*, vol. 17, no. 7, pp. 651–654, 2010.

[37] V. Cevher, R. Chellappa, and J. H. McClellan, "Gaussian approximations for energy-based detection and localization in sensor networks," in *2007 IEEE/SP 14th Workshop on Statistical Signal Processing*. IEEE, 2007, pp. 655–659.

[38] D. Cabric, A. Tkachenko, and R. W. Brodersen, "Experimental study of spectrum sensing based on energy detection and network cooperation," in *Proceedings of the first international workshop on Technology and policy for accessing spectrum*. ACM, 2006, p. 12.

[39] S. M. Kay, "Fundamentals of statistical signal processing, volume i: estimation theory," 1993.

[40] N. Hoven, R. Tandra, and A. Sahai, "Some fundamental limits on cognitive radio," *Wireless Foundations EECS, Univ. of California, Berkeley*, 2005.

[41] D. Cabric, S. M. Mishra, and R. W. Brodersen, "Implementation issues in spectrum sensing for cognitive radios," in *Signals, systems and computers, 2004.*

Conference record of the thirty-eighth Asilomar conference on, vol. 1. IEEE, 2004, pp. 772–776.

[42] A. Tkachenko, D. Cabric, and R. W. Brodersen, "Cyclostationary feature detector experiments using reconfigurable bee2," *Proceedings of the DySPAN*, pp. 216–219, 2007.

[43] S. Xu, Z. Zhao, and J. Shang, "Spectrum sensing based on cyclostationarity," in *Power Electronics and Intelligent Transportation System, 2008. PEITS'08. Workshop on*. IEEE, 2008, pp. 171–174.

[44] D. Bhargavi and C. R. Murthy, "Performance comparison of energy, matched-filter and cyclostationarity-based spectrum sensing," in *Signal Processing Advances in Wireless Communications (SPAWC), 2010 IEEE Eleventh International Workshop on*. IEEE, 2010, pp. 1–5.

[45] Y. Zeng and Y.-C. Liang, "Maximum-minimum eigenvalue detection for cognitive radio," in *2007 IEEE 18th International Symposium on Personal, Indoor and Mobile Radio Communications*. IEEE, 2007, pp. 1–5.

[46] S. Dikmese, J. L. Wong, A. Gokceoglu, E. Guzzon, M. Valkama, and M. Renfors, "Reducing computational complexity of eigenvalue based spectrum sensing for cognitive radio," in *8th International Conference on Cognitive Radio Oriented Wireless Networks*. IEEE, 2013, pp. 61–67.

[47] S. Dikmese, A. Gokceoglu, M. Valkama, and M. Renfors, "Reduced complexity spectrum sensing based on maximum eigenvalue and energy," *ISWCS 2013*, 2013.

[48] N. Pillay and H. Xu, "Eigenvalue-based spectrum sensing using the exact distribution of the maximum eigenvalue of a wishart matrix," *IET Signal Processing*, vol. 7, no. 9, pp. 833–842, 2013.

[49] Z. Tian and G. B. Giannakis, "A wavelet approach to wideband spectrum sensing for cognitive radios," in *2006 1st International Conference on Cognitive Radio Oriented Wireless Networks and Communications*. IEEE, 2006, pp. 1–5.

[50] Y. Zeng, Y.-C. Liang, and M. W. Chia, "Edge based wideband sensing for cognitive radio: algorithm and performance evaluation," in *New Frontiers in Dynamic*

Spectrum Access Networks (DySPAN), 2011 IEEE Symposium on. IEEE, 2011, pp. 538–544.

[51] S. H. Kamel, S. E. El-Khamy, and M. B. Abdel-Malek, "An improved compressed wideband spectrum sensing technique based on stationary wavelet transform in cognitive radio systems," in *General Assembly and Scientific Symposium (URSI GASS), 2014 XXXIth URSI*. IEEE, 2014, pp. 1–4.

[52] C. R. Stevenson, G. Chouinard, Z. Lei, W. Hu, S. J. Shellhammer, and W. Caldwell, "Ieee 802.22: The first cognitive radio wireless regional area network standard," *IEEE communications magazine*, vol. 47, no. 1, pp. 130–138, 2009.

[53] W. S. Jeon, D. G. Jeong, J. A. Han, G. Ko, and M. S. Song, "An efficient quiet period management scheme for cognitive radio systems," *IEEE Transactions on Wireless Communications*, vol. 7, no. 2, pp. 505–509, 2008.

[54] L. Luo, N. M. Neihart, S. Roy, and D. J. Allstot, "A two-stage sensing technique for dynamic spectrum access," *IEEE transactions on wireless communications*, vol. 8, no. 6, pp. 3028–3037, 2009.

[55] H. Qing, Y. Liu, G. Xie, and J. Gao, "Wideband spectrum sensing for cognitive radios: A multistage wiener filter perspective," *IEEE Signal Processing Letters*, vol. 22, no. 3, pp. 332–335, 2015.

[56] N. Gunichetty, S. Hiremath, and S. Patra, "Two stage spectrum sensing for cognitive radio using cmme," in *Communications and Signal Processing (ICCSP), 2015 International Conference on*. IEEE, 2015, pp. 1075–1079.

[57] S. Geethu and G. L. Narayanan, "A novel high speed two stage detector for spectrum sensing," *Procedia Technology*, vol. 6, pp. 682–689, 2012.

[58] M. Lin, A. P. Vinod, and C. M. S. See, "A new flexible filter bank for low complexity spectrum sensing in cognitive radios," *Journal of Signal Processing Systems*, vol. 62, no. 2, pp. 205–215, 2011.

[59] Y. Cui, Z. Zhao, and H. Zhang, "Novel filter banks based wireless microphone detection in ieee 802.22 wran," in *Communications and Networking in China (CHINACOM), 2010 5th International ICST Conference on*. IEEE, 2010, pp. 1–5.

[60] M. Narendar, A. P. Vinod, A. Madhukumar, and A. K. Krishna, "A tree-structured dft filter bank based spectrum detector for estimation of radio channel edge frequencies in cognitive radios," *Physical Communication*, vol. 9, pp. 45–60, 2013.

[61] P. Paysarvi-Hoseini and N. C. Beaulieu, "On the benefits of multichannel/wideband spectrum sensing with non-uniform channel sensing durations for cognitive radio networks," *IEEE Transactions on Communications*, vol. 60, no. 9, pp. 2434–2443, 2012.

[62] Z. Quan, S. Cui, A. H. Sayed, and H. V. Poor, "Wideband spectrum sensing in cognitive radio networks," in *2008 IEEE International Conference on Communications*. IEEE, 2008, pp. 901–906.

[63] ——, "Optimal multiband joint detection for spectrum sensing in cognitive radio networks," *IEEE Transactions on Signal Processing*, vol. 57, no. 3, pp. 1128–1140, 2009.

[64] G. Hattab and M. Ibnkahla, "Multiband spectrum access: great promises for future cognitive radio networks," *Proceedings of the IEEE*, vol. 102, no. 3, pp. 282–306, 2014.

[65] B. Farhang-Boroujeny, "Filter bank spectrum sensing for cognitive radios," *Signal Processing, IEEE Transactions on*, vol. 56, no. 5, pp. 1801–1811, 2008.

[66] M. Rashidi, K. Haghighi, A. Owrang, and M. Viberg, "A wideband spectrum sensing method for cognitive radio using sub-nyquist sampling," in *Digital Signal Processing Workshop and IEEE Signal Processing Education Workshop (DSP/SPE), 2011 IEEE*. IEEE, 2011, pp. 30–35.

[67] Z. Tian and G. B. Giannakis, "Compressed sensing for wideband cognitive radios," in *2007 IEEE International Conference on Acoustics, Speech and Signal Processing-ICASSP'07*, vol. 4. IEEE, 2007, pp. IV–1357.

[68] J. Liang, Y. Liu, W. Zhang, Y. Xu, X. Gan, and X. Wang, "Joint compressive sensing in wideband cognitive networks," in *2010 IEEE Wireless Communication and Networking Conference*. IEEE, 2010, pp. 1–5.

[69] Z. Tian, Y. Tafesse, and B. M. Sadler, "Cyclic feature detection with sub-nyquist sampling for wideband spectrum sensing," *IEEE Journal of Selected topics in signal processing*, vol. 6, no. 1, pp. 58–69, 2012.

[70] F. Zeng, C. Li, and Z. Tian, "Distributed compressive spectrum sensing in cooperative multihop cognitive networks," *IEEE Journal of Selected Topics in Signal Processing*, vol. 5, no. 1, pp. 37–48, 2011.

[71] M. Mishali and Y. C. Eldar, "Blind multiband signal reconstruction: Compressed sensing for analog signals," *IEEE Transactions on Signal Processing*, vol. 57, no. 3, pp. 993–1009, 2009.

[72] R. Venkataramani and Y. Bresler, "Perfect reconstruction formulas and bounds on aliasing error in sub-nyquist nonuniform sampling of multiband signals," *IEEE Transactions on Information Theory*, vol. 46, no. 6, pp. 2173–2183, 2000.

[73] B. Farhang-Boroujeny and R. Kempter, "Multicarrier communication techniques for spectrum sensing and communication in cognitive radios," *IEEE Communications Magazine*, vol. 46, no. 4, pp. 80–85, 2008.

[74] P. R. Parekh and M. B. Shah, "Spectrum sensing in wideband ofdm based cognitive radio," in *Communications and Signal Processing (ICCSP), 2014 International Conference on*. IEEE, 2014, pp. 1476–1481.

[75] T. Weiss, J. Hillenbrand, A. Krohn, and F. K. Jondral, "Mutual interference in ofdm-based spectrum pooling systems," in *Vehicular Technology Conference, 2004. VTC 2004-Spring. 2004 IEEE 59th*, vol. 4. IEEE, 2004, pp. 1873–1877.

[76] K. Maliatsos, A. Adamis, and A. G. Kanatas, "Elaborate analysis and design of filter-bank-based sensing for wideband cognitive radios," *EURASIP Journal on Advances in Signal Processing*, vol. 2014, no. 1, p. 1, 2014.

[77] P. Amini, P. Kempter, R. R. Chen, L. Lin, and B. Farhang-Boroujeny, "Filter bank multitone: A physical layer candidate for cognitive radios," in *Proc. of the SDR Forum technical Conference*, 2005, pp. 14–18.

[78] P. Amini, R. Kempter, and B. Farhang-Boroujeny, "A comparison of alternative filterbank multicarrier methods for cognitive radio systems," in *Proc. of the SDR Technical Conference and Product Exposition*, 2006.

[79] D. J. Thomson, "Spectrum estimation and harmonic analysis," *Proceedings of the IEEE*, vol. 70, no. 9, pp. 1055–1096, 1982.

[80] Z. Zhao, H. Zhang, and Y. Cui, "An efficient filter banks based multicarrier system in cognitive radio networks," *Radioengineering*, 2010.

[81] H. Zhang, D. L. Ruyet, D. Roviras, and H. Sun, "Polyphase filter bank based multi-band spectrum sensing in cognitive radio systems," *International Journal of Communication Systems*, 2014.

[82] S. Dikmese, S. Srinivasan, and M. Renfors, "Fft and filter bank based spectrum sensing and spectrum utilization for cogntive radios," in *Communications Control and Signal Processing (ISCCSP), 2012 5th International Symposium on*. IEEE, 2012, pp. 1–5.

[83] S. Dikmese and M. Renfors, "Optimized fft and filter bank based spectrum sensing for bluetooth signal," in *2012 IEEE Wireless Communications and Networking Conference (WCNC)*. IEEE, 2012, pp. 792–797.

[84] M. Lin and A. Vinod, "Progressive decimation filter banks for variable resolution spectrum sensing in cognitive radios," in *Telecommunications (ICT), 2010 IEEE 17th International Conference on*. IEEE, 2010, pp. 857–863.

[85] T. Karp and N. J. Fliege, "Modified dft filter banks with perfect reconstruction," *IEEE Transactions on Circuits and Systems II: Analog and Digital Signal Processing*, vol. 46, no. 11, pp. 1404–1414, 1999.

[86] N. J. Fliege, *Multirate digital signal processing: multirate systems, filter banks, wavelets*. John Wiley & Sons, Inc., 1994.

[87] A. Viholainen, M. Bellanger, and M. Huchard, "Prototype filter and structure optimization," *PHYDYAS project, January*, 2009.

[88] M. G. Bellanger, "Specification and design of a prototype filter for filter bank based multicarrier transmission," in *Acoustics, Speech, and Signal Processing, 2001. Proceedings.(ICASSP'01). 2001 IEEE International Conference on*, vol. 4. IEEE, 2001, pp. 2417–2420.

[89] S. Mirabbasi and K. Martin, "Overlapped complex-modulated transmultiplexer filters with simplified design and superior stopbands," *IEEE Transactions on Circuits and Systems II: Analog and Digital Signal Processing*, vol. 50, no. 8, pp. 456–469, 2003.

[90] A. Datar, A. Jain, and P. C. Sharma, "Design of kaiser window based optimized prototype filter for cosine modulated filter banks," *Signal processing*, vol. 90, no. 5, pp. 1742–1749, 2010.

[91] P. Martín-Martín, R. Bregovic, A. Martín-Marcos, F. Cruz-Roldán, and T. Saramaki, "A generalized window approach for designing transmultiplexers," *IEEE Transactions on Circuits and Systems I: Regular Papers*, vol. 55, no. 9, pp. 2696–2706, 2008.

[92] C. D. Creusere and S. K. Mitra, "A simple method for designing high-quality prototype filters for m-band pseudo qmf banks," *Signal Processing, IEEE Transactions on*, vol. 43, no. 4, pp. 1005–1007, 1995.

[93] Y.-P. Lin and P. Vaidyanathan, "A kaiser window approach for the design of prototype filters of cosine modulated filterbanks," *IEEE Signal Processing Letters*, vol. 5, no. 6, pp. 132–134, 1998.

[94] F. Cruz-Roldán, P. Amo-López, S. Maldonado-Bascón, and S. S. Lawson, "An efficient and simple method for designing prototype filters for cosine-modulated pseudo-qmf banks," *IEEE Signal Processing Letters*, vol. 9, no. 1, pp. 29–31, 2002.

[95] F. Beaulieu and B. Champagne, "Multicarrier modulation using perfect reconstruction dft filter bank transceivers," in *2005 5th International Conference on Information Communications & Signal Processing*. IEEE, 2005, pp. 111–115.

[96] S.-M. Phoong, Y. Chang, and C.-Y. Chen, "Dft-modulated filterbank transceivers for multipath fading channels," *IEEE Transactions on Signal Processing*, vol. 53, no. 1, pp. 182–192, 2005.

[97] A. Kumar, G. Singh, and R. Anand, "A simple design method for the cosine-modulated filter banks using weighted constrained least square technique," *Journal of the Franklin Institute*, vol. 348, no. 4, pp. 606–621, 2011.

[98] S. W. Bergen and A. Antoniou, "An efficient closed-form design method for cosine-modulated filter banks using window functions," *Signal Processing*, vol. 87, no. 5, pp. 811–823, 2007.

[99] G. Doblinger, "A fast design method for perfect-reconstruction uniform cosine-modulated filter banks," *IEEE Transactions on Signal Processing*, vol. 60, no. 12, pp. 6693–6697, 2012.

[100] W.-S. Lu, T. Saramaki, and R. Bregovic, "Design of practically perfect-reconstruction cosine-modulated filter banks: A second-order cone programming approach," *IEEE Transactions on Circuits and Systems I Regular Papers*, vol. 51, no. 3, pp. 552–563, 2004.

[101] Z.-J. Zhang, "Efficient design of cosine modulated filter banks based on gradient information," *IEEE signal processing letters*, vol. 14, no. 12, pp. 940–943, 2007.

[102] Z.-J. Zhang, P.-L. Shui, and T. Su, "Efficient design of high-complexity cosine modulated filter banks using th band conditions," *IEEE Transactions on Signal Processing*, vol. 56, no. 11, pp. 5414–5426, 2008.

[103] D. Chen, D. Qu, T. Jiang, and Y. He, "Prototype filter optimization to minimize stopband energy with npr constraint for filter bank multicarrier modulation systems," *IEEE Transactions on Signal Processing*, vol. 61, no. 1, pp. 159–169, 2013.

[104] D. Chen, D. Qu, and T. Jiang, "Novel prototype filter design for fbmc based cognitive radio systems through direct optimization of filter coefficients," in *Wireless Communications and Signal Processing (WCSP), 2010 International Conference on*. IEEE, 2010, pp. 1–6.

[105] S. Yin, S.-C. Chan, and K. M. Tsui, "On the design of nearly-pr and pr fir cosine modulated filter banks having approximate cosine-rolloff transition band," *IEEE Transactions on Circuits and Systems II: Express Briefs*, vol. 55, no. 6, pp. 571–575, 2008.

[106] N. Zhao, F. Pu, X. Xu, and N. Chen, "Cognitive wideband spectrum sensing using cosine-modulated filter banks," *International Journal of Electronics*, vol. 102, no. 11, pp. 1890–1901, 2015.

[107] T. A. Weiss and F. K. Jondral, "Spectrum pooling: an innovative strategy for the enhancement of spectrum efficiency," *IEEE Communications Magazine*, vol. 42, no. 3, pp. S8–14, 2004.

[108] A. Rizos, J. Proakis, and T. Nguyen, "Comparison of dft and cosine modulated filter banks in multicarrier modulation," in *Global Telecommunications Conference, 1994. GLOBECOM'94. Communications: The Global Bridge., IEEE*, vol. 2. IEEE, 1994, pp. 687–691.

[109] B. Farhang-Boroujeny, "Multicarrier modulation with blind detection capability using cosine modulated filter banks," *IEEE Transactions on Communications*, vol. 51, no. 12, pp. 2057–2070, 2003.

[110] G. Cherubini, E. Eleftheriou, S. Oker, and J. M. Cioffi, "Filter bank modulation techniques for very high speed digital subscriber lines," *IEEE Communications Magazine*, vol. 38, no. 5, pp. 98–104, 2000.

[111] N. Zhao, F. Pu, X. Xu, and N. Chen, "Cosine-modulated transceivers for tv white space cognitive access," *Chin. J. Electron*, vol. 21, no. 2, pp. 362–366, 2012.

[112] S. M. Kay, *Fundamentals of Statistical Signal Processing: Practical Algorithm Development*. Pearson Education, 2013, vol. 3.

[113] N. M. Neihart, S. Roy, and D. J. Allstot, "A parallel, multi-resolution sensing technique for multiple antenna cognitive radios," in *2007 IEEE International Symposium on Circuits and Systems*. IEEE, 2007, pp. 2530–2533.

[114] S. Chen, K. Zeng, and P. Mohapatra, "Hearing is believing: detecting wireless microphone emulation attacks in white space," *IEEE transactions on mobile computing*, vol. 12, no. 3, pp. 401–411, 2013.

[115] C. J. Kim *et al.*, "Fractional bw usage for wran systems," *IEEE 802.22-06/0117r0*, 2006.

[116] S. J. Shellhammer, A. K. Sadek, and W. Zhang, "Technical challenges for cognitive radio in the tv white space spectrum," in *Information Theory and Applications Workshop, 2009*. IEEE, 2009, pp. 323–333.

[117] Y. Zeng, Y.-C. Liang, A. T. Hoang, and R. Zhang, "A review on spectrum sensing for cognitive radio: challenges and solutions," *EURASIP Journal on Advances in Signal Processing*, vol. 2010, no. 1, p. 1, 2010.

[118] H.-S. Chen and W. Gao, "Spectrum sensing for fm wireless microphone signals," in *New Frontiers in Dynamic Spectrum, 2010 IEEE Symposium on*. IEEE, 2010, pp. 1–5.

[119] S. Lim, S. Kim, C. Park, and M. Song, "The detection and classification of the wireless microphone signal in the ieee 802.22 wran system," in *2007 Asia-Pacific Microwave Conference*. IEEE, 2007, pp. 1–4.

[120] J. Unnikrishnan and S. Shellhammer, "Simulation of eigenvalue based sensing of wireless mics," *IEEE P802*, vol. 22, pp. 802–22, 2007.

[121] M. Ghosh, V. Gaddam, G. Turkenich, and K. Challapali, "Spectrum sensing prototype for sensing atsc and wireless microphone signals," in *2008 3rd International Conference on Cognitive Radio Oriented Wireless Networks and Communications (CrownCom 2008)*. IEEE, 2008, pp. 1–7.

[122] Y. Cui, Z. Zhao, and H. Zhang, "An efficient filter banks based multicarrier system in cognitive radio networks," *Radioengineering*, vol. 19, no. 4, p. 479, 2010.

[123] S. Dikmese, S. Srinivasan, M. Shaat, F. Bader, and M. Renfors, "Spectrum sensing and resource allocation for multicarrier cognitive radio systems under interference and power constraints," *EURASIP Journal on Advances in Signal Processing*, vol. 2014, no. 1, p. 1, 2014.

[124] M. Lin and A. P. Vinod, "A low complexity high resolution cooperative spectrum-sensing scheme for cognitive radios," *Circuits, Systems, and Signal Processing*, vol. 31, no. 3, pp. 1127–1145, 2012.

[125] K. G. Smitha and A. P. Vinod, "A reconfigurable channel filter for software defined radio using rns," *Journal of Signal Processing Systems*, vol. 67, no. 3, pp. 229–237, 2012.

[126] Y. Cui, Z. Zhao, and H. Zhang, "Adaptive threshold enhanced filter banks for wireless microphone detection in ieee 802.22 wran," in *21st Annual IEEE In-*

ternational Symposium on Personal, Indoor and Mobile Radio Communications. IEEE, 2010, pp. 2727–2732.

[127] C. Clanton, M. Kenkel, and Y. Tang, "Wireless microphone signal simulation method," *IEEE 802.22-07/0124r0*, 2007.

[128] A. Kumar, G. Singh, and S. Anurag, "An optimized cosine-modulated nonuniform filter bank design for subband coding of ecg signal," *Journal of King Saud University-Engineering Sciences*, vol. 27, no. 2, pp. 158–169, 2015.

[129] S. Kalathil, B. S. Kumar, and E. Elias, "Efficient design of multiplier-less digital channelizers using recombination non-uniform filter banks," *Journal of King Saud University-Engineering Sciences*, 2015.

[130] S. Kalathil and E. Elias, "Design of multiplier-less sharp non-uniform cosine modulated filter banks for efficient channelizers in software defined radio," *Engineering Science and Technology, an International Journal*, vol. 19, no. 1, pp. 147–160, 2016.

[131] J. Kovacevic and M. Vetterli, "Perfect reconstruction filter banks with rational sampling factors," *IEEE Transactions on Signal Processing*, vol. 41, no. 6, pp. 2047–2066, 1993.

[132] R. Cox, "The design of uniformly and nonuniformly spaced pseudoquadrature mirror filters," *IEEE transactions on acoustics, speech, and signal processing*, vol. 34, no. 5, pp. 1090–1096, 1986.

[133] S. Anurag and A. Kumar, "An improved design technique for multichannel non-uniform filter bank," *Int. Jr. of Advanced Computer Engineering & Architecture*, vol. 2, no. 2, pp. 161–170, 2012.

[134] A. Kumar, G. K. Singh, and S. Anurag, "Design of nearly perfect reconstructed non-uniform filter bank by constrained equiripple fir technique," *Applied Soft Computing*, vol. 13, no. 1, pp. 353–360, 2013.

[135] A. Eghbali, H. Johansson, and P. Lowenborg, "A multimode transmultiplexer structure," *IEEE Transactions on Circuits and Systems II: Express Briefs*, vol. 55, no. 3, pp. 279–283, 2008.

[136] S. Akkarakaran and P. Vaidyanathan, "New results and open problems on nonuniform filter-banks," in *Acoustics, Speech, and Signal Processing, 1999. Proceedings., 1999 IEEE International Conference on*, vol. 3. IEEE, 1999, pp. 1501–1504.

[137] M. Wang, J. Wan, and Y. Zhao, "Design of linear phase nonuniform filter banks with interpolated prototype filters," *Procedia Engineering*, vol. 29, pp. 435–440, 2012.

[138] J.-J. Lee and B. G. Lee, "A design of nonuniform cosine modulated filter banks," *IEEE Transactions on Circuits and Systems II: Analog and Digital Signal Processing*, vol. 42, no. 11, pp. 732–737, 1995.

[139] J. Li, T. Q. Nguyen, and S. Tantaratana, "A simple design method for near-perfect-reconstruction nonuniform filter banks," *IEEE Transactions on Signal Processing*, vol. 45, no. 8, pp. 2105–2109, 1997.

[140] S. Chan, X. Xie, and T. Yuk, "Theory and design of a class of cosine-modulated non-uniform filter banks," in *Acoustics, Speech, and Signal Processing, 2000. ICASSP'00. Proceedings. 2000 IEEE International Conference on*, vol. 1. IEEE, 2000, pp. 504–507.

[141] B. W.-K. Ling, C. Y.-F. Ho, K.-L. Teo, W.-C. Siu, J. Cao, and Q. Dai, "Optimal design of cosine modulated nonuniform linear phase fir filter bank via both stretching and shifting frequency response of single prototype filter," *IEEE Transactions on Signal Processing*, vol. 62, no. 10, pp. 2517–2530, 2014.

[142] F. Argenti and E. Del Re, "Non-uniform filter banks based on a multi-prototype cosine modulation," in *Acoustics, Speech, and Signal Processing, 1996. ICASSP-96. Conference Proceedings., 1996 IEEE International Conference on*, vol. 3. IEEE, 1996, pp. 1511–1514.

[143] S. Srinivasan, S. Dikmese, and M. Renfors, "Spectrum sensing and spectrum utilization model for ofdm and fbmc based cognitive radios," in *2012 IEEE 13th International Workshop on Signal Processing Advances in Wireless Communications (SPAWC)*. IEEE, 2012, pp. 139–143.

[144] S. Huang, A. Ephremides, and D. Yuan, "A non-uniform bandwidth allocation scheme for efficient cognitive spectrum access," in *2015 IEEE International Conference on Communications (ICC)*. IEEE, 2015, pp. 7725–7730.

[145] ——, "Improving the cognitive access efficiency by non-uniform bandwidth allocation," *IEEE Transactions on Wireless Communications*, vol. 14, no. 11, pp. 6435–6447, 2015.

[146] K. El Baamrani, A. A. Ouahman, and S. Allaki, "Rate adaptive resource allocation for ofdm downlink transmission," *AEU-International Journal of Electronics and Communications*, vol. 61, no. 1, pp. 30–34, 2007.

[147] A. Leke and J. M. Cioffi, "A maximum rate loading algorithm for discrete multitone modulation systems," in *Global Telecommunications Conference, 1997. GLOBECOM'97., IEEE*, vol. 3. IEEE, 1997, pp. 1514–1518.

[148] P. S. Chow, J. M. Cioffi, J. Bingham *et al.*, "A practical discrete multitone transceiver loading algorithm for data transmission over spectrally shaped channels," *IEEE Transactions on communications*, vol. 43, no. 234, pp. 773–775, 1995.

[149] R. F. Fischer and J. B. Huber, "A new loading algorithm for discrete multitone transmission," in *Global Telecommunications Conference, 1996. GLOBECOM'96.'Communications: The Key to Global Prosperity*, vol. 1. IEEE, 1996, pp. 724–728.

[150] D. Hughes-Hartogs, "Ensemble modem structure for imperfect transmission media," May 23 1989, uS Patent 4,833,706.

[151] B. S. Krongold, K. Ramchandran, and D. L. Jones, "Computationally efficient optimal power allocation algorithms for multicarrier communication systems," *IEEE Transactions on Communications*, vol. 48, no. 1, pp. 23–27, 2000.

[152] S. Sadr, A. Anpalagan, and K. Raahemifar, "Suboptimal rate adaptive resource allocation for downlink ofdma systems," *International Journal of Vehicular Technology*, vol. 2009, 2009.

[153] A. Mahmood and J.-C. Belfiore, “An efficient algorithm for optimal discrete bit-loading in multicarrier systems,” *IEEE transactions on communications*, vol. 58, no. 6, pp. 1627–1630, 2010.

[154] Y.-P. Lin, S.-M. Phoong, and P. Vaidyanathan, *Filter bank transceivers for OFDM and DMT systems*. Cambridge University Press, 2010.

APPENDIX A

Centroid of Trapezoid

The energy distribution in two subband bins are modeled as a trapezoid and shown in Figure A.1, where a and b represent the energy in the subband bins and h the spectral resolution of the subband.

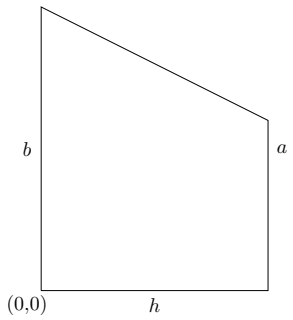

Figure A.1: Centroid of trapezoid

We consider the bottom edge to be perpendicular to the left and right sides of the trapezoid. The bottom left corner is considered as the point $(0, 0)$. The top edge is then defined by the linear function

$$f(x) = b + \frac{x}{h}(a - b), \tag{A.1}$$

where, $f(0) = b$ and $f(h) = b + \dfrac{x}{h}(a - b)$.

The area of the trapezoid is given by $A = \dfrac{h}{2}(a + b)$. A trapezoid is a quadrilateral with two parallel sides and the centroid lies between the two bases. That is, centroid of a trapezoid geometrically lies on the median. Therefore,

$$A\bar{x} = \int_0^h xf(x)dx \tag{A.2}$$

$$= \int_0^h x\left(b + \frac{x}{h}(a - b)\right)dx \tag{A.3}$$

$$= \left[\frac{1}{2}bx^2 + \frac{1}{3h}(a - b)x^3\right]_0^h \tag{A.4}$$

$$= \frac{h^2}{6}(2a + b) \tag{A.5}$$

Hence,

$$\bar{x} = \frac{\frac{h^2}{6}(2a+b)}{\frac{h}{2}(a+b)} \tag{A.6}$$

$$= \frac{h(2a+b)}{3(a+b)} \tag{A.7}$$

The centroid can be verified for the following conditions:

1. If $a = 0$ the trapezoid becomes a right triangle, and then Equation A.6 becomes $\bar{x} = \frac{h}{3}$.
2. If $a = b$ the trapezoid becomes a rectangle and Equation A.6 becomes $\bar{x} = \frac{h}{2}$.

LIST OF PAPERS BASED ON THESIS

Papers in Refereed International Journals

1. A Low Complexity Multistage Polyphase Filter Bank For Wireless Microphone Detection in CR, *Circuits, Systems, and Signal Processing, Springer*, **36**, 1671-1685 (2016).

2. An Iterative Design with Variable Step Prototype Filter for Cosine Modulated Filter Bank, *Radioengineering*, **25**, 156-160 (2016).

3. Rate Request Sequenced Bit Loading Secondary User Reallocation Algorithm for DMT Systems in Cognitive Radio, *International Journal of Vehicular Technology*, **Article ID 685491** (2015)

4. Filter bank design using multiprototype approach for variable granularity bands, *International Journal On Smart Sensing And Intelligent Systems*, **9**, 733-751 (2016).

5. Spectral Detection with Multistage Granularity Bands using Filter Bank Techniques for CR Applications, *International Journal of Wireless and Mobile Computing, Inderscience*, **12**, 62-67 (2017).

A.0.1 Papers Communicated and Under Review

(a) A Novel Center of Mass method for Estimation of Center Frequency and Spectral Edges in CR using Filter Banks - under review.

(b) A Non-Contiguous Bandwidth Allocation with Filter Bank Multicarrier Technique for Multiple Users - under review

Presentations in Conferences

1. *A channel combiner approach for the design of near perfect reconstruction non uniform filter banks* at the **IEEE International Conference on Communication and Signal Processing (ICSSP 2014)** Tamil Nadu, 3-5th April 2014.

2. *Analysis of multiprototype over single prototype filters for non uniform filter banks* at the **IEEE (INDICON 2014)** Pune, 11-13th Dec 2014.

3. *Spectrum Sensing in Multipath fading channels using Cosine Modulated Filter Bank for Cognitive Radio Applications* at the **IEEE International conference on Electrical, Computers and Communication Technology** Tamil Nadu, 5-7th March 2015.

4. *Spectrum Sensing with Programmable Granularity Bands Using Cosine Modulated Filter Bank for Cognitive Radio* at the **IEEE International Conference on Communication and Signal Processing (ICSSP 2015)** Tamil Nadu, 2-4th April 2015.

5. *CMFB for Spectrum Detection and Utilization in CR Application* at the **International Conference on Computing and Network Communications (CoCoNet 2015)** Trivandrum, 16-19th Dec 2015.